

CIE 5060

**Study and Comparison of
Shell Design Codes**

*For Adaptation to Design Geometrically
Complex Steel Shell Structures*



A Master's thesis submitted in part fulfilment of
the requirements for the degree of
Master of Science of Civil Engineering

by

Eoin Dunphy

Student No.: 4035879

March 1, 2013

ABSTRACT

The Eurocode and American Bureau of Shipping code analytical methods of determining the buckling resistance of 6 axially loaded steel shell cylinders was studied. The Eurocode MNA/LBA and GMNIA numerical methods were also studied using finite element analysis and compared against the results of the analytical methods. Following these comparisons the intention was to give an overview of the different methods and their applicability. Further suggestions were then made on how these methods could be used in the future analyses of more geometrically complex steel shell structures.

It was found that the Eurocode significantly underestimates the buckling resistance of ring and stringer stiffened cylindrical shells when compared to the ABS code (34% to 54% lower). The MNA/LBA numerical method currently allows the determination of the buckling resistance of simple structures under load conditions not covered by the classical theory. The MNA/LBA method shows potential for greater usage in more geometrically complex analyses provided that the required buckling parameters for its use are pre-determined. If these parameters are available the MNA/LBA method would be a less time consuming design method than the more rigorous GMNIA method.

The GMNIA method is the most complex analysis and as it is purely computational the importance of correctly modelling the structure and its imperfections is paramount in the determination of a realistic buckling resistance. The pitfalls of these requirements is that the correct imperfection type is difficult and time consuming to determine and the introduction of these imperfections has implications on further modelling of the structure. However, the GMNIA method is adaptable to unique cases without precedent and there is potential for research based on its usage as opposed to through physical experimentation.

ACKNOWLEDGEMENTS

I would like to show my gratitude to my thesis committee; Prof. ir. Jan Rots, Dr. ir. Jeroen Coenders, Ir. Andrew Borgart and Dr. ir. Pierre Hoogenboom for their guidance, support and their help throughout the course of this graduation project.

I would also like to sincerely thank all my family and friends for their continued support and encouragement.

Eoin Dunphy

TABLE OF CONTENTS

Abstract	i
Acknowledgements	ii
1 Introduction	1
1.1 General	1
1.2 Shell Structures	1
1.3 Buckling	3
1.3.1 Bifurcation of Equilibrium	3
1.3.2 Limit Load Buckling	5
1.3.3 Buckling Modes	6
1.4 Flat Plates and Curved Panels	8
1.4.1 Plate	9
1.4.2 Shell panel	11
1.5 Eurocode	14
1.5.1 EN 1993-1-6: Strength and stability of shell structures	14
1.5.2 EN 1993-4-1: Silos	16
1.6 American Bureau of Shipping	16
2 Problem Definition	19
2.1 Objective	20
3 Theoretical Background	21
3.1 Axial Buckling of Cylindrical Shells	21
3.2 External Pressure Buckling of Cylindrical Shells	24
3.3 Imperfections	25
3.4 Finite Elements	27
4 Methodology	29
4.1 Eurocode: EN 1993-1-6	29
4.1.1 Meridional Buckling	29
4.1.2 Circumferential Buckling	31
4.1.3 Stress Design Method	32
4.2 Eurocode: EN 1993-4-1	34
4.3 ABS	37
4.3.1 Unstiffened or Ring-Stiffened Cylinders	38
4.3.2 Ring and Stringer-stiffened Shells	41
4.4 Computational Analysis	44
4.4.1 Static Structural Stress Analysis	45

4.4.2	Linear Buckling Analysis	46
4.4.3	Introduction of Imperfections	47
4.4.4	Non-Linear Analysis	47
5	Design Code Analytical Method	54
5.1	Ring Stiffened Cylinders	54
5.1.1	Cylinder IC-1	54
5.1.2	Cylinder 1	63
5.1.3	Cylinder 6.1	64
5.2	Ring and Stringer Stiffened Cylinders	64
5.2.1	Cylinder IC6	64
5.2.2	Cylinder 2-1C	65
5.2.3	Cylinder 2-1B	66
6	Computational Method	68
6.1	Ring Stiffened Cylinders	68
6.1.1	Cylinder IC-1	68
6.1.2	Cylinder 1	83
6.1.3	Cylinder 6.1 - First Eigenmode	86
6.1.4	Cylinder 6.1 - Second Eigenmode	90
6.2	Ring and Stringer Stiffened Cylinders	92
6.2.1	Cylinder IC6	92
6.2.2	Cylinder 2-1C	95
6.2.3	Cylinder 2-1B	99
6.2.4	Mesh Sensitivity	103
7	Comparison	104
7.1	Analytical Comparison	105
7.1.1	Ring Stiffened Cylinders	105
7.1.2	Ring- and Stringer Stiffened Cylinders	112
7.2	Computational Comparison	114
7.2.1	Ring-stiffened Cylinders	114
7.2.2	Ring- and Stringer-stiffened Cylinders	115
8	Discussion	117
8.1	General Discussion	117
8.2	Computational Method Discussion	120
8.2.1	The MNA/LBA Method	120
8.2.2	The GMNIA method	125
9	Conclusions and Recommendations for Further Study	129
9.1	Recommendations for Further Study	130
	References	134

I	Appendix A - Singly curved plate example	139
II	Appendix B - Matlab ABS Script	141
III	Appendix C - Eurocode Script	152
IV	Appendix D - ANSYS Element Types	161
V	Appendix E - Sample ANSYS Report	164

LIST OF SYMBOLS

χ	Buckling resistance reduction factor
χ_{ov}	Overall buckling resistance reduction factor for complete shell
β	Plastic range factor in buckling interaction
ϵ	Strain
η	Interaction exponent for buckling
γ	Partial factor
ν	Poisson's ratio
σ_{CExR}	Classical axial buckling stress of a cylinder
σ_{ExB}	Elastic compressive buckling stress for an imperfect cylindrical shell
λ	Relative slenderness of shell
λ_0	squash limit relative slenderness (value of λ at which stability reductions commence)
λ_{ov}	Overall relative slenderness for the complete shell (multiple segments)
λ_p	plastic limit relative slenderness (value of λ below which plasticity affects the stability)
ω	Relative length parameter for shell
ρ_{xP}	Lower bound knock down factor
σ_{CExR}	The classical buckling stress of a cylinder under axial loading
σ_{ExB}	The elastic compressive buckling stress of an imperfect stringer-stiffened shell
σ_{cr}	Critical buckling stress
σ_c	Classical buckling stress
σ_s	The elastic buckling stress of a stringer stiffened shell
E	Material modulus of elasticity
I	Second moment of area of section
N	Applied load
$R_{cr,perfect}$	Geometrically and materially non-linear resistance of perfect shell
I_{se}	The moment of inertia of stringer stiffener plus associated effective shell plate width

N_{cr}	Critical buckling load
R_{cr}	Elastic critical buckling resistance of a perfect shell
R_{pl}	Plastic critical buckling resistance of a perfect shell
a	Amplitude of geometric imperfection
l	Length
r	Radius to middle surface of shell
t	Thickness of plate/shell
w	Displacement
a	Length of panel
b	Width of panel
k	Boundary condition parameter
s_e	Reduced effective width of shell
z_b	The Batdorf width parameter

1 INTRODUCTION

1.1 General

In the field of civil engineering the design codes and guidelines for to designing steel shells are of very limited use when it comes to geometrically complex structures. The typical steel shells that civil engineers are principally concerned with are silos, tanks, pipelines, chimneys, towers and masts which are covered in Eurocode 3. For larger scale steel shells of increased geometrical complexity there is little guidance as current knowledge of shell structures is dominated by and based upon shells of revolution (Rotter; 1998). As such, when it comes to structures like the Yas Hotel bridge (Figure: 1.1) which are neither pure shells nor typical beam and column structures the design can be approached in a number of ways; from complicated modelling from the beginning of the design process, to developing a design based on a simplification on the structure. To base the design of such a building on a model with too many simplifications could lead to neglecting some very important and advantageous characteristics of shell behaviour, resulting in inefficiently designed, wasteful and potentially unsafe structures. Similarly, it is impractical and time consuming to design such a structure from the early design stages using detailed computational models and it can be difficult to accurately model the design situation. A solution may be to have some guidelines or rules of thumb around which the preliminary design of the structure may be based which takes into account the structurally advantageous behaviour of shells.

1.2 Shell Structures

Shell structures have a long history and have existed since before structural engineering and architecture were even recognised sciences; one of the oldest known example of a concrete shell being the Pantheon dome in Rome which was completed sometime around 125AD. From an early age the aesthetics of shells and their natural strength and stability has been well known, despite the lack of mathematical reasoning behind them. Dome structures continued to be the most significant shell structure for quite some time and are visible throughout history as part of many cathedrals, mosques and mausoleums up until the early



Figure 1.1: Yas Hotel Bridge, Abu Dhabi

20th century where shell structures underwent a revival.

During the 20th century a greater understanding of the mechanical properties of shell structures was developed, not only were their aesthetics appreciated but also the economy of such structures due to their efficient load distribution. This knowledge however was mainly only applicable to geometrically regular curved surfaces which can be easily described by analytical mathematical functions. With the advent of computational technology and in particular FEM (Finite Element Modelling) engineers and architects could model more complex shapes and venture into the analysis of more free form structures. The increased capability and desire for free form shell structures is evident in many designs from well-known architects such as Zaha Hadid architects, Future Systems, ONL Oosterhuis, Norman Foster and Partners, Asymptote Architects and UN Studios. With this drive toward more complex geometry there is a demand for increased research and design procedures for these structures and in the instance of shells, where form and force are so intricately linked, it seems that the engineering aspects are lagging behind the architectural demand. Interestingly there have been some projects in which shipbuilding companies have designed and built steel civil engineering structures using steel or aluminium plates such as the Yas hotel link bridge in Abu Dhabi and the J.P. Morgan media centre in Lords Cricket Ground in London. This meeting of two disciplines of design poses interesting research topics into how applicable approaches from other disciplines are to the design of civil engineering struc-

tures and what assumptions remain valid or could be modified for better design as despite being based on the same theory, different approaches may be taken in design.

1.3 Buckling

Buckling is an important behaviour in the design of metal structures. Generally buckling may be defined as the sudden failure, or instability, of a structural member subject to compressive stress. This instability occurs at a maximum point on the load-deflection curve at which point instability may fall into one of two categories:

1. Bifurcation of equilibrium or;
2. Limit load buckling

1.3.1 Bifurcation of Equilibrium

If a perfect member is subject to an external load and initially deforms in one configuration, then at a critical load the deformation of this structure changes to another pattern (referred to as the buckling mode), the instability is said to be “bifurcation buckling”, it occurs when two (or more) equilibrium paths pass through the same point. Take for instance a column subject to axial loading; initially the column will shorten, then at a critical load the column will begin to bend. This type of buckling can be found in structures such as axially compressed columns, plates and cylindrical shells and may be further broken down based on postbuckling behaviour to i) stable postbuckling or ii) unstable post buckling.

1.3.1.1 Stable Postbuckling

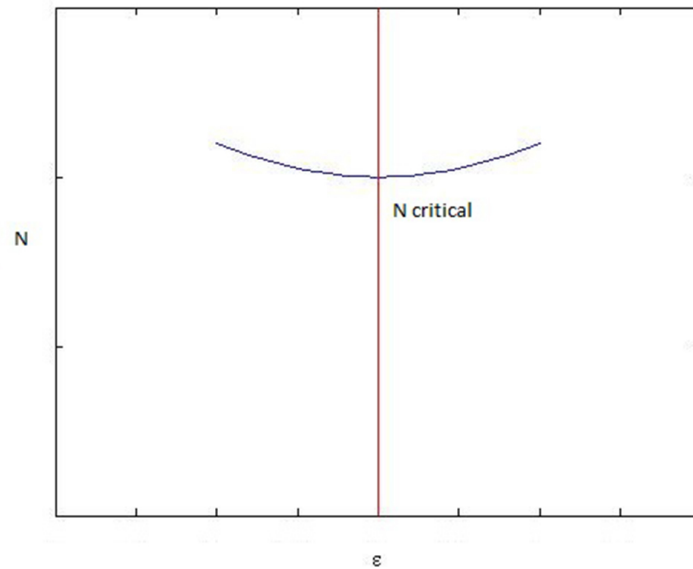


Figure 1.2: Stable postbuckling curve

The load required to keep the structure in a deformed configuration increases as the deformation increases in magnitude. For example, an axially compressed plate will develop tensile membrane stresses as it deforms which will result in an increase of stiffness.

1.3.1.2 Unstable Postbuckling

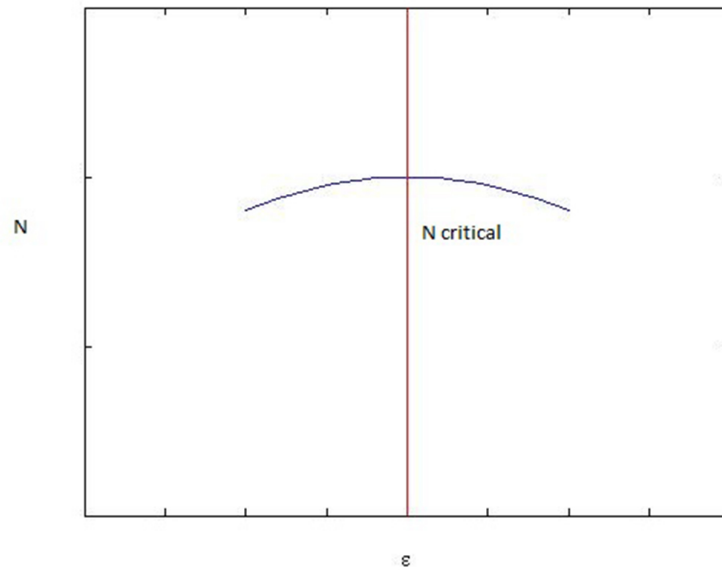


Figure 1.3: Unstable postbuckling curve

The external load required to maintain equilibrium decreases as the postbuckling deformation increases, e.g. an axially compressed cylindrical shell.

1.3.2 Limit Load Buckling

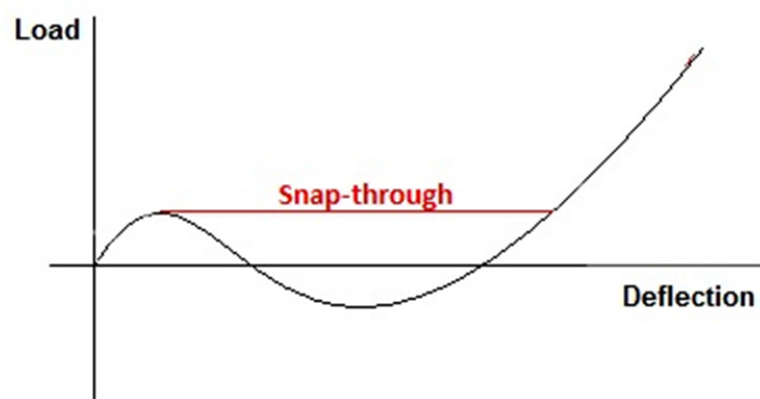


Figure 1.4: Limit load buckling

When the initially stable path loses its stability at the “limit point” of the system and there is a jump, or “snap through” non-equilibrium states to another stable path this is known as limit load, or snap-through buckling. This behaviour may be seen in buckling of shallow arches or spherical caps.

1.3.3 Buckling Modes

For stiffened structures buckling may occur at different levels, or modes, which can be generalised as a scale of buckling. The failure of plates and stiffened panels can be further subdivided into three of these modes or levels, namely, the plate level; which is local buckling between minor stiffeners. The stiffened panel level; which is larger scale buckling between more major stiffeners and the entire grillage level; which is buckling at a global level (see Figure: 1.5)

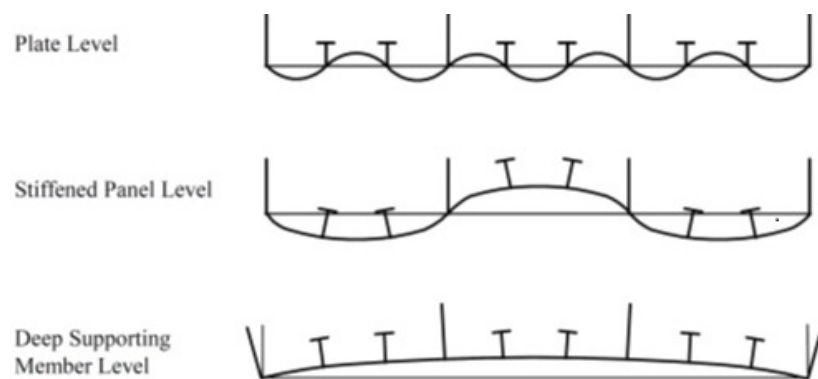


Figure 1.5: Stiffened panel failure levels (*American Bureau of Shipping - Guide for buckling and ultimate strength assessment for offshore structures*; 2004)

Similarly, such a distinction can be made with shell structures, for instance the probable buckling modes of ring- and/or stringer-stiffened cylindrical shells can be sorted as follows:

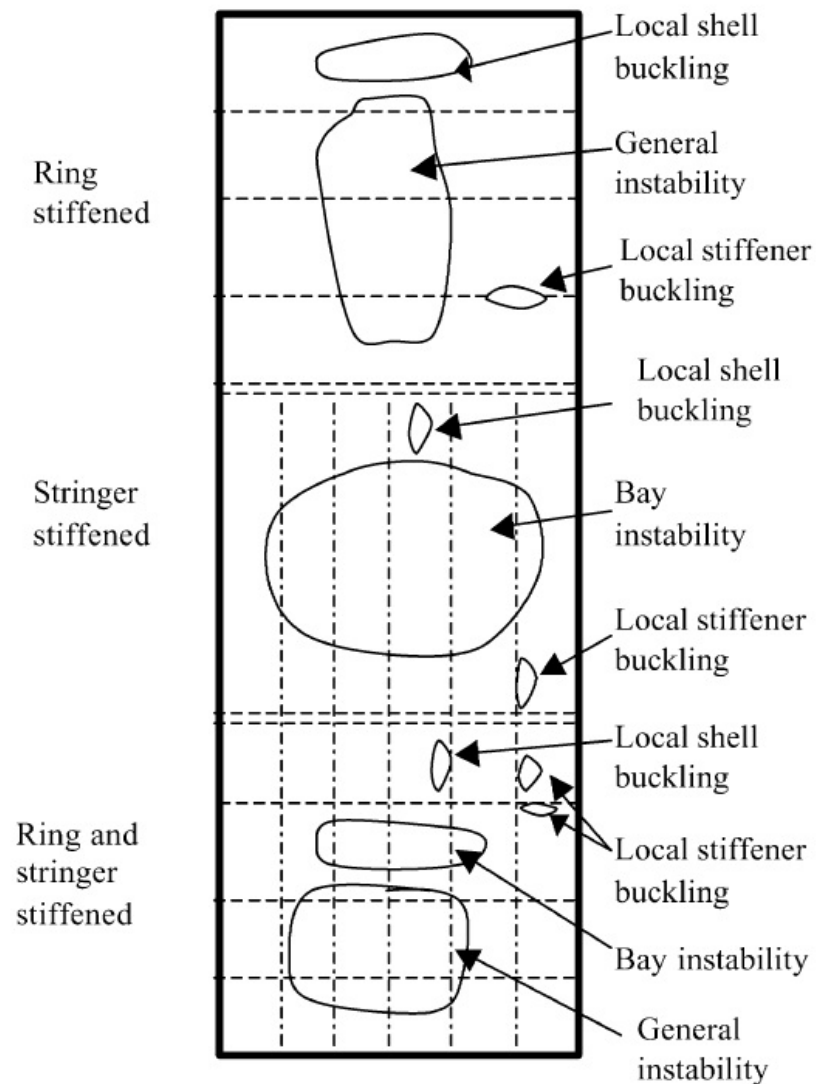


Figure 1.6: Buckling modes of stiffened cylindrical shells (Das et al.; 2003)

These categories of buckling are of particular interest for shell structures and are examined in detail within the *American Bureau of Shipping - Guide for buckling and ultimate strength assessment for offshore structures* (2004) and can be described as follows:

- Local shell or curved panel buckling (i.e., buckling of the shell between adjacent stiffeners). The stringers remain straight and the ring stiffeners remain round.
- Bay buckling (i.e., buckling of the shell plating together with the stringers, if present, between adjacent ring stiffeners). The ring stiffeners and the ends of the cylindrical

shells remain round.

- General buckling, (i.e., buckling of one or more ring stiffeners together with the attached shell plus stringers, if present).

Additionally, the ABS guidelines for buckling of offshore structures also examines the following:

- Local stiffener buckling (i.e., torsional/flexural buckling of stiffeners, ring or stringer, or local buckling of the web and flange). The shell remains undeformed.
- Column buckling (i.e., buckling of cylindrical shell as a column).

1.4 Flat Plates and Curved Panels

A plated structure as defined by Eurocode EN 1993-1-5 is “a structure built up from nominally flat plates which are connected together [where] the plates may be stiffened or unstiffened” and a stiffener is defined as a plate or section attached to the plate to resist buckling or to strengthen the plate. Structural plates and panels are very common in the fields of civil engineering and also in other disciplines such as marine and offshore engineering. In typical civil engineering structures they are often seen as elements in built up sections, such as plate girders or columns which primarily function as beams, but due to their geometrical aspects must be considered as plates.

It is important to note that mathematically we can define three different types of plates: (1) thin plates with small deflections, (2) thin plates with large deflections and (3) thick plates, each with their own theory and conditions. As this thesis is concerned with buckling of thin shell elements the most closely related category is that of thin plates with large deflections.

Eurocode EN 1993-1-6:2007 Strength and Stability of Shell Structures defines a shell panel as “an incomplete shell of revolution”, or more explicitly that “the shell form is defined by a rotation of the generator about the axis through less than 2 radians.” The main suppositions of the theory of thin plates also form the basis for the usual theory of thin shells. There exists, however, a substantial difference in the behaviour of plates and shells under the action of external loading. The static equilibrium of a plate element under a lateral load is only possible by action of bending and twisting moments, usually accompanied by shearing forces, while a shell, in general, is able to transmit the surface load by “membrane”



Figure 1.7: Steel plate girder

stresses which act parallel to the tangential plane at a given point of the middle surface and are distributed uniformly over the thickness of the shell. “This property of shells makes them, as a rule, a much more rigid and a more economical structure than a plate would be under the same conditions” (Timoshenko and Woinowsky-Krieger; 1959).

The advantage of introducing curvature can be demonstrated using a simple example:

Given the same geometrical properties i.e a thickness of 5mm, height of 1000mm and a loaded edge length of 1570.8mm. Both the plate and the curved panel are simply supported on all four edges and are loaded by an evenly distributed force on the short edge.

1.4.1 Plate

The classical buckling strength of a flat plate loaded in plane which is simply supported on its sides is (Timoshenko and Gere; 1961, p.353):

$$\sigma_c = k \frac{\pi^2 E}{12(1 - \nu^2)(b/t)^2} \quad (1.1)$$

where:

a is the length of the plate,

b is the width of the plate,

t is the thickness of the plate,

E is the modulus of elasticity of the material,

ν is Poisson's ratio and;

$$k = \left(\frac{b}{a} + \frac{a}{b}\right)^2 \quad (1.2)$$

So for the given boundary conditions $k=4.873$.

So;

$$\sigma_c = 4.873 \frac{\pi^2 \times (2 \times 10^5)}{12(1 - 0.3^2)(1570.8/5)^2}$$

$$\sigma_c = 8.92 \text{ N/mm}^2$$

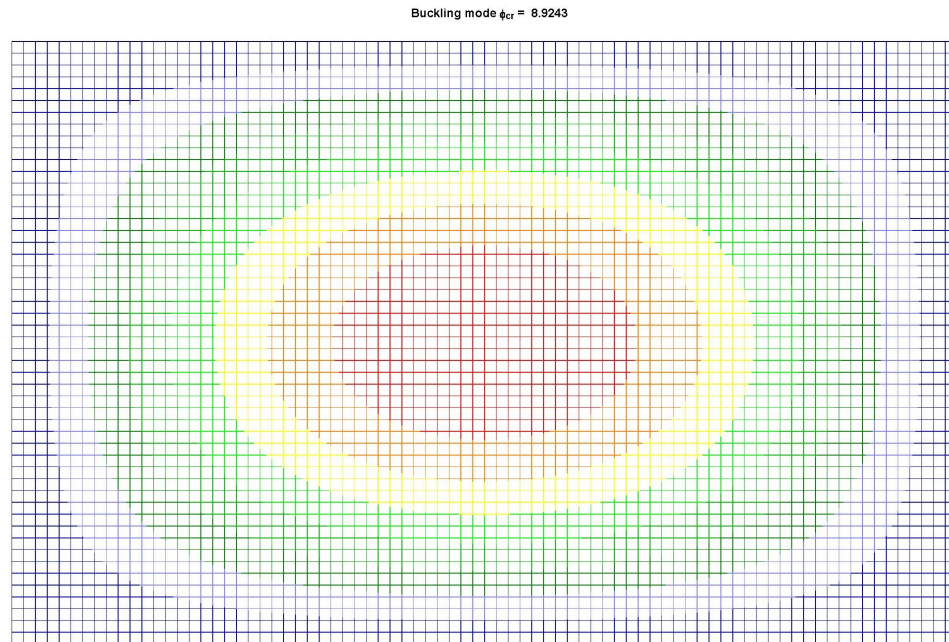


Figure 1.8: First buckling mode of flat plate - deformed shape and stress

This result is compared to a finite element computation (see Figure: 1.9). A linear buckling analysis on the plate gives a load factor of 62466 to a load of 1N distributed over the short edge. Therefore the buckling load is 62kN which is 11% smaller than the hand calculation. In reality the plate strength would probably be larger due to the stable post buckling behaviour.

1.4.2 Shell panel

If the same dimensions are used but a large curvature is introduced, the buckling strength of the plate increases significantly. A MATLAB script (See Appendix A) was used to determine the buckling stress of the same plate curved with a radius of 500mm into a semi circular shape. By adapting the theory for flat plates the compressive buckling coefficient is changed (Gerard and Becker; 1957) to:

$$k = \frac{(n^2 + \beta^2)^2}{\beta^2} + \frac{12z_b^2\beta^2}{\pi^4(n^2 + \beta^2)^2} \quad (1.3)$$

Where:

$$z_b = (b^2/rt)(1 - \nu^2)^{1/2} \quad (1.4)$$

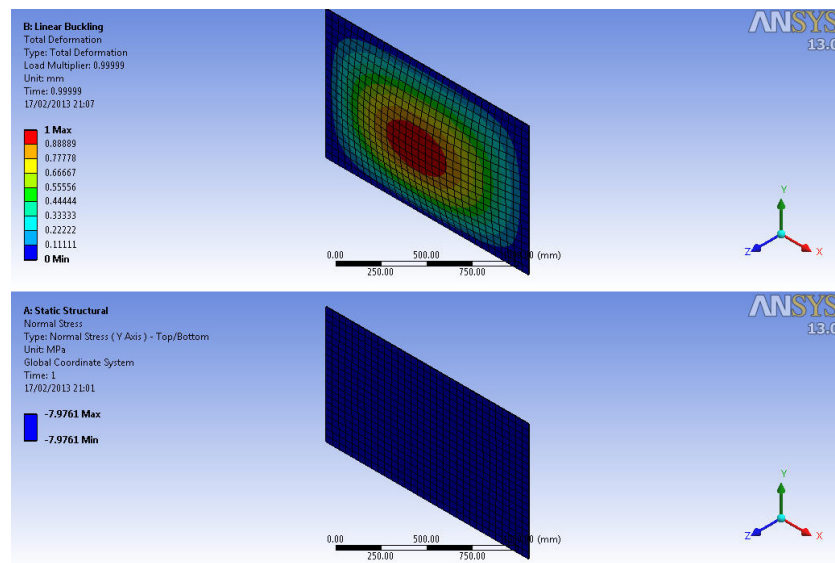


Figure 1.9: ANSYS - First buckling mode flat plate and buckling stress

$$\beta = b/\lambda \quad (1.5)$$

$$\lambda = \frac{(\pi r)}{n} \quad (1.6)$$

This equation for k is minimised to determine n , the wave number in the circumferential direction of cylinders and singly curved plates. For this example it can be seen from the MATLAB plot (Figure: 1.10) that this results in 5 waves. This is also illustrated graphically by an ANSYS linear buckling analysis of the same plate (Figure: 1.11).

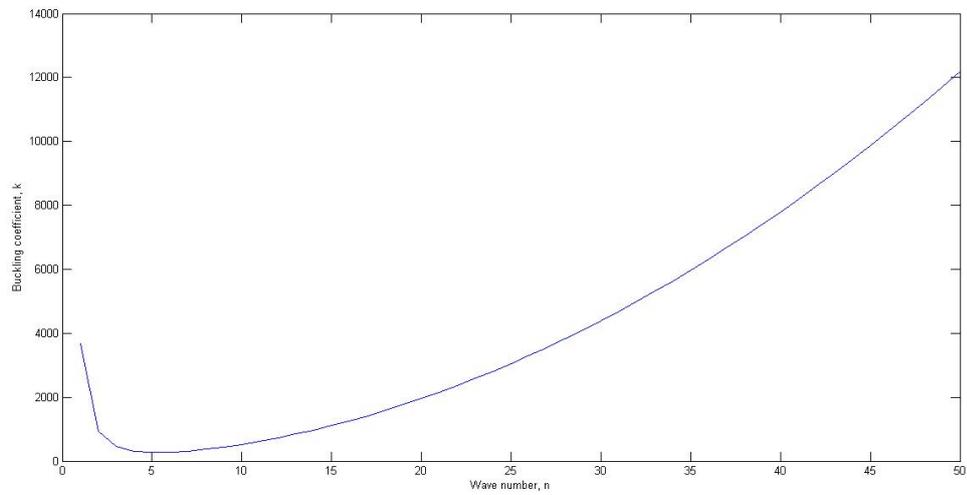


Figure 1.10: Wave number vs. Buckling coefficient

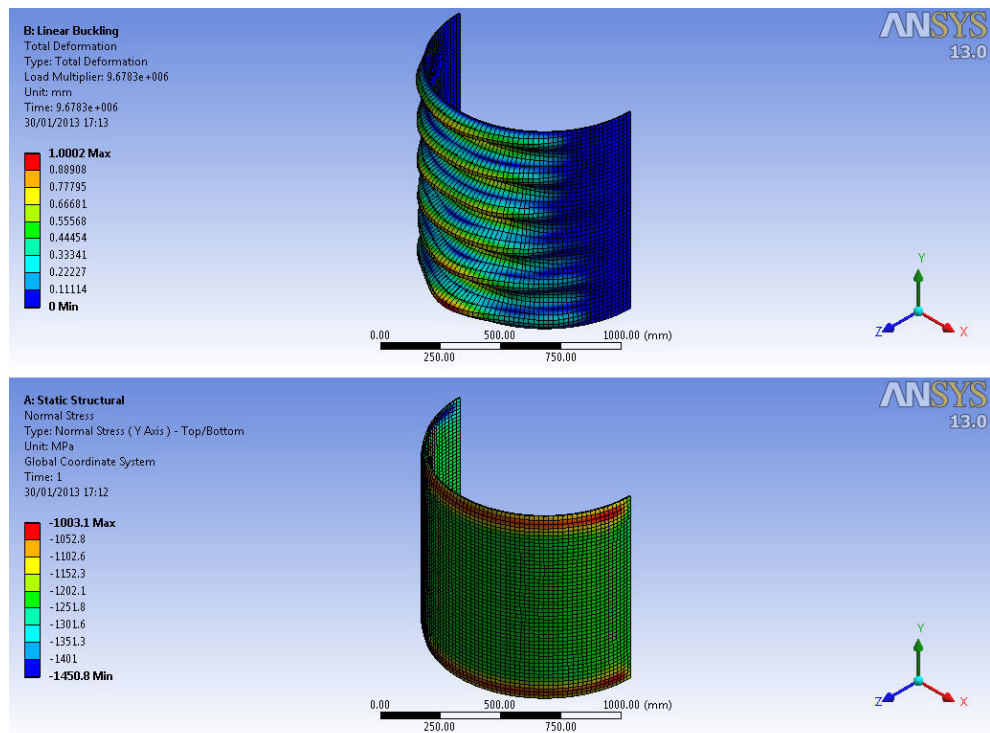


Figure 1.11: First buckling mode of curved panel - deformed shape and stress

This gives a value of $k=269.06$ which results in a critical buckling stress for the curved plate of:

$$\sigma_{cr} = 1215.9N/mm^2$$

Or, for the sake of comparison with the ANSYS model, the buckling force multiplier is = 9.6783e+006. Giving a buckling force of:

$$N_{cr} = 9.6783e + 006 \quad N$$

Over an area of:

$$Area = \pi r t = 7854 \quad mm^2$$

Resulting in a buckling stress of:

$$\sigma_{cr} = 1232.3 \quad N/mm^2$$

1.5 Eurocode

“The EN Eurocodes are a series of 10 European Standards, EN 1990 - EN 1999, providing a common approach for the design of buildings and other civil engineering works and construction products” (*The EN Eurocodes*; n.d.).

Methods based on two Eurocode documents are used in this study. These documents are *Eurocode 3 - Design of steel structures - Part 1-6: Strength and stability of shell structures* (2007), which applies to the structural design of plated steel structures that have the form of a shell of revolution, and *Eurocode 3 - Design of steel structures - Part 4-1: Silos* (2007).

1.5.1 EN 1993-1-6: Strength and stability of shell structures

Part 1-6: Shells deals with four different limit states for shell structures: Plastic limit, cyclic plasticity, buckling and fatigue however the area of interest for this study was on buckling so this section will be explained. There are different methodologies for analysis mentioned in *Part 1-6: Shells*; one set being hand calculations (referred to as “stress design”) which are based on existing membrane theory formulae, the other methodologies being numerical analysis which are computational.

The following types of shell analysis are defined in *EN 1993-1-6*:

Type of analysis	Shell Theory	Material Law	Shell Geometry
Membrane theory of shells	membrane equilibrium	not applicable	perfect
Linear elastic shell analysis (LA)	linear buckling and stretching	linear	perfect
Linear elastic bifurcation analysis (LBA)	linear bending and stretching	linear	perfect
Geometrically non-linear elastic analysis (GNA)	non-linear	linear	perfect
Materially non-linear analysis (MNA)	linear	non-linear	perfect
Geometrically and materially non-linear analysis (GMNA)	non-linear	non-linear	perfect
Geometrically non-linear elastic analysis with imperfections (GNIA)	non-linear	linear	imperfect
Geometrically and materially non-linear analysis with imperfections (GMNIA)	non-linear	non-linear	imperfect

Figure 1.12: Types of shell analysis

The Annexes of *Part 1-6: Shells* contain much information relating to hand calculations of shell structures which are broken down as follows:

- Annex A - Membrane theory stresses in shells
- Annex B - Additional expressions for plastic collapse resistances
- Annex C - Expressions for linear elastic membrane and bending stresses
- Annex D - Expressions for buckling design

The most relevant to this study being Annex D which contains semi empirical formulae for determining the buckling strength of cylindrical shells for various load cases such as; axial compression, external pressure, shear and combinations of pressurised and axial compression and a transformation of wind loading to an external pressure distribution. This method of determining the buckling resistance is essentially the traditional method and is known as design by means of buckling stresses in the Eurocode. The semi-empirical element of this method is that it is a lower bound approach, that is that is that the yield stress is knocked down by under predicting the strength by a specific percentile calibrated from test specimens which were examined under the same phenomena. There are two other approaches approved by the Eurocode, both of which are computational and are defined as:

- Design by means of a global numerical GMNIA analysis

- Design by means of a global numerical MNA/LBA analysis

1.5.2 EN 1993-4-1: Silos

This standard is concerned with the resistance and stability of silo structures and is broken down into the design of many aspects of silo structures; from rectangular silos, to cylindrical silos, conical hoppers, and roof structures. *EN 1993-4-1* covers limit state design where the ultimate limit state is defined that the design resistance of the structure must be greater than the design loads.

$$S_d < R_d$$

Where S and R represent any appropriate limit state action and resistance respectively.

Though *Part 4-1: Silos* states that the modelling of the structural shell should follow the requirements of *Part 1-6: Shells* and that the method of analysis should also be carried out according to the requirements of *EN 1993-1-6* it was deemed appropriate to study the document related to silos in order to compare the approaches for the design of cylinders. *Part 4-1: Silos* includes a different analytical method to determine the axial buckling stress (*Eurocode 3 - Design of steel structures - Part 4-1: Silos*; 2007, p. 53-54) and external buckling stress (*Eurocode 3 - Design of steel structures - Part 4-1: Silos*; 2007, p. 56-57) for stiffened orthotropic cylindrical walls compared to that of Annex D of *Part 1-6: Shells*. This orthotropic method takes into account the contributions of the stiffeners making it more comparable to the method used in the *American Bureau of Shipping - Guide for buckling and ultimate strength assessment for offshore structures*. As a study, this method has been adjusted so that it can model stiffened isotropic cylindrical walls (see Weingarten et al. (1968) and Baruch and Singer (1963)).

1.6 American Bureau of Shipping

The American Bureau for Shipping is an offshore and marine classification society which establishes rules and standards for the design and construction of offshore structures and marine vessels. The *American Bureau of Shipping - Guide for buckling and ultimate strength assessment for offshore structures* (2004) (ABS) approaches the design of shell structures in a similar, though not identical, manner as the Eurocode buckling stresses method.

Whereas the Eurocode has a lower bound approach to strength assessment there is another method of strength formulation which can be used known as the mean value formulation. This approach predicts the strength as the mean value based on all test specimens and is implemented in some, though not all, of the buckling stress predictions of certain buckling modes in the ABS guide.

Taking for instance the bay buckling strength assessment for an unstiffened or ring stiffened cylinder. This buckling strength is determined by a lower bound approach similar to that adopted in the Eurocode. Whereby the elastic compressive buckling stress for an imperfect cylindrical shell is given by:

$$\sigma_{ExR} = \rho_{xR} C \sigma_{CExR}$$

where:

ρ_{xR} is the lower-bound knock down factor to account for shape imperfections,

C is a length dependent coefficient and;

σ_{CExR} is the classical buckling stress.

Differences in the strength predictions occur, however, for curved panels. In this instance the elastic buckling stress for an imperfect curved panel between adjacent stringer stiffeners is given as:

$$\sigma_{ExP} = B_{xP} \rho_{xP} C \sigma_{CExP}$$

where:

ρ_{xP} is once again a lower bound knock down factor and;

B_{xP} is another factor to compensate for the lower bound nature of ρ_{xP} .

Though not explicitly stated in the ABS guide, it can be read in *“Buckling and ultimate strength criteria of stiffened shells under combined loading for reliability analysis”* Das et al. (2003), upon which the ABS guide is based that B is a mean bias factor which would increase the buckling stress from a lower-bound prediction, to a less conservative mean value based prediction. Apart from this difference the strength prediction is similar to the Eurocode where as in this instance the classical buckling stress of a curved panel is based on the theory used in the shell panel example given in the introduction (Subsection: 1.4.2).

The ABS method for determining the buckling stress for ring and stringer stiffened shells is also semi-empirical and is quite different from the Eurocode approach. The elastic compressive buckling stress of an imperfect stringer-stiffened shell is given as:

$$\sigma_{ExB} = \sigma_s + \sigma_c$$

where:

σ_s is the elastic buckling stress of a stringer stiffened shell

$$\sigma_s = \rho_{xB} \frac{0.605E(t/r)}{1 + (A_s/st)}$$

E is the modulus of elasticity

A_s is the cross sectional area of the stringer stiffener

s is the distance between stringer stiffeners

Which is the classical buckling stress of a column reduced by a constant imperfection factor of $\rho_{xB} = 0.75$ and further reduced by a parameter dependent on the area and the spacing of the stringer stiffeners.

σ_c is the elastic buckling stress of a column

$$\sigma_c = \frac{\pi^2 EI_{se}}{l^2(A_s + s_e t)}$$

I_{se} is the moment of inertia of stringer stiffener plus associated effective shell plate width

s_e is the reduced effective width of shell

l is the length of the shell segment

Which is the classical Euler buckling stress formula for a column, but incorporating the associated shell width of the cylinder.

Similarly the critical buckling stress for a ring and stringer stiffened cylinder is also determined semi-empirically incorporating the properties of the stiffeners into derivation.

These are some examples of differences between the ABS code and the Eurocode, the differences between the methods shown in greater detail in the Methodology section (Chapter: 4).

2 PROBLEM DEFINITION

One of the major problems with constructing such structures is that there are few guidelines for the design of geometrically complex shell structures or for structures with curved steel panels in the field of civil engineering. The purpose of this thesis is to explore another disciplines of design, maritime engineering, and to see if the codes or design guidelines from this field could be adapted to be used for civil engineering structures.



Figure 2.1: Yas hotel link bridge stiffeners

The Yas hotel was mentioned earlier as an example of a steel shell structure. Though not a ‘pure’ shell, this structure exhibits shell behaviour. Some of the structural engineers that were involved in the design of the Yas hotel bridge were contacted and they mentioned several topics that could have influenced the design but which there was insufficient information to be found on¹. These topics were:

- Design of stiffening beams and incorporating effective widths of shell segments

¹Stated in an e-mail conversation with a structural engineer that worked on the Yas Marina Bridge project, Abu Dhabi whose name has purposefully not be printed to maintain confidentiality

- The effect of curvature on the buckling of the steel panels
- Modelling of minor stiffeners
- Stiffener orientation (orthogonal, radial, stress flow driven)

It was decided that the most interesting topic to investigate would be methods to determine the buckling resistance of steel shell structures and to investigate the approaches these methods take in accounting for the stiffeners in these shell structures. By researching these topics perhaps some useful conclusions could be drawn that will aid designers in having a greater understanding of the behaviour of steel shell structures, and could lead to a more accurate reflection of the behaviour of these stiffened structures which could lead to better, safer and more economically designed buildings.

It was decided that the *American Bureau of Shipping - Guide for buckling and ultimate strength assessment for offshore structures* (2004) would be an appropriate code to compare with the Eurocode. The ABS code was developed by a classification society with a long history in the development of standards for the design and construction of large steel structures. Their work involves the standardisation of marine vessels and offshore structures the likes of which companies such as *centraalstaal* design and build. As *centraalstaal* are now working to design and build geometrically complex steel shell structures it was regarded as befitting that a set of standards that the company would be familiar with be studied.

2.1 Objective

- The objective of this Master's thesis is to investigate and compare the Eurocode and the American Bureau of Shipping methods of analytically determining the buckling resistance of steel shell cylindrical structures.
- Following this a comparison of the numerical methods of determining buckling resistance of shell structures is to be made with particular focus on the two Eurocode methods specified in EN 1993-1-6: Strength and stability of shell structures
- Upon comparison, to make recommendations as to how these methods may be adapted or adopted to approach the design of more geometrically complex steel structures.

3 THEORETICAL BACKGROUND

3.1 Axial Buckling of Cylindrical Shells

The theoretical buckling stresses of cylindrical shells are misleading as they may substantially overestimate the actual carrying resistance of the shell. This will be illustrated through the derivation of the theoretical buckling stress of an elastic, thin cylinder of medium length. Assuming that the buckled shape will give radial displacements according to the expression:

$$w = -A \sin \frac{m\pi x}{l} \quad (3.1)$$

This assumption is important as we can already predict the shape at which we expect the cylinder to buckle across length, l , according to each mode, m .

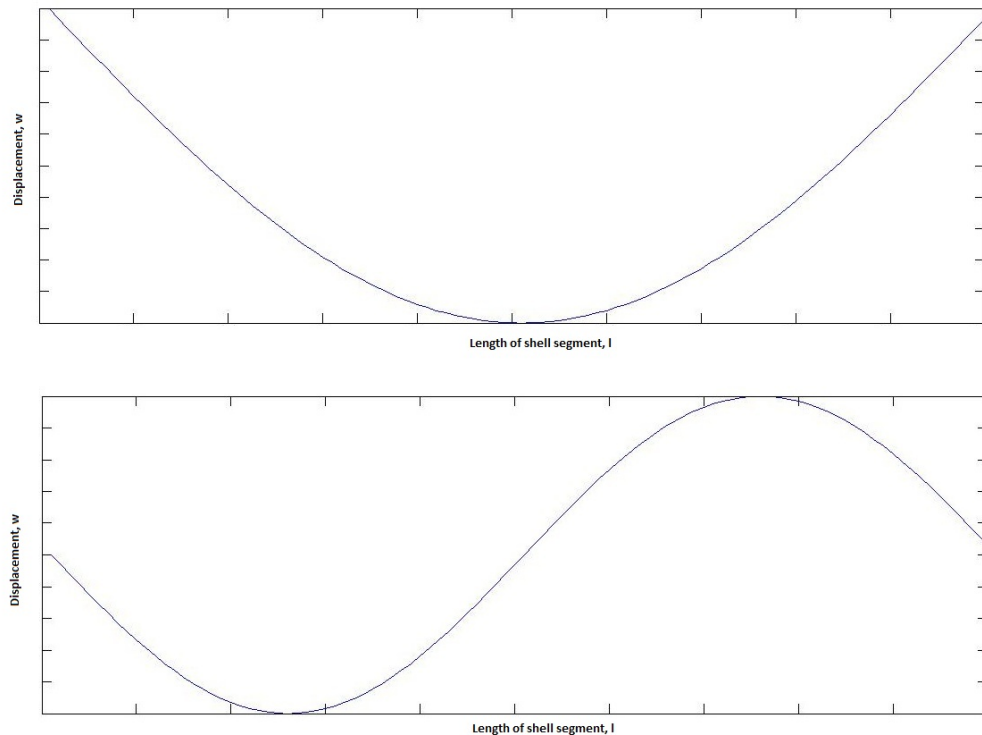


Figure 3.1: First and second modal shapes

The strain in the axial direction, ϵ_1 and the strain in the circumferential direction, ϵ_2 can be obtained by applying the condition that the axial compressive force during buckling, N_{cr} , remains constant.

The axial strain before buckling is given by the following expression:

$$\epsilon_0 = -\frac{N_{cr}}{Et} \quad (3.2)$$

Applying the above constant compressive force condition:

$$\epsilon_1 + \nu\epsilon_2 = (1 - \nu^2)\epsilon_0 \quad (3.3)$$

It can be observed that the strain in the circumferential direction is:

$$\epsilon_2 = -\nu\epsilon_0 - \frac{w}{r} \quad (3.4)$$

Substituting in the assumed radial displacement:

$$\epsilon_2 = -\nu\epsilon_0 + \frac{A}{r} \sin \frac{m\pi x}{l} \quad (3.5)$$

We also find that:

$$\epsilon_1 = \epsilon_0 - \nu \frac{A}{r} \sin \frac{m\pi x}{l} \quad (3.6)$$

The change of curvature in the axial plane is given as:

$$\chi_x = \frac{\partial^2 w}{\partial x^2} = A \frac{m^2 \pi^2}{l^2} \sin \frac{m\pi x}{l} \quad (3.7)$$

Using the energy method (Equation: 3.8) the obtained solutions for ϵ_1 , ϵ_2 and χ_x are substituted into the equations for the strain energy of a deformed shell due to bending:

$$U_1 = \frac{1}{2} D \int \int [(\chi_x + \chi_y)^2 - 2(1 - \nu)(\chi_x \chi_y - \chi_{xy}^2)] dA \quad (3.8)$$

and the strain energy of a deformed shell due to stretching of the middle surface:

$$U_2 = \frac{Et}{2(1 - \nu^2)} \int \int [(\epsilon_1 + \epsilon_2)^2 - 2(1 - \nu)(\epsilon_1 \epsilon_2 - \frac{1}{4}\gamma^4)] dA \quad (3.9)$$

Where D is the flexural rigidity given by:

$$D = \frac{Et}{12(1 - \nu^2)} \quad (3.10)$$

We find that the increase of the strain energy during buckling is given by the equation:

$$\Delta U = -2\pi t E \nu \epsilon_0 \int_0^l A \sin \frac{m\pi x}{l} dx + \frac{\pi A^2 E t l}{2r} + A^2 \frac{\pi^4 m^4}{2l^4} \pi r l D \quad (3.11)$$

And the work done by compressive forces during buckling is:

$$\Delta T = 2\pi N_{cr} \left(\nu \int_0^l A \sin \frac{m\pi x}{l} dx + \frac{r}{4} A^2 \frac{m^2 \pi^2}{l} \right) \quad (3.12)$$

Where:

$$\nu \int_0^l A \sin \frac{m\pi x}{l} dx \quad \text{is due to the change of } \epsilon_1 - \epsilon_0 \text{ of the axial strain and;}$$

$$\frac{r}{4} A^2 \frac{m^2 \pi^2}{l} \quad \text{is due to the bending of the generators given by the assumed radial displacement, } w.$$

Equating the work done by the compressive forces during buckling with the increase of strain energy during buckling gives us:

$$\sigma_{cr} = \frac{N_{cr}}{t} = D \left(\frac{m^2 \pi^2}{t l^2} + \frac{E}{r^2 D} \frac{l^2}{m^2 \pi^2} \right) \quad (3.13)$$

And assuming that there are many waves formed along the length of the cylinder during buckling and considering σ_{cr} as a continuous function of m/l , we find that the minimum value of the critical buckling stress is:

$$\sigma_{cr} = \frac{2}{rt} \sqrt{EDt} = \frac{Et}{r \sqrt{3(1 - \nu^2)}} \quad (3.14)$$

And substituting in the Poisson's ratio for steel, $\nu = 0.3$ the theoretical critical buckling

stress for perfect elastic steel cylinders may be given as:

$$\sigma_{cr} = 0.605 \frac{Et}{r} \quad (3.15)$$

Which occurs at:

$$\frac{m\pi}{l} = \sqrt[4]{\frac{Et}{r^4 D}} \quad (3.16)$$

So, the length of the half-waves into which the shell buckles (in it's first mode, m=1) can be given as:

$$\frac{l}{m} = \pi \sqrt[4]{\frac{r^2 D}{Et}} = \pi \sqrt[4]{\frac{r^2 t^2}{12(1-\nu^2)}} \approx 1.72\sqrt{rt} \quad (3.17)$$

The theoretical basis of this approach is that at loads lower than the elastic critical load, the gain of strain energy in the elements is less than the potential energy of the loads. A condition of instability is defined, as the stage when the change of the above two energies is zero, that is, the stiffness of the structure is zero. Then the structure will not resist any random disturbance. (Mahfouz; 1999)

Readers requiring a more detailed coverage of shell buckling are advised to consult “*Theory of elastic stability*” (Timoshenko and Gere; 1961)

This theoretical buckling stress for elastic thin shells is used both in the Eurocode and the ABS guide to buckling for offshore structures.

In the ABS code it is denoted as the classical compressive buckling stress for a perfect cylindrical shell:

$$\sigma_{CExR} = 0.605 \frac{Et}{r}$$

Whereas in the Eurocode this stress is denoted as the critical buckling stress of the isotropic wall or the meridional critical buckling stress resistance:

$$\sigma_{x,Rcr} = \frac{E}{\sqrt{3(1-\nu^2)}} \frac{t}{r} = 0.605 \frac{Et}{r}$$

3.2 External Pressure Buckling of Cylindrical Shells

The theory used to determine the external buckling pressure of cylindrical shells differs slightly between the two design codes examined. The Eurocode is based on a simplification of the method described in “*Theory of elastic stability*” (Timoshenko and Gere; 1961, p.474)

where the three simultaneous partial differential equations representing the relationships between the displacement in the axial, circumferential and radial directions were simplified by neglecting higher-order terms (Donnell; 1933). This simplification was adopted by Batdorf (Batdorf; 1947) and the Eurocode equation for the critical circumferential buckling stress was obtained from this (Rotter; 2008, p.176), but with some changes to the coefficients relating to the boundary conditions and geometry of the cylinder (which will be explained in further detail in Chapter 5).

Though the references for the theory on the calculation of the circumferential buckling stresses are not explicitly stated in the *ABS buckling guide* it is assumed that they were also at some stage derived from the method derived by Batdorf (Batdorf; 1947) as the “Batdorf parameter” is used. There are, however, some differences between the ABS method and the Eurocode method relating to the parameters accounting for geometrical properties and boundary conditions. *American Bureau of Shipping - Commentary on the guide for buckling and ultimate Strength assessment for offshore structures* (2005) states that much of the *ABS buckling guide* recommendations are based on experimental data of past and current offshore-related research and references a report on such experimental data (Das et al.; 2003).

3.3 Imperfections

It has already been stated that the bifurcation process is purely mathematical and the end result is the theoretical upper limit for the strength of a structure. However, when geometrical imperfections, material non-linearity, residual stresses etc. are taken into account the critical buckling load may be significantly lower than the theoretical load anticipates; the primary source of these discrepancies being shape imperfections. It is not correct to assume that all shells are highly sensitive to imperfections. The sensitivity depends on the type of shell and the type of loading. For instance, a cylindrical shell is highly imperfection sensitive to a wide range of imperfection forms when compressed in the meridional direction, however their imperfection sensitivity is quite low under uniform external pressure for example. This sensitivity is of course dependent on the type of imperfection and it should be noted that cylindrical shells are extremely sensitive to axisymmetric geometric imperfections (Forasassi and Frano; 2006). For eigenmode pre-deformed shells it can even be the case that the buckling stress of a cylindrical shell under uniform external pressure can be

higher than that of a perfect cylindrical shell under uniform external pressure Schneider and Brede (2005).



Figure 3.2: A geometric imperfection illustrated as a crease in a cylinder

This difference relates to the buckling modes, under axial loading the buckling modes are characterised by waves which, compared to the diameter are short in both the longitudinal and circumferential direction. Small imperfections on the surface of the shell are likely to have the same characteristic shape as some of the critical buckles and will tend to deepen under increasing load and trigger “snap-through” buckling at an earlier loading stage. The buckling pattern under external pressure consists of buckles which are longer in the meridional direction and less numerous in the hoop direction, therefore these buckles are probably considerably larger than the initial imperfections (Faculty of Civil and Geodetic Engineering, University of Ljubljana; n.d.).

Sensitivity to geometric imperfections is dependant on both the form and the amplitude of the imperfection, it can be the case that imperfections strengthen the structure, in fact, large amplitude imperfections may raise the strength of the structure above what is associated with smaller amplitudes and unfortunately the form of geometric imperfection that is most critical in determining the strength of a structure cannot be easily defined (Rotter; 2008).

3.4 Finite Elements

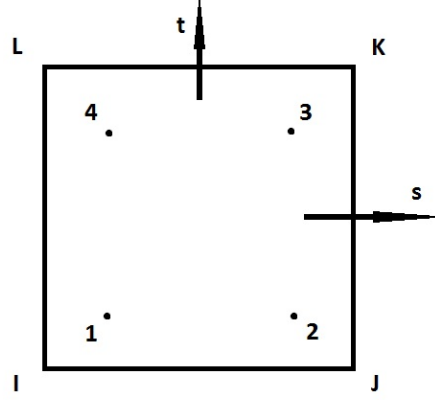


Figure 3.3: 4-noded quadrilateral shell element

The main finite elements types used were 4-noded shell elements (Figure: 3.3) which can account for both membrane and bending forces. Each of the four nodes has six degrees of freedom (three translational, three rotational) with the following translational and rotational polynomials (see Figure: 3.4):

$$u = \frac{1}{4}(u_I(1-s)(1-t) + u_j(1+s)(1-t) + u_k(1+s)(1+t) + u_L(1-s)(1+t)) \quad (3.18)$$

$$v = \frac{1}{4}(v_I(1-s)(1-t) + v_j(1+s)(1-t) + v_k(1+s)(1+t) + v_L(1-s)(1+t)) \quad (3.19)$$

$$w = \frac{1}{4}(w_I(1-s)(1-t) + w_j(1+s)(1-t) + w_k(1+s)(1+t) + w_L(1-s)(1+t)) \quad (3.20)$$

$$\theta_x = \frac{1}{4}(\theta_x(1-s)(1-t) + \theta_x(1+s)(1-t) + \theta_x(1+s)(1+t) + \theta_x(1-s)(1+t)) \quad (3.21)$$

$$\theta_y = \frac{1}{4}(\theta_y(1-s)(1-t) + \theta_y(1+s)(1-t) + \theta_y(1+s)(1+t) + \theta_y(1-s)(1+t)) \quad (3.22)$$

$$\theta_z = \frac{1}{4}(\theta_z(1-s)(1-t) + \theta_z(1+s)(1-t) + \theta_z(1+s)(1+t) + \theta_z(1-s)(1+t)) \quad (3.23)$$

The number of integration points through the thickness of this element can be chosen as 1, 3, 5, 7 or 9. The default option is three integration points (top, middle and bottom) however when plasticity is present the minimum number of integration points is five. Full integration was used as opposed to reduced integration, which is not recommended, according to:

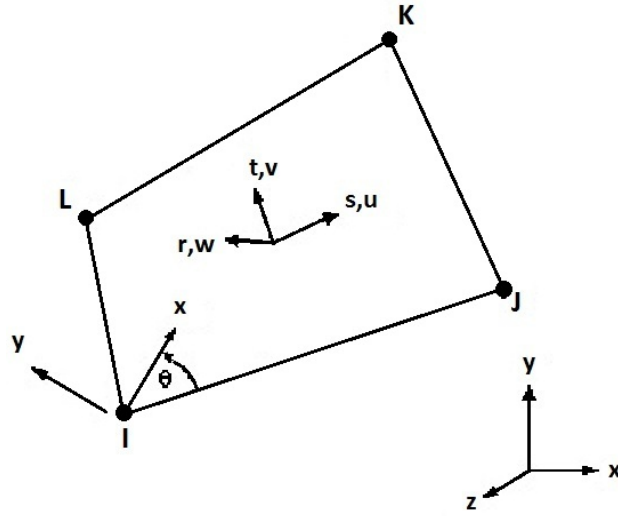


Figure 3.4: 4 node shell

$$\int_{-1}^1 \int_{-1}^1 f(x, y) dx dy = \sum_{j=1}^m \sum_{i=1}^l H_j H_i f(x_i, y_j) \quad (3.24)$$

Where:

- $f(x, y)$ is the function to be integrated,
- H_i and H_j are weighting factors,
- x_i and y_j are the locations to evaluate the function and;
- l and m are the number of integration points.

The basic functions for the transverse shear strain have been changed to avoid shear locking by use of the Mixed Interpolation of Tensorial Components (MITC) method (For further reading consult Dvorkin (1984), Dvorkin and Bathe (1984) and Bathe and Dvorkin (1986)). “The basic idea of the MITC technique is to interpolate displacements and strains separately and “connect” these interpolations at “tying points” (Lee and Bathe; 2004).

Other Finite Elements may be found in Appendix D

4 METHODOLOGY

4.1 Eurocode: EN 1993-1-6

The following equations from *Eurocode 3 - Design of steel structures - Part 1-6: Strength and stability of shell structures* (2007) were used in the design code comparison and have been transcribed here for easy reference.

The length of the shell segment is characterised in terms of the dimensionless length parameter ω ;

$$\omega = \frac{l}{r} \sqrt{\frac{r}{t}} = \frac{l}{\sqrt{rt}} \quad (4.1)$$

The boundary conditions are defined in the Eurocode in Figure 4.1.

Boundary condition code	Simple term	Description	Normal displacements	Vertical displacements	Meridional rotation
BC1r	Clamped	radially restrained meridionally restrained rotation restrained	$w = 0$	$u = 0$	$\beta_\phi = 0$
BC1f		radially restrained meridionally restrained rotation free	$w = 0$	$u = 0$	$\beta_\phi \neq 0$
BC2r		radially restrained meridionally free rotation restrained	$w = 0$	$u \neq 0$	$\beta_\phi = 0$
BC2f	Pinned	radially restrained meridionally free rotation free	$w = 0$	$u \neq 0$	$\beta_\phi \neq 0$
BC3	Free edge	radially free meridionally free rotation free	$w \neq 0$	$u \neq 0$	$\beta_\phi \neq 0$

Figure 4.1: Eurocode defined boundary conditions

4.1.1 Meridional Buckling

The critical meridional buckling stress, using a value of C_x should be obtained from:

$$\sigma_{xRc} = 0.605EC_x \frac{t}{r} \quad (4.2)$$

For short cylinders with:

$$\omega \leq 1.7$$

$$C_x = 1.36 - \frac{1.83}{\omega} + \frac{2.07}{\omega^2} \quad (4.3)$$

For medium cylinders with:

$$1.7 \leq \omega \leq 0.5 \frac{r}{t}$$

$$C_x = 1 \quad (4.4)$$

For long cylinders with:

$$0.5 \frac{r}{t} < \omega$$

$$C_x = 1 + \frac{0.2}{C_{xb}} \left[1 - 2\omega \frac{t}{r} \right] \quad (4.5)$$

but $C_x \geq 0.6$

Table 4.1: Parameter C_{xb} for the effect of boundary conditions on the critical meridional buckling stress in long cylinders

Case	Cylinder end	Boundary condition	C_{xb}
1	end 1 end 2	BC 1 BC 1	6
2	end 1 end 2	BC 1 BC 2	3
3	end 1 end 2	BC 2 BC 2	1

The meridional elastic imperfection factor should be obtained from:

$$\alpha_x = \frac{0.62}{1 + 1.91(\Delta w_k/t)^{1.44}} \quad (4.6)$$

where Δw_k is the characteristic imperfection amplitude

$$\Delta w_k = \frac{1}{Q} \sqrt{\frac{r}{t}} t \quad (4.7)$$

Where Q is the meridional compression fabrication quality parameter.

Table 4.2: Values of fabrication quality parameter Q

Fabrication Quality Class	Description	Q
Class A	Excellent	40
Class B	High	25
Class C	Normal	16

The meridional squash limit slenderness $\bar{\lambda}_{x0}$, the plastic range factor β , and the interaction exponent η should be taken as:

$$\bar{\lambda}_{x0} = 0.2 \quad \beta = 0.6 \quad \eta = 1.0$$

Cylinders need not be checked against meridional shell buckling if they satisfy:

$$\frac{r}{t} \leq 0.04 \frac{E}{f_{y,k}}$$

4.1.2 Circumferential Buckling

For short cylinders with:

$$\frac{\omega}{C_\theta} < 20$$

the critical circumferential buckling stress should be obtained from:

$$\sigma_{\theta Rc} = 0.92E \frac{C_{\theta s} t}{\omega r} \quad (4.8)$$

For medium-length cylinders with:

$$20 \leq \frac{\omega}{C_\theta} \leq 1.63 \frac{r}{t}$$

the critical circumferential buckling stress should be obtained from:

$$\sigma_{\theta Rc} = 0.92E \frac{C_\theta t}{\omega r} \quad (4.9)$$

For long cylinders with:

$$\frac{\omega}{C_\theta} > 1.63 \frac{r}{t}$$

the critical circumferential buckling stress should be obtained from:

$$\sigma_{\theta Rc} = E \left(\frac{t}{r}\right)^2 [0.275 + 2.03 \left(\frac{C_\theta r}{\omega t}\right)^4] \quad (4.10)$$

The meridional squash limit slenderness $\bar{\lambda}_{\theta 0}$, the plastic range factor β , and the interaction exponent η should be taken as:

$$\bar{\lambda}_{\theta 0} = 0.4 \quad \beta = 0.6 \quad \eta = 1.0$$

Cylinders need not be checked against circumferential shell buckling if they satisfy:

$$\frac{r}{t} \leq 0.21 \sqrt{\frac{E}{f_{y,k}}}$$

Table 4.3: Values of α_θ based on fabrication quality

Fabrication quality class	Description	α_θ
Class A	Excellent	0.75
Class B	High	0.65
Class C	Normal	0.50

4.1.3 Stress Design Method

The buckling resistance should be represented by the buckling stresses as defined in 1.4.5.

The design buckling stresses should be obtained from:

$$\sigma_{x,Rd} = \sigma_{x,Rk} / \gamma_M \quad (4.11)$$

$$\sigma_{\theta,Rd} = \sigma_{\theta,Rk} / \gamma_M \quad (4.12)$$

The characteristic buckling strengths should be obtained by multiplying the characteristic yield strength by the reduction factors:

$$\sigma_{x,Rk} = \chi_x f_{y,k} \quad (4.13)$$

Table 4.4: External pressure buckling factors for medium-length cylinders C_θ

Case	Cylinder end	Boundary condition	Value of C_θ
1	end 1	BC 1	1.5
	end 2	BC 1	
2	end 1	BC 1	1.25
	end 2	BC 2	
3	end 1	BC 2	1
	end 2	BC 2	
4	end 1	BC 1	0.6
	end 2	BC 3	
5	end 1	BC 2	0
	end 2	BC 3	
6	end 1	BC 3	0
	end 2	BC 3	

Table 4.5: External pressure buckling factors for short cylinders C_{θ_s}

Case	Cylinder end	Boundary condition	C_{θ_s}
1	end 1	BC 1	$1.5 + \frac{10}{\omega^2} - \frac{5}{\omega^3}$
	end 2	BC 1	
2	end 1	BC 1	$1.25 + \frac{8}{\omega^2} - \frac{4}{\omega^3}$
	end 2	BC 2	
3	end 1	BC 2	$1.0 + \frac{3}{\omega^3}$
	end 2	BC 2	
4	end 1	BC 1	$0.6 + \frac{1}{\omega^2} - \frac{0.3}{\omega^3}$
	end 2	BC 3	

$$\sigma_{\theta,Rk} = \chi_{\theta} f_{y,k} \quad (4.14)$$

The reduction factors χ_x and χ_{θ} should be determined as a function of the relative slenderness of the shell $\bar{\lambda}$ from:

$$\begin{aligned} \chi &= 1 && \text{when } \bar{\lambda} \leq \bar{\lambda}_0 \\ \chi &= 1 - \beta \left(\frac{\bar{\lambda} - \bar{\lambda}_0}{\bar{\lambda}_p - \bar{\lambda}_0} \right)^{\eta} && \text{when } \bar{\lambda}_0 \leq \bar{\lambda} \leq \bar{\lambda}_p \\ \chi &= \frac{\alpha}{\bar{\lambda}^2} && \text{when } \bar{\lambda} \geq \bar{\lambda}_p \end{aligned}$$

where:

$$\bar{\lambda}_p = \sqrt{\frac{\alpha}{1 - \beta}}$$

$$\bar{\lambda}_x = \sqrt{f_{y,k} / \sigma_{xRc}}$$

$$\bar{\lambda}_{\theta} = \sqrt{f_{y,k} / \sigma_{\theta Rc}}$$

4.2 Eurocode: EN 1993-4-1

The following equations from *Eurocode 3 - Design of steel structures - Part 4-1: Silos* (2007) were used in the design code comparison and have been transcribed here for easy reference.

Eurocode EN 1993-4-1 states that the buckling resistance for isotropic walls should use the method described above. For determining the buckling resistance of isotropic walls with vertical stiffeners (and the spacing of the stringer stiffeners is less than $2\sqrt{rt}$ which is the case for the stringer stiffened cylinders studied) the designer is given the option to design the shell wall in the same manner as an unstiffened wall, or by the global analysis procedure in EN 1993-1-6.

There is, however, another design approach for stiffened corrugated shells which are treated as stiffened orthotropic shells. This method is of interest as it incorporates the properties of the stiffening members, making it comparable to the ABS design method. However, as this method is for orthotropic shells with stiffening members the equations had to be

altered to make it applicable for isotropic walls with vertical stiffeners. This was performed by changing the equations to match those given in Weingarten et al. (1968, p.25). The Eurocode does not state that this method in determining the buckling stresses is allowed but it was deemed interesting to examine. In order for this to be done the flexural stiffness must be changed from:

$$D_{\phi} = \frac{Et^3}{12(1-\nu^2)} \frac{1}{\left(1 + \frac{\pi^2 d^2}{4l^2}\right)}$$

$$D_{\theta} = 0.13Et d^2$$

$$D_{\phi\theta} = \frac{Gt^3}{12} \left(1 + \frac{\pi^2 d^2}{4l^2}\right)$$

to flexural stiffness's for isotropic cylinders:

$$D_{\phi} = \frac{Et^3}{12(1-\nu^2)}$$

$$D_{\theta} = \frac{Et^3}{12(1-\nu^2)}$$

$$D_{\phi\theta} = 2D_{\phi}$$

The critical buckling stress resultant $n_{x,Rcr}$ per unit circumference of the orthotropic shell should be evaluated at each appropriate level in the silo by minimising the following expression with respect to the critical circumferential wave number j and the buckling height l_i :

$$n_{x,Rcr} = \frac{1}{j^2 \omega^2} \left(A_1 + \frac{A_2}{A_3} \right) \quad (4.15)$$

The critical buckling stress for uniform external pressure $p_{n,Rcru}$ should be evaluated by minimising the following expression with respect to the critical circumferential wave number, j :

$$p_{n,Rcru} = \frac{1}{r j^2} \left(A_1 + \frac{A_2}{A_3} \right) \quad (4.16)$$

with:

$$A_1 = j^4 [\omega^4 C_{44} + 2\omega^2 (C_{45} + C_{66}) + C_{55}] + C_{22} + 2j^2 C_{25} \quad (4.17)$$

$$A_2 = 2\omega^2(C_{12} + C_{33})(C_{22} + j^2C_{25})(C_{12} + j^2\omega^2C_{14}) - (\omega^2C_{11} + C_{33})(C_{22} + j^2C_{25})^2 \quad (4.18)$$

$$- \omega^2(C_{22} + \omega^2C_{33})(C_{12} + j^2\omega^2C_{14})^2$$

$$A_3 = (\omega^2C_{11} + C_{33})(C_{22} + C_{25} + \omega^2C_{33}) - \omega^2(C_{12} + C_{33})^2 \quad (4.19)$$

with:

$$C_{11} = C_\phi + EA_s/d_s \quad (4.20)$$

$$C_{12} = \nu\sqrt{C_\phi C_\theta} \quad (4.21)$$

$$C_{14} = e_s EA_s/(rd_s) \quad (4.22)$$

$$C_{22} = C_\theta + EA_r/d_r \quad (4.23)$$

$$C_{25} = e_r EA_r/(rd_r) \quad (4.24)$$

$$C_{33} = C_{\phi\theta} \quad (4.25)$$

$$C_{44} = [D_\phi + EI_s/d_s + EA_s e_s^2/d_s]/r^2 \quad (4.26)$$

$$C_{45} = \nu\sqrt{D_\phi D_\theta}/r^2 \quad (4.27)$$

$$C_{55} = [D_\theta + EI_r/d_r + EA_r e_r^2/d_r]/r^2 \quad (4.28)$$

$$C_{66} = [D_{\phi\theta} + 0.5(GI_{ts}/d_s + GI_{tr}/d_r)]/r^2 \quad (4.29)$$

$$\omega = \frac{\pi r}{jl_i} \quad (4.30)$$

where:

l_i is the half wavelength of the potential buckle in the vertical direction

A_s is the cross-sectional area of a stringer stiffener

I_s is the second moment of area of a stringer stiffener about the circumferential axis (vertical bending)

d_s is the separation between stringer stiffeners

I_{ts} is the uniform torsion constant of a stringer stiffener

e_s is the outward eccentricity from the shell middle surface of a stringer stiffener

A_r is the cross-sectional area of a ring stiffener

- I_r is the second moment of area of a ring stiffener about the vertical axis (circumferential bending)
- d_r is the separation between ring stiffeners
- I_{tr} is the uniform torsion constant of a ring stiffener
- e_r is the outward eccentricity from the shell middle surface of a ring stiffener
- C_ϕ is the sheeting stretching stiffness in the axial direction
- C_θ is the sheeting stretching stiffness in the circumferential direction
- $C_{\phi\theta}$ is the sheeting stretching stiffness in membrane shear
- D_ϕ is the sheeting flexural rigidity in the axial direction
- D_θ is the sheeting flexural rigidity in the circumferential direction
- $D_{\phi\theta}$ is the sheeting twisting flexural rigidity in twisting
- r is the radius of the silo.

The characteristic buckling stress may be determined from this critical buckling stress resultant from:

$$n_{x,Rk} = \chi_{glob} t_m f_{y,k}$$

where:

$$\begin{aligned} \chi_{glob} &= \sqrt{\frac{t_m f_{y,k}}{n_{x,Rcr}}} \\ t_m &= \text{“smeared” wall thickness} \\ &= t + A_s/b \end{aligned}$$

This method has been verified by comparing the value of ω from EN 1993-4-1 (Equation: 4.30) with that of the Eurocode method in Annex D of EN 1993-1-6 (Equation: 4.1). If these values match it is noted in the results table with a ‘Yes’. It should be noted that the method adopted for this study is a very simplified approach to this theory, a more detailed method based on this theory may be found in *“Buckling of axially compressed cylinders”* (Miller; 1977,).

4.3 ABS

The following equations from *American Bureau of Shipping - Guide for buckling and ultimate strength assessment for offshore structures* (2004) were used in the design code comparison and have been transcribed here for easy reference.

4.3.1 Unstiffened or Ring-Stiffened Cylinders

4.3.1.1 Critical Buckling Stress for Axial Compression or Bending Moment

The critical buckling stress of unstiffened or ring-stiffened cylindrical shell subjected to axial compression or bending moment may be taken as:

$$\sigma_{CxR} = \begin{cases} \sigma_{ExR} & \sigma_{ExR} \leq P_r \sigma_0 \\ \sigma_0 [1 - P_r (1 - P_r) \frac{\sigma_0}{\sigma_{ExR}}] & \sigma_{ExR} > P_r \sigma_0 \end{cases}$$

where:

P_r = proportional linear elastic limit of the structure, which may be taken as 0.6 for steel

σ_{ExR} = elastic compressive buckling stress for an imperfect cylindrical shell

$$= \rho_{xR} C \sigma_{CExR}$$

σ_{CExR} = classical compressive buckling stress for a perfect cylindrical shell

$$= 0.605 \frac{Et}{r}$$

C = length dependant coefficient

$$= \begin{cases} 1.0 & z \geq 2.85 \\ 1.425/z + 0.175z & z < 2.85 \end{cases}$$

ρ_{xR} = nominal or lower bound knock-down factor to allow for shape imperfections

$$= \begin{cases} 0.75 + 0.003z(1 - \frac{r}{300t}) & z < 1 \\ 0.75 - 0.142(z - 1)^{0.4} + 0.003z(1 - \frac{r}{300t}) & 1 \leq z \leq 20 \\ 0.35 - 0.0002 \frac{r}{t} & z \geq 20 \end{cases}$$

z = Batdorf parameter

$$= \frac{l^2}{rt} \sqrt{1 - \nu^2}$$

l = length between adjacent ring stiffeners (unsupported)

r = mean radius of cylindrical shell

t	=	thickness of cylindrical shell
E	=	modulus of elasticity
ν	=	Poissons ratio, 0.3 for steel
σ_0	=	specified minimum yield point

4.3.1.2 Critical Buckling Stress for External Pressure

The critical buckling stress for an unstiffened or ring-stiffened cylindrical shell subjected to external pressure may be taken as:

$$\sigma_{C\theta R} = \Phi \sigma_{E\theta R}$$

where:

Φ	=	plasticity reduction factor
	=	1 for $\Delta \leq 0.55$
	=	$\frac{0.45}{\Delta} + 0.18$ for $0.55 < \Delta \leq 1.6$
	=	$\frac{1.31}{1 + 1.15\Delta}$ for $1.6 < \Delta < 6.25$
	=	$1/\Delta$ for $\Delta \geq 6.25$

$$\Delta = \frac{\sigma_{E\theta R}}{\sigma_0}$$

$$\begin{aligned} \sigma_{E\theta R} &= \text{elastic hoop buckling stress for an imperfect cylindrical shell} \\ &= \rho_{\theta R} \frac{q_{CE\theta R}(r+0.5t)}{t} K_{\theta} \end{aligned}$$

$$\begin{aligned} \rho_{\theta R} &= \text{nominal or lower bound knock-down factor to allow for shape imperfections} \\ &= 0.8 \end{aligned}$$

$$K_{\theta} = \text{coefficient to account for the effect of ring stiffener}$$

$$q_{CE\theta R} = \text{elastic buckling pressure}$$

$$= \begin{cases} \frac{1.27E}{A_L^{1.18} + 0.5} \frac{t^2}{r} & A_L \leq 2.5 \\ \frac{0.92E}{A_L} \frac{t^2}{r} & 2.5 < A_L \leq 0.208 \leq \frac{r}{t} \\ 0.836C_p^{-1.061} E \frac{t^3}{r} & 0.208 \frac{r}{t} < A_L \leq 0.285 \frac{r}{t} \\ 0.275E \frac{t^3}{r} & 0.285 \leq \frac{r}{t} < A_L \end{cases}$$

$$A_L = \frac{\sqrt{z}}{(1 - \nu^2)^{1/4}} - 1.17 + 1.068k$$

$$\begin{aligned} k &= 0 \text{ for lateral pressure} \\ &= 0.5 \text{ for hydrostatic pressure} \end{aligned}$$

where K_θ is defined as:

$$K_\theta = 1 - \frac{1 - k\nu}{1 + t(t_w + l\bar{\omega})/\bar{A}_R} G_\alpha$$

$$\bar{A}_R = A_R \left(\frac{r}{r_R}\right)^2$$

$$\bar{\omega} = \frac{\cosh 2\alpha - \cos 2\alpha}{\alpha(\sinh 2\alpha + \sin 2\alpha)}$$

$$\alpha = \frac{l}{1.56\sqrt{rt}}$$

$$G_\alpha = 2 \frac{\sinh \alpha \cos \alpha + \cosh \alpha \sin \alpha}{\sinh 2\alpha + \sin 2\alpha} \geq 0$$

$$\begin{aligned} k &= N_x/N_\theta \text{ for lateral pressure} \\ &= N_x/N_\theta + 0.5 \text{ for hydrostatic pressure} \\ A_R &= \text{cross sectional area of ring stiffener} \\ N_x &= \text{axial load per unit length} \end{aligned}$$

N_θ	=	circumferential load per unit length
r_R	=	radius to centroid of ring stiffener
t	=	thickness of cylindrical shell
t_w	=	stiffener web thickness
l	=	length between adjacent ring stiffeners (unsupported)

4.3.2 Ring and Stringer-stiffened Shells

4.3.2.1 Critical Buckling Stress for Axial Compression or Bending Moment

$$\sigma_{CxB} = \begin{cases} \sigma_{ExB} & \sigma_{ExB} \leq P_r \sigma_0 \\ \sigma_0 \left[1 - P_r (1 - P_r) \frac{\sigma_0}{\sigma_{ExB}} \right] & \sigma_{ExB} > P_r \sigma_0 \end{cases}$$

where:

P_r	=	proportional linear elastic limit of the structure, which may be taken as 0.6 for steel
σ_{ExB}	=	elastic compressive buckling stress for an imperfect cylindrical stringer stiffened shell
	=	$\sigma_c + \sigma_s$
σ_s	=	elastic compressive buckling stress of stringer-stiffened shell

$$= \rho_{xB} \frac{0.605E(t/r)}{1 + \frac{A_s}{st}}$$

ρ_{xB}	=	0.75
σ_c	=	elastic buckling stress of column

$$= \frac{\pi^2 E I_{se}}{l^2 (A_s + s_e t)}$$

I_{se}	=	moment of inertia of stringer stiffener plus associated effective shell plate width
----------	---	---

$$= I_s + A_s z_{st}^2 \frac{s_e t}{A_s + s_e t} + \frac{s_e t^3}{12}$$

I_s	=	moment of inertia of stringer stiffener about its own centroid axis
z_{st}	=	distance from centerline of shell to the centroid of stringer stiffener
A_s	=	cross sectional area of stringer stiffener
s_e	=	reduced effective width of shell
	=	$\frac{0.53}{\lambda_{xP}}s$ for $\lambda_{xP} > 0.53$
	=	s for $\lambda_{xP} \leq 0.53$
s	=	shell plate width between adjacent stringers
λ_{xP}	=	reduced shell slenderness ratio
	=	$\sqrt{\frac{\sigma_0}{\sigma_{Exp}}}$
σ_{Exp}	=	elastic compressive buckling stress for imperfect curved panel between adjacent stringer stiffeners

σ_{Exp} is defined in another section of the ABS code as:

$$\sigma_{Exp} = B_{xP} \rho_{xP} \sigma_{CEXP}$$

where:

σ_{CEXP}	=	classical buckling stress for a perfect curved panel between adjacent stringer stiffeners
	=	$K_{xP} \frac{\pi^2 E}{12(1-\nu^2)} \left(\frac{t}{s}\right)^2$
K_{xP}	=	$4 + \frac{3z_s^2}{\pi^4}$ for $z_s \leq 11.4$
	=	0.702 z_s for $z_s > 11.4$
ρ_{xP}	=	nominal or lower bound knock-down factor to allow for shape imperfections
	=	$1 - 0.019z_s^{1.25} + 0.002z_s \left(1 - \frac{r}{300t}\right)$ for $z_s \leq 11.4$

$$= 0.27 + \frac{1.5}{z_s} + \frac{27}{z_s^2} + 0.008\sqrt{z_s}\left(1 - \frac{r}{300t}\right) \quad \text{for } z_s > 11.4$$

$$\begin{aligned} B_{xP} &= \text{factor compensating for the lower bound nature of } \rho_{xP} \\ &= \begin{cases} 1.15 & \text{for } \lambda_n > 1 \\ 1 + 0.15\lambda_n & \text{for } \lambda_n \leq 1 \end{cases} \end{aligned}$$

$$\lambda_n = \sqrt{\frac{\sigma_0}{\rho_{xP}\sigma_{CExP}}}$$

$$z_s = \sqrt{1 - \nu^2} \frac{s^2}{rt}$$

s = spacing of stringer stiffeners

4.3.2.2 Critical Buckling Stress for External Pressure

The critical buckling stress for ring and stringer-stiffened cylindrical shells subjected to external pressure may be taken as:

$$\sigma_{C\theta B} = (\sigma_{C\theta R} + \sigma_{sp})K_p \leq \sigma_0$$

where:

$\sigma_{C\theta R}$ = critical hoop buckling stress for the unstiffened shell

σ_{sp} = collapse hoop stress for a stringer stiffener plus its associated shell plating

$$= \frac{q_s(r + 0.5t)}{t} K_\theta$$

q_s = collapse pressure of a stringer stiffener plus its associated shell plating

$$= \frac{16}{st^2} A_s |z_{st}| \sigma_0$$

z_{st} = distance from centerline of shell to the centroid of stringer stiffener

K_p = effective pressure correction factor

$$= 0.25 + \frac{0.85}{500}g \quad \text{for } g \leq 500$$

$$= 1.10 \quad \text{for } g > 500$$

g = geometrical parameter

$$= 2\pi \frac{l^2 A_s}{N_s I_s}$$

N_s = number of stringer stiffeners

4.4 Computational Analysis

For this study Ansys Workbench version 13.0.0 was used. The cylinders were drawn in AutoCAD 2013 by first creating a base circle representing the base of the cylinder; this base circle was then copied using the array function with spacing equal to the spacing between the ring stiffeners. A thin surface was then extruded from each circle to the next, creating a separate surface between each circle, where each circular line represents a ring stiffener.

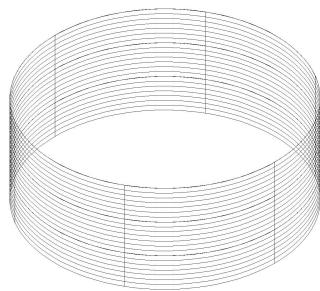


Figure 4.2: Wireframe model

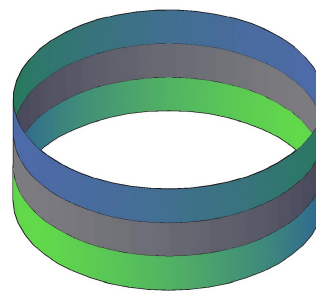


Figure 4.3: Separation of surfaces

The AutoCAD file was then saved as an Initial Graphics Exchange Specification (IGES) file, which was then imported into the Ansys workbench geometry modeller (called “DesignModeller”). The option to “stitch surfaces” was disabled so that each of the individual surfaces were kept separate and the option to “process line bodies” was enabled so that the lines representing the ring stiffeners could be imported.

Within the DesignModeller the ring stiffener cross section was defined and then assigned to each of the line bodies representing the ring stiffeners. These were then offset from their centroidal axis so that they were correctly positioned and orientated. A thickness was then defined for the imported surfaces thereby rendering the geometric modelling of the structure complete. Using the defined geometry a number of analyses were run:

4.4.1 Static Structural Stress Analysis

A linear buckling analysis must be preceded by a static structural analysis.

Supports:

The base of the cylinder was defined as simply supported. The top ring of the cylinder was radially constrained, i.e. it could only move in the vertical direction. The ring stiffeners for the linear buckling analysis were modelled as cross-sectional elements.

Mesh:

The typical mesh size of each analysis is a minimum edge length of 10mm and a maximum edge length of 30mm. The meshes were quadrilateral shell elements (a description of which is given in Section: 3.4) and were “pinched” or matched at the intersections between two surfaces and the ring stiffeners so that the structure was modelled as one contiguous part.

Loading:

Two loadcases were examined for the linear analyses: axial loading, and external pressure loading (See Figures: 4.4 and 4.5). For the axial loading case a vertical compressive load of 1N was distributed on the top of the cylinder, whereas for the external buckling case, a uniform pressure of 1Pa was placed acting externally on each of the shell segments.

Steps and substeps:

For this type of analysis there was only one step and substep required as it is a direct (as opposed to iterative) solution process.

Solution process:

A sparse matrix direct solver process was used and there were six degrees of freedom per

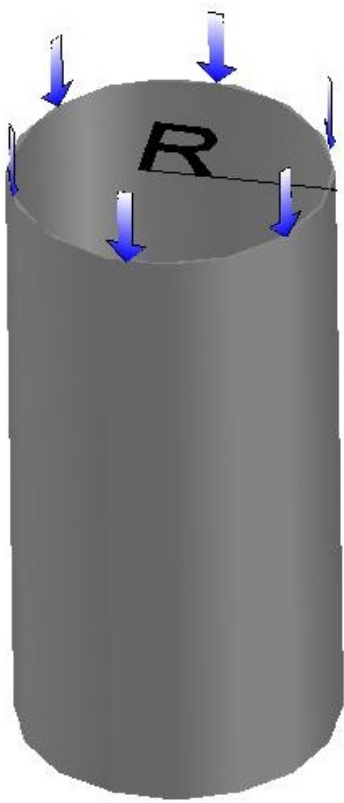


Figure 4.4: Axial loading

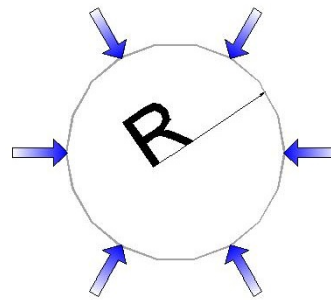


Figure 4.5: External pressure loading

node; three translational and three rotational.

4.4.2 Linear Buckling Analysis

The Block Lanczos method was used to extract the first three modal buckling shapes (Further information on this method can be found in Rajakumar and Rogers (1991)).

The result of a linear buckling analysis is a load factor that when multiplied by the load applied in the previous static analysis will result in buckling. So, if a load of 10N were applied in the preceding static structural analysis and the result of the linear buckling analysis is a load factor of 550 then the buckling load is $10 \times 550 = 5500\text{N}$.

4.4.3 Introduction of Imperfections

The modal buckling shapes that have been extracted from a linear buckling analysis can be scaled and the shape exported for further analysis. For this study the first modal shape was extracted and scaled by a number of values, and a non-linear buckling analysis was performed on each of these geometries.

Taking Cylinder IC1 as an example:

- A linear buckling analysis was performed, the first three modal shapes and buckling factors were determined
- The geometry of the first modal shape was extracted
- The deformation of the first modal shape was scaled by 1 and a non-linear analysis was performed on the resulting geometry
- The first modal shape was scaled by a factor of 5 and a non-linear analysis was performed on the resulting geometry
- The first modal shape was scaled by a factor of 10 and a non-linear analysis was performed on the resulting geometry etc.

This allowed an imperfection sensitivity analysis to be performed when the resulting buckling stresses from the non-linear analyses were compared.

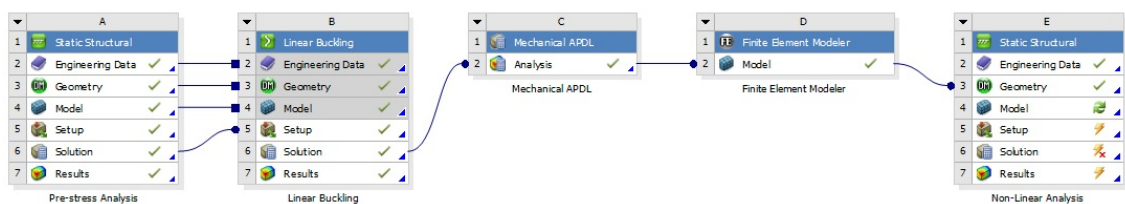


Figure 4.6: Computational analysis procedure

4.4.4 Non-Linear Analysis

Multiple non-linear analyses were performed on each cylinder in this study. The Eurocode section describes some of these in detail. The following description is the methodology for the geometrically and materially non-linear analysis of a cylinder of perfect geometry

(That is that the modal imperfection shape was not used, the geometry is the same as the linear analysis i.e. geometric imperfection free) and a description of the non-linear analysis performed on each cylinder with introduced imperfections (Geometrically, materially non-linear analysis with included imperfections of which, approximately 30 of these analyses were performed). The external uniform pressure loadcase was not analysed non-linearly, it was decided that axial loading was of greater interest as axial loading of cylindrical shells has more critical post-buckling behaviour. Given the limitation of time and computational storage space non-linear analyses of axial loading alone was deemed sufficient. Further information on non-linear analyses of cylindrical shells under uniform external pressure may be found in “*Consistent equivalent geometric imperfections for the numerical buckling strength verification of cylindrical shells under uniform external pressure*” Schneider and Brede (2005).

Supports:

The base of the cylinder was defined as simply supported. The top ring of the cylinder was radially constrained, i.e. it could only move in the vertical direction. The ring stiffeners for the non-linear buckling analysis were modelled as infinitely radially stiff¹ i.e. that they could not displace laterally but were free to move in the vertical direction.

Mesh:

The typical mesh size of each analysis is a minimum edge length of 10mm and a maximum edge length of 30mm. The meshes were quadrilateral elements and were “pinched” or matched at the intersections between two surfaces and the ring stiffeners so that the structure was modelled as one contiguous part.

Loading:

The loading procedure for the non-linear analyses was to apply a vertical displacement to the top of each cylinder in the direction of the base putting the cylinder under compression. The imposed displacement varied per analysis. The procedure was to perform an initial

¹This was a requirement as the surfaces of the buckled shape could not be ‘split’ and a supporting line element could not be introduced. Therefore constraints were placed directly on the nodes at the locations of the stiffeners, a comparison was performed between a case where line elements could be used and a case where nodal constraints were used, this is discussed in more detail in the discussion of computational results section

buckling analysis with a large imposed displacement then once convergence was lost, the displacement at which the structure became unstable was determined. Upon inspection of the load vs. displacement diagram it was determined if this instability was induced by buckling (or improper modelling). The applied displacement was then adjusted to a value closer to that which induced buckling and the analysis was run again. This resulted in smaller load increments allowing the resulting buckling load to be more accurately determined.

Steps and substeps:

For each analysis there was one load step which was further subdivided into substeps. The initial subdivision into substeps was performed automatically by the program until an approximate buckling load (from induced displacement) was determined. After an approximate buckling load was determined the substeps were typically set to a minimum of 50. This meant that for each substep the load increment was the (imposed displacement/50). After 50 steps, the total imposed displacement was then equal to the applied displacement. Analysing the model in 50 substeps allowed the load vs. displacement diagram to be giving the behaviour of the structure in good detail. A greater number of substeps would result in greater computation time, but more accurate results. The accuracy given with 50 substeps was considered sufficient for this study.

Solution process:

The non-linear analysis was analysed using the full Newton-Raphson method with sparse matrix direct solver and the convergence criteria used was an L2-norm (Weisstein; n.d.) of force (and moment) tolerance equal to 0.5%.

Once again the nodes had six degrees of freedom; six translational and six rotational.

4.4.4.1 Global numerical MNA/LBA analysis

This approach is given in section 8.6 of *Part 1-6: Shells* and is explained in (Figure: 4.7) and has essentially the same basis of the traditional stress design buckling approach.

1. Firstly a linear buckling analysis (LBA) is performed - this determines the elastic critical buckling resistance R_{cr} of a perfect shell.
2. A material non-linear, or elastic-plastic, analysis is performed to determine the plastic reference resistance of the shell R_{pl}

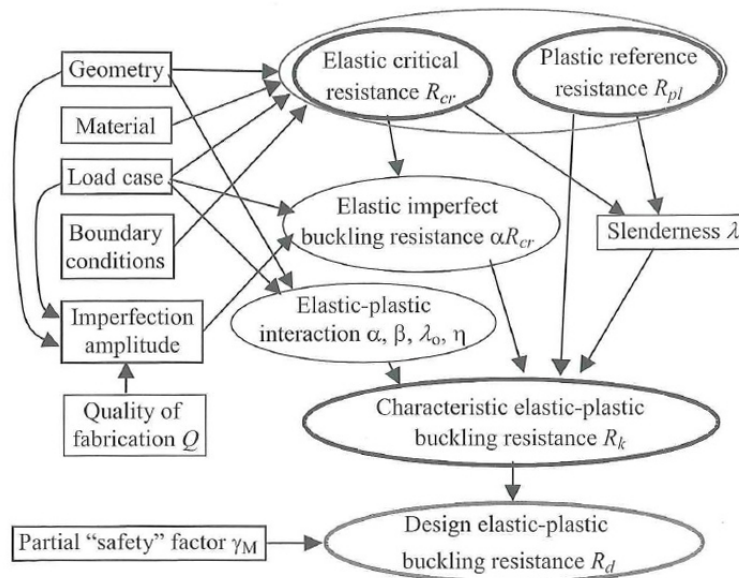


Figure 4.7: Steps in buckling strength assessment using design by global numerical MNA/LBA analysis (Rotter; 2008)

3. The relative slenderness, λ_{ov} , is deduced where:

$$\lambda_{ov} = \sqrt{R_{pl}/R_{cr}} \quad (4.31)$$

4. The overall buckling reduction factor χ_{ov} is then determined from:

$$\begin{aligned} \chi_{ov} &= 1 & \text{when } \lambda_{ov} &\leq \lambda_{ov,0} \\ \chi_{ov} &= 1 - \beta_{ov} \left(\frac{\lambda_{ov} - \lambda_{ov,0}}{\lambda_{ov,p} - \lambda_{ov,0}} \right)^{\eta_{ov}} & \text{when } \lambda_{ov,0} < \lambda < \lambda_{ov,p} \\ \chi_{ov} &= \frac{\alpha_{ov}}{\lambda_{ov}^2} & \text{when } \lambda_{ov,p} &\leq \lambda_{ov} \end{aligned}$$

where:

$$\lambda_{ov,p} = \sqrt{\frac{\alpha_{ov}}{1 - \beta_{ov}}}$$

As the analyses are of cylinders under meridional loading, λ_{ov} , β_{ov} and η_{ov} were chosen as the same as λ_x , β_x and η_x , so the elastic imperfection factor α_{ov} is also determined the same way as a cylinder under meridional loading.

$$\alpha_{ov} = \frac{0.62}{1 + 1.91(\Delta w_k/t)^{1.44}} \quad (4.32)$$

and Δw_k is determined by Equation: 4.7

5. The characteristic buckling resistance, R_k , is then obtained from:

$$R_k = \chi_{ov} R_{pl}$$

6. and the design buckling resistance, R_d , is given by:

$$R_d = R_k / \gamma_M$$

where:

γ_{M1} is the partial factor for resistance

4.4.4.2 Global numerical GMNIA analysis

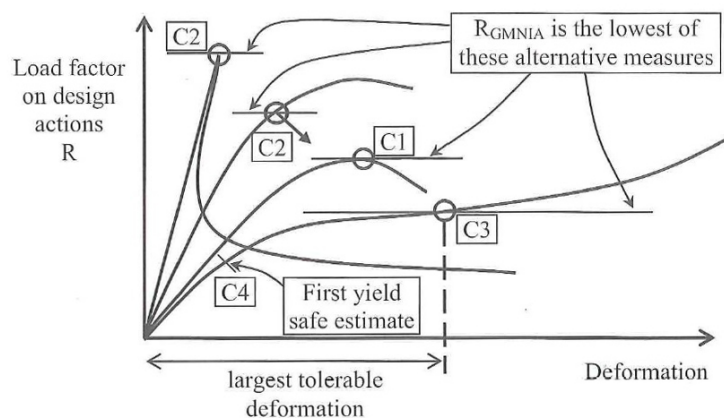


Figure 4.8: Definition of buckling resistance from global GMNIA analysis Rotter (2008)

The procedure is summarised as follows:

1. Firstly a linear buckling analysis (LBA) is performed - this determines the elastic critical buckling resistance R_{cr} of a perfect shell.
2. A materially non-linear analysis is performed on a perfect shell - this determines the plastic reference resistance R_{pl} of a perfect shell.

3. These two resistances are used to establish the overall relative slenderness λ_{ov} of the shell.
4. Next geometrically and materially non-linear analysis are performed using a number of imposed imperfection amplitudes on the same cylinder to determine the imperfect elastic-plastic critical buckling resistance R_{GMNIA} , which is determined as one of the values (Figure: 4.8):
 - The maximum load factor (limit load) on the load-deformation curve C1
 - The bifurcation load factor, where this occurs before the limit load is reached C2
 - The largest tolerable deformation C3
 - The load factor at which the equivalent stress at the most highly stressed point on the shell surface reaches the design value of the yield stress.
 - The buckling loads were graphed in non-dimensional form. the buckling load for each imperfection amplitude (N_{cr} , also denoted R_{GMNIA}) was divided by the buckling load for the perfect cylinder ($N_{cr,perfect}$, also denoted R_{GMNA}) and the imperfection amplitude was divided by the shell thickness.
5. For the buckling design by global numerical GMNIA analysis a required amplitude of the adopted equivalent geometric imperfection form, $\Delta w_{0,eq}$, was determined from the larger of:

$$\Delta w_{0,eq,1} = l_g U_{n1}$$

$$\Delta w_{0,eq,2} = n_i t U_{n2}$$

where:

- | | |
|-----------------------|---|
| l_g | is the relevant gauge length |
| n_i | is a multiplier to achieve an appropriate tolerance level
($n_i = 25$ is recommended) |
| U_{n1} and U_{n2} | are the dimple imperfection factors given in Table: 4.6: |

6. The imperfect elastic-plastic critical buckling resistance, R_{GMNIA} , for this amplitude was then determined from linear interpolation of the previous GMNIA results (see Figure:

Table 4.6: Recommended values for dimple imperfection parameters (*Eurocode 3 - Design of steel structures - Part 1-6: Strength and stability of shell structures*; 2007)

Fabrication quality class	Description	Recommended U_{n1}	Recommended U_{n2}
Class A	Excellent	0.01	0.01
Class B	High	0.016	0.016
Class C	Normal	0.025	0.025

7. The characteristic buckling resistance should be obtained from:

$$R_k = k_{GMNIA} R_{GMNIA}$$

Where k_{GMNIA} is the calibration factor and was assumed to be 1 (one)².

8. The design buckling resistance, R_d , is given by:

$$R_d = R_k / \gamma_M$$

where:

γ_{M1} is the partial factor for resistance

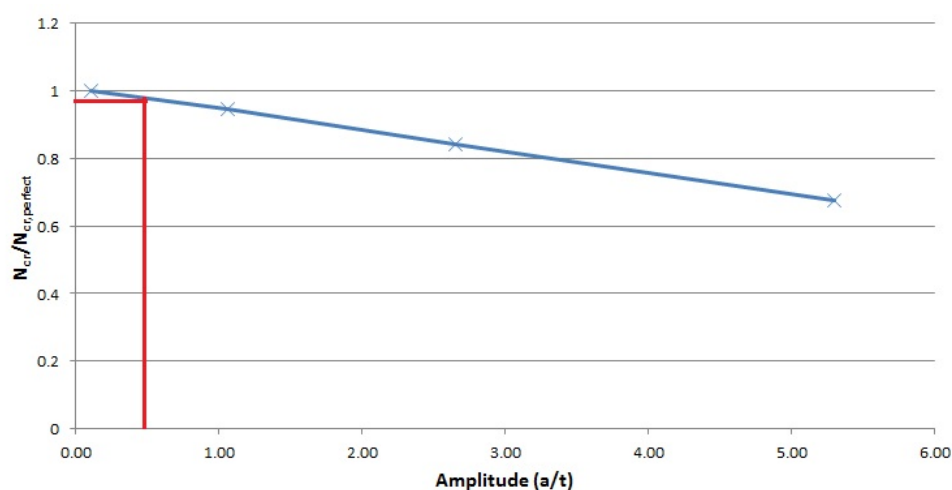


Figure 4.9: Example interpolation of the R_{GMNIA} for the amplitude of the adopted equivalent geometric imperfection

² k_{GMNIA} can lie between 0.8 and 1.2 but if it falls outside this range the analytical results are deemed invalid, it is determined through comparison with known results or tests

5 DESIGN CODE ANALYTICAL METHOD

American Bureau of Shipping - Commentary on the guide for buckling and ultimate Strength assessment for offshore structures (2005) has six example steel structures to which the guide was applied to. Three cylinders stiffened only with ring stiffeners and three cylinders with both ring and stringer stiffeners. These examples were used to verify the Matlab script written for the ABS the guide for buckling and ultimate strength assessment for offshore structures (see Appendix B) but these structures were also designed using the Eurocode and finite element analysis to compare the design approaches and see what range of buckling stresses are given for the different design approaches. The basic geometric information is given in Tables 5.1 and 5.8 but for further details such as stiffener dimensions, loading etc. please consult the ABS commentary (2005). This chapter will present the results of the design methods, their results will be compared and discussed in Chapters 6 and 8.

5.1 Ring Stiffened Cylinders

Table 5.1: Ring stiffened shell geometry

Model Name		IC-1	1	6.1
Total Length(Assumed)	L (mm)	2239.5	2438.49	2522.1
Length between ring stiffeners	l (mm)	746.5	812.83	840.7
Mean radius	r (mm)	749.7	197.2	3175
Thickness	t (mm)	3.52	12.57	6.35
Specified minimum yield stress	$\sigma_0(N/mm^2)$	281	301	276
Modulus of elasticity	E (N/mm^2)	2.05E+05	2.04E+05	1.99E+05
Poisson's ratio	ν	0.3	0.3	0.3

5.1.1 Cylinder IC-1

Ring stiffened steel cylinder subject to axial loading only.

For this first example the equations will be written but for further examples only the key values will be given.

5.1.1.1 Eurocode - Meridional (Axial) Loading

The length of the shell segment is characterised in terms of the dimensionless length parameter ω :

$$\omega = \frac{l}{r} \sqrt{\frac{r}{t}} = \frac{l}{\sqrt{rt}}$$

$$\omega = \frac{746.5}{\sqrt{749.7 \times 3.52}} = 14.53$$

The critical meridional buckling stress, using a value of C_x , should be obtained from:

$$\sigma_{xRc} = 0.605EC_x \frac{t}{r}$$

where the coefficient C_x is a length dependent factor and as:

$$1.7 \leq \omega \leq 0.5 \frac{r}{t}$$

the cylinder is classified as medium length so:

$$C_x = 1$$

The critical meridional buckling stress can be determined as:

$$\sigma_{xRc} = 0.605 \times (2.05 \times 10^5) \times 1 \times \frac{3.52}{749.7} = 582.32 \text{ N/mm}^2$$

The meridional elastic imperfection factor should be obtained from:

$$\alpha_x = \frac{0.62}{1 + 1.91(\Delta w_k/t)^{1.44}}$$

where Δw_k is the characteristic imperfection amplitude:

$$\Delta w_k = \frac{1}{Q} \sqrt{\frac{r}{t}} t$$

where Q is the meridional compression fabrication quality parameter (see Table: 4.2), which for this study is assumed to be “excellent”¹, so:

$$\Delta w_k = \frac{1}{40} \sqrt{\frac{749.7}{3.52}} 3.52 = 1.28$$

and:

$$\alpha_x = \frac{0.62}{1 + 1.91(1.28/3.52)^{1.44}}$$

$$\alpha_x = 0.4284$$

The meridional squash limit slenderness $\bar{\lambda}_{x0}$, the plastic range factor β , and the interaction exponent η should be taken as:

$$\bar{\lambda}_{x0} = 0.2 \quad \beta = 0.6 \quad \eta = 1.0$$

So, determining the reduction factor χ_x :

$$\bar{\lambda}_p = \sqrt{\frac{\alpha}{1 - \beta}}$$

$$\bar{\lambda}_p = \sqrt{\frac{0.4284}{1 - 0.6}} = 1.03$$

and:

$$\bar{\lambda}_x = \sqrt{f_{y,k}/\sigma_{xRc}}$$

$$\bar{\lambda}_x = \sqrt{281/582.32} = 0.6947$$

as

$$\bar{\lambda}_0 \leq \bar{\lambda}_x \leq \bar{\lambda}_p$$

The reduction factor χ_x may be taken as:

$$\chi_x = 1 - \beta \left(\frac{\bar{\lambda}_x - \bar{\lambda}_0}{\bar{\lambda}_p - \bar{\lambda}_0} \right)$$

¹This is a significant assumption but the fabrication quality of a manufacturer is difficult to determine. A manufacturer was approached about their fabrication tolerances but they never responded so an assumption was required. Reducing the fabrication quality to “High” results in a design buckling stress of $148.37N/mm^2$ which is a 10% reduction of the “Excellent” value. If the quality was reduced to “Normal” the buckling strength would be $120.42N/mm^2$, a 26% reduction of the “Excellent” value.

$$\chi_x = 1 - 0.6 \left(\frac{0.6947 - 0.2}{1.03 - 0.2} \right) = 0.64$$

The characteristic buckling strengths should be obtained by multiplying the characteristic yield strength by the reduction factors:

$$\sigma_{x,Rk} = \chi_x f_{y,k}$$

$$\sigma_{x,Rk} = 0.64 \times 281 = 181.11 \quad N/mm^2$$

Although for this study the characteristic buckling stresses are compared, for the sake of completeness the Eurocode design buckling stresses should be obtained from:

$$\sigma_{x,Rd} = \sigma_{x,Rk} / \gamma_M$$

$$\sigma_{x,Rd} = 181.11 / 1.1 = 164.65 \quad N/mm^2$$

5.1.1.2 ABS - Axial Loading

The elastic buckling stress for an imperfect cylindrical shell is defined as:

$$\sigma_{ExR} = \rho_{xR} C \sigma_{CExR}$$

where ρ_{xR} , the nominal or lower bound knock-down factor and the length dependent coefficient, C, are dependent on the Batdorf parameter, z:

$$z = \frac{l^2}{rt} \sqrt{1 - \nu^2}$$

$$z = \frac{746.5^2}{749.7 \times 3.52} \sqrt{1 - 0.3^2} = 201.44$$

in this case, where:

$$20 \leq z$$

then ρ_{xR} is determined by:

$$\rho_{xR} = 0.35 - 0.0002 \frac{r}{t}$$

$$\rho_{xR} = 0.35 - 0.0002 \frac{749.7}{3.52} = 0.3074$$

for the length dependent coefficient when:

$$z \geq 2.85$$

then C is defined as:

$$C = 1$$

The classical compressive buckling stress σ_{CExR} for a cylinder is the same that was derived in theory (see Section: 3.1):

$$\sigma_{CExR} = 0.605 \frac{Et}{r}$$

$$\sigma_{CExR} = 0.605 \frac{(2.05 \times 10^5) \times 3.52}{749.7} = 582.32 \quad N/mm^2$$

so the elastic buckling stress for an imperfect cylindrical shell is:

$$\sigma_{ExR} = 0.3074 \times 1 \times 582.32 = 179.01 \quad N/mm^2$$

but as the elastic buckling stress for an imperfect cylindrical shell falls into the elastic-plastic range:

$$\sigma_{ExR} > P_r \sigma_0$$

the critical buckling stress of unstiffened or ring-stiffened cylindrical shell subjected to axial compression or bending moment may be taken as:

$$\sigma_{CxR} = \sigma_0 \left[1 - P_r (1 - P_r) \frac{\sigma_0}{\sigma_{ExR}} \right]$$

$$\sigma_{CxR} = 281 \left[1 - 0.6(1 - 0.6) \frac{281}{179.00} \right] = 175.14 \quad N/mm^2$$

Table 5.2: Cylinder IC-1 - Axial

Eurocode		ABS	
Plasticity	Elasto-plastic	Plasticity	Plastic effects
Length coefficient, C_x	1	Length coefficient, C	1
Elastic stress, $\sigma_{x,Rc}$	582.32 N/mm^2	Elastic stress, σ_{ExR}	582.32 N/mm^2
Critical stress, $\sigma_{x,Rk}$	181.11 N/mm^2	Critical stress, σ_{CxR}	175.14 N/mm^2

5.1.1.3 Eurocode - Circumferential Loading

The equation for the critical buckling stress for circumferential is length dependent so firstly the non-dimensional length of the cylinder must be defined using ω and C_θ . The value for ω has already been determined, and the value for C_θ is dependent on the boundary conditions (see Table: 4.4) which were assumed to be “pinned-pinned”². For “pinned-pinned” conditions the value of C_θ may be taken as:

$$C_\theta = 1$$

As the non-dimensional length is:

$$\frac{\omega}{C_\theta} < 20$$

the critical circumferential buckling stress should be obtained from:

$$\sigma_{\theta Rc} = 0.92E \frac{C_{\theta s} t}{\omega r}$$

where the value for $C_{\theta s}$ is taken from Table 4.5 which for “pinned-pinned” conditions is defined as:

$$C_{\theta s} = 1 + \frac{3}{\omega^{1.35}}$$

$$C_{\theta s} = 1 + \frac{3}{14.53^{1.35}} = 1.08$$

The critical circumferential buckling stress can then be determined as:

$$\sigma_{\theta Rc} = 0.92E \frac{C_{\theta s} t}{\omega r}$$

$$\sigma_{\theta Rc} = 0.92 \times (2.05 \times 10^5) \left(\frac{1.08}{14.53} \right) \left(\frac{3.52}{749.7} \right) = 65.87 \text{ N/mm}^2$$

The value for α_θ is based on the fabrication quality and is taken from Table 4.3:

$$\alpha_\theta = 75$$

The meridional squash limit slenderness $\bar{\lambda}_{\theta 0}$, the plastic range factor β , and the interaction exponent η should be taken as:

²This is the boundary condition which most closely matched the ABS code

$$\bar{\lambda}_{\theta 0} = 0.4 \quad \beta = 0.6 \quad \eta = 1.0$$

So, determining the reduction factor χ_{θ} :

$$\bar{\lambda}_p = \sqrt{\frac{\alpha}{1 - \beta}}$$

$$\bar{\lambda}_p = \sqrt{\frac{0.75}{1 - 0.6}} = 2.07$$

and:

$$\bar{\lambda}_{\theta} = \sqrt{f_{y,k} / \sigma_{\theta Rc}}$$

$$\bar{\lambda}_{\theta} = \sqrt{281 / 65.87} = 2.07$$

as

$$\bar{\lambda}_{\theta} \geq \bar{\lambda}_p$$

The reduction factor χ_{θ} may be taken as:

$$\chi_{\theta} = \frac{\alpha}{\bar{\lambda}_{\theta}^2}$$

$$\chi_{\theta} = \frac{0.75}{2.07^2} = 0.1758$$

The characteristic buckling strengths should be obtained by multiplying the characteristic yield strength by the reduction factors:

$$\sigma_{\theta, Rk} = \chi_{\theta} f_{y,k}$$

$$\sigma_{\theta, Rk} = 0.1758 \times 281 = 49.4 \quad N/mm^2$$

Although for this study the characteristic buckling stresses are compared, for the sake of completeness the Eurocode design buckling stresses should be obtained from:

$$\sigma_{\theta, Rd} = \sigma_{\theta, Rk} / \gamma_M$$

$$\sigma_{\theta, Rd} = 49.4 / 1.1 = 44.91 \quad N/mm^2$$

5.1.1.4 ABS - External Pressure Loading

Firstly A_L will be calculated:

$$A_L = \frac{\sqrt{z}}{(1 - \nu^2)^{1/4}} - 1.17 + 1.068k$$

where:

$$k = 0 \text{ for lateral pressure}$$

$$z = 201.44$$

the elastic buckling pressure is dependent on A_L , so

$$A_L = \frac{\sqrt{201.44}}{(1 - 0.3^2)^{1/4}} - 1.17 + (1.068 \times 0) = 13.36$$

which falls into the range of

$$2.5 < A_L \leq 0.208 \leq \frac{r}{t}$$

then the elastic buckling pressure is determined as

$$q_{CE\theta R} = \frac{0.92E t^2}{A_L r}$$

$$q_{CE\theta R} = \frac{0.92 \times 2.05 \times 10^5}{13.36} \frac{3.52^2}{749.7} = 0.31Pa$$

Next the coefficient to account for the effect of ring stiffener, K_θ , must be determined:

$$K_\theta = 1 - \frac{1 - k\nu}{1 + t(t_w + l\bar{\omega})/\bar{A}_R} G_\alpha$$

$$\bar{A}_R = A_R \left(\frac{r}{r_R}\right)^2$$

$$\bar{\omega} = \frac{\cosh 2\alpha - \cos 2\alpha}{\alpha(\sinh 2\alpha + \sin 2\alpha)}$$

$$\alpha = \frac{l}{1.56\sqrt{rt}}$$

$$G_\alpha = 2 \frac{\sinh \alpha \cos \alpha + \cosh \alpha \sin \alpha}{\sinh 2\alpha + \sin 2\alpha} \geq 0$$

k	=	N_x/N_θ for lateral pressure
	=	$N_x/N_\theta + 0.5$ for hydrostatic pressure
A_R	=	cross sectional area of ring stiffener
N_x	=	axial load per unit length
N_θ	=	circumferential load per unit length
r_R	=	radius to centroid of ring stiffener
t	=	thickness of cylindrical shell
t_w	=	stiffener web thickness
l	=	length between adjacent ring stiffeners (unsupported)

Substituting in the known values results in:

N_x	=	624.14
N_θ	=	0
k	=	0
α	=	9.32
G_α	=	0
$\bar{\omega}$	=	0.11
\bar{A}_R	=	173.39

Giving a coefficient to account for the effect of ring stiffener of

$$K_\theta = 1$$

The elastic hoop buckling stress for an imperfect cylindrical shell is:

$$\sigma_{E\theta R} = \rho_{\theta R} \frac{q_{CE\theta R}(r+0.5t)}{t} K_\theta = 53.14 \text{ N/mm}^2$$

and Δ is:

$$\Delta = \frac{\sigma_{E\theta R}}{\sigma_0}$$

$$\Delta = \frac{53.14}{281} = 0.19$$

which falls into the range:

$$\Delta \leq 0.55$$

so

$$\Phi = 1$$

which means the critical buckling stress for an unstiffened or ring-stiffened cylindrical shell subjected to external pressure may be taken as:

$$\sigma_{C\theta R} = \Phi \sigma_{E\theta R}$$

$$\sigma_{C\theta R} = 1 \times 53.14 = 53.14 \text{ N/mm}^2$$

Table 5.3: Cylinder IC1 - External Pressure

Eurocode			ABS		
Plasticity	Elastic		Plasticity	Elastic	
Circumferential stress, $\sigma_{\theta,Rc}$	65.87	N/mm^2	Hoop stress, $\sigma_{E\theta R}$	53.14	N/mm^2
Characteristic stress, $\sigma_{\theta,Rk}$	44.91	N/mm^2	Critical stress, $\sigma_{C\theta R}$	53.14	N/mm^2

5.1.2 Cylinder 1

Ring stiffened cylinder subject to hydrostatic pressure only. The stiffeners of this structure are located externally.

Table 5.4: Cylinder 1 - Axial

Eurocode			ABS		
Plasticity	Elasto-plastic		Plasticity	Plastic effects	
Length coefficient, C_x	0.6		Length coefficient, C	1	
Elastic stress, $\sigma_{x,Rc}$	4720.25	N/mm^2	Elastic stress, σ_{ExR}	2728.8	N/mm^2
Critical stress, $\sigma_{x,Rk}$	291.56	N/mm^2	Critical stress, σ_{CxR}	293.03	N/mm^2

Table 5.5: Cylinder 1 - External Pressure

Eurocode			ABS		
Plasticity	Elasto-Plastic		Plasticity	Plastic effects	
Circumferential stress, $\sigma_{\theta,Rc}$	783.43	N/mm^2	Hoop stress, $\sigma_{E\theta R}$	571.95	N/mm^2
Characteristic stress, $\sigma_{\theta,Rk}$	260.04	N/mm^2	Critical stress, $\sigma_{C\theta R}$	235.23	N/mm^2

5.1.3 Cylinder 6.1

Ring stiffened cylinder subject to combined radial pressure and axial loading.

Table 5.6: Cylinder 6.1 - Axial

Eurocode			ABS		
Plasticity	Elastic		Plasticity	Elastic	
Length coefficient, C_x	1		Length coefficient, C	1	
Elastic stress, $\sigma_{x,Rc}$	240.79	N/mm^2	Elastic stress, σ_{ExR}	240.79	N/mm^2
Critical stress, $\sigma_{x,Rk}$	81.73	N/mm^2	Critical stress, σ_{CxR}	60.20	N/mm^2

Table 5.7: Cylinder 6.1 - External Pressure

Eurocode			ABS		
Plasticity	Elastic		Plasticity	Elastic	
Circumferential stress, $\sigma_{\theta,Rc}$	78.66	N/mm^2	Hoop stress, $\sigma_{E\theta R}$	61.72	N/mm^2
Characteristic stress, $\sigma_{\theta,Rk}$	58.99	N/mm^2	Critical stress, $\sigma_{C\theta R}$	61.72	N/mm^2

5.2 Ring and Stringer Stiffened Cylinders

Table 5.8: Ring and stringer stiffened cylinders geometry

Model Name		IC6	2-1C	2-1B
Total length(Assumed)	$L (mm)$	2847.36	9909.97	9919.09
Length between ring stiffeners	$l (mm)$	180	228.6	228.6
Mean radius	$r (mm)$	160	571.4	571.1
Thickness	$t (mm)$	0.84	1.96	1.97
Specified minimum yield stress	$\sigma_0(N/mm^2)$	348	393.2	395.7
Modulus of elasticity	$E(N/mm^2)$	2.01E+05	2.16E+05	2.18E+05
Poisson's ratio	ν	0.3	0.3	0.3

5.2.1 Cylinder IC6

Axial force alone.

Table 5.9: Cylinder IC6 - Axial

Eurocode			ABS		
Plasticity	Elasto-plastic		Plasticity	Plastic effects	
Elastic stress, $\sigma_{x,Rc}$	638.43	N/mm^2	Elastic stress, σ_{ExB}	1400.77	N/mm^2
Critical stress, $\sigma_{x,Rk}$	215.38	N/mm^2	Critical stress, σ_{CxB}	327.25	N/mm^2

Table 5.10: Cylinder IC6 - External pressure

Eurocode			ABS		
Plasticity	Elastic		Plasticity	Elastic	
Circumferential stress, $\sigma_{\theta,Rc}$	67.15	N/mm^2	Unstiffened stress, $\sigma_{C\theta R}$	54.24	N/mm^2
Characteristic stress, $\sigma_{\theta,Rk}$	50.37	N/mm^2	Critical stress, $\sigma_{C\theta B}$	126.49	N/mm^2

Table 5.11: Cylinder IC6 - Alternative Eurocode

EN 1993-4-1 Method					
Axial			External Pressure		
Omega match	Yes				
Critical stress, $n_{x,Rcr}$	107.62	N/mm^2	Critical stress, $P_{n,Rcr}$	39.99	N/mm^2

5.2.2 Cylinder 2-1C

Radial pressure alone.

Table 5.12: Cylinder 2-1C - Axial

Eurocode			ABS		
Plasticity	Elasto-plastic		Plasticity	Plastic effects	
Elastic stress, $\sigma_{x,Rc}$	448.25	N/mm^2	Elastic stress, σ_{ExB}	3.88e+03	N/mm^2
Critical stress, $\sigma_{x,Rk}$	175.06	N/mm^2	Critical stress, σ_{CxB}	383.63	N/mm^2

Table 5.13: Cylinder 2-1C - External pressure

Eurocode			ABS		
	Plasticity	Plastic		Plasticity	Plastic
	Circumferential stress, $\sigma_{\theta,Rc}$	122.18	N/mm^2	Unstiffened stress, $\sigma_{C\theta R}$	96.50
	Characteristic stress, $\sigma_{\theta,Rk}$	91.62	N/mm^2	Critical stress, $\sigma_{C\theta B}$	184.28
				N/mm^2	

Table 5.14: Cylinder 2-1C - Alternative Eurocode

EN 1993-4-1 Method					
Axial			External Pressure		
	Omega match	Yes			
	Critical stress, $N_{x,Rcr}$	142.17	N/mm^2	Critical stress, $P_{n,Rcr}$	68.66
				N/mm^2	

5.2.3 Cylinder 2-1B

Combined loading of radial pressure and axial load.

Table 5.15: Cylinder 2-1B - Axial

Eurocode			ABS		
	Plasticity	Elasto-plastic		Plasticity	Plastic effects
	Elastic stress, $\sigma_{x,Rc}$	454.95	N/mm^2	Elastic stress, σ_{ExB}	3.94e+03
	Critical stress, $\sigma_{x,Rk}$	177.55	N/mm^2	Critical stress, σ_{CxB}	386.16
				N/mm^2	

Table 5.16: Cylinder 2-1B - External pressure

Eurocode			ABS		
	Plasticity	Plastic		Plasticity	Plastic effects
	Circumferential stress, $\sigma_{\theta,Rc}$	124.34	N/mm^2	Unstiffened stress, $\sigma_{C\theta R}$	98.21
	Characteristic stress, $\sigma_{\theta,Rk}$	93.25	N/mm^2	Critical stress, $\sigma_{C\theta B}$	188.92
				N/mm^2	

Table 5.17: Cylinder 2-1B - Alternative Eurocode

EN 1993-4-1 Method					
Axial			External Pressure		
Omega match	Yes				
Critical stress, $N_{x,Rcr}$	143.16	N/mm^2	Critical stress, $P_{n,Rcr}$	71.06	N/mm^2

6 COMPUTATIONAL METHOD

In the following section the analytical results are given for each of the cylinders. The results of linear buckling analyses for axial loading and external pressure loading are given followed by non-dimensionalised results for the non-linear analyses of each cylinder with varying imperfection amplitudes to illustrate the effect that such imperfections have on the structures. These analytical results are then used to determine the buckling resistances of the cylinders according to the analytical methods defined in *Eurocode 3 Part 1-6: Strength and stability of shell structures*.

6.1 Ring Stiffened Cylinders

6.1.1 Cylinder IC-1

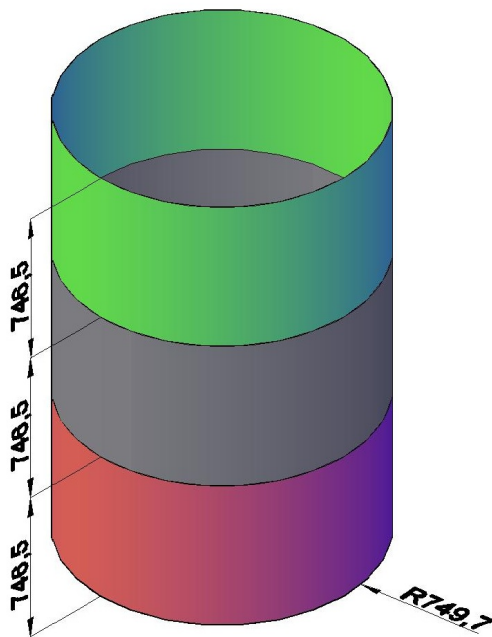


Figure 6.1: Cylinder IC1 AutoCAD model

Geometry:

The cylinder geometry was defined in AutoCAD as a 3D structure with three cylindrical surfaces representing the shell surface between the ring stiffeners and four circular line bodies to represent the ringstiffeners. The geometry was saved as an Initial Graphics Exchange Specification (IGES) file and then imported into the Ansys workbench DesignModeller.

Within the DesignModeller a thickness of 3.52mm was assigned to the three surface bodies and a cross section was defined for the ring stiffeners. The cross sectional dimensions of the ring stiffeners are taken from the ABS commentary, for cylinder IC1 the ring stiffeners had a thickness of 3.52mm and depth of 48mm (Figure: 6.2).

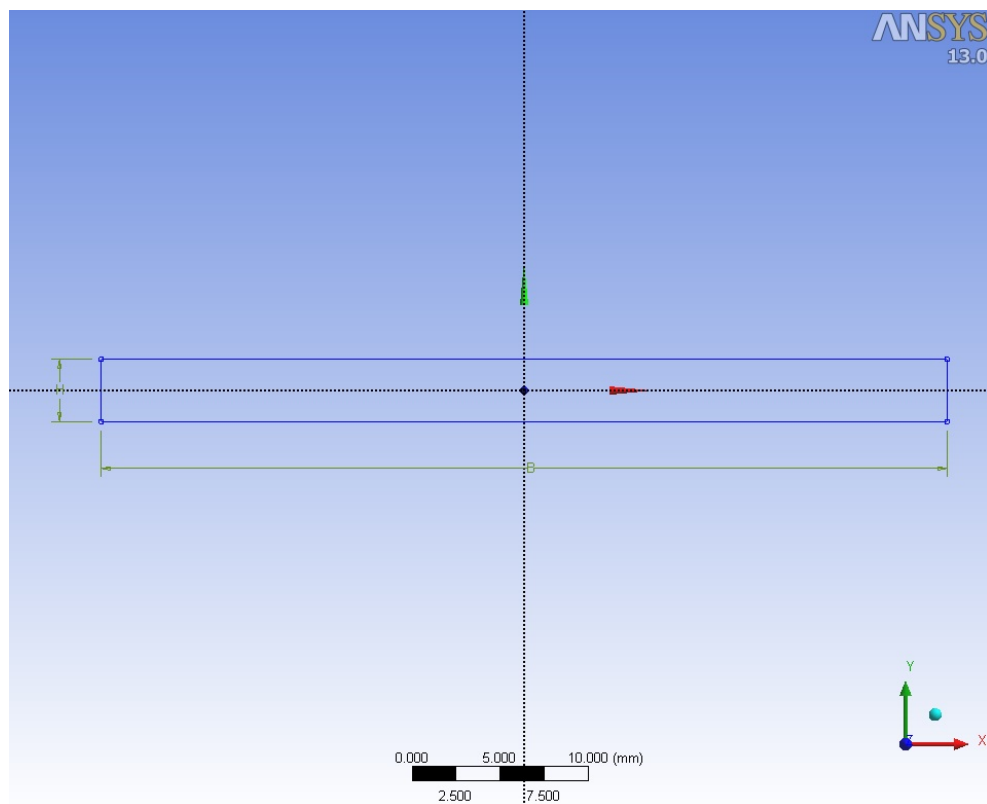


Figure 6.2: Cylinder IC1 - Cross section of ring stiffeners

The Ring stiffeners were offset so that they were orientated in the corrected direction and in contact with the cylinder on the interior of the cylinder.

Supports:

Next the support conditions of the cylinder were defined. The base of the cylinder was

defined as pinned, as there 6 degrees of freedom per node this meant restraint in the x- y- and z- translational directions, with no rotational restraint. The top nodes of the cylinder were radially constrained. Lateral translation (x- and y- directions) was constrained but the nodes were not restrained in the vertical (z) direction (see Figure: 6.3). The ring stiffener supports were included as the structural elements as can be seen in Figure: 6.4.

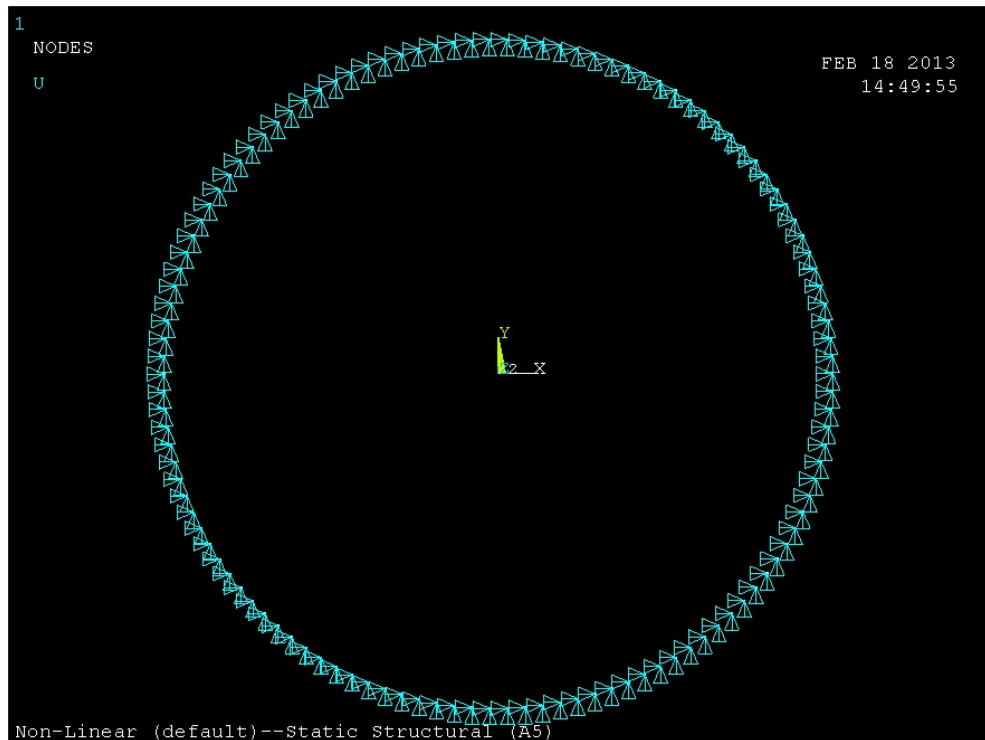


Figure 6.3: Cylinder IC1 - Radial constraints on top nodes

Mesh:

The mesh defined was a quadrilateral mesh with a face size of 25mm and the mesh was matched at the interfaces between the shell surfaces and the ring stiffeners so that the structure was modelled as a contiguous structure. The shell elements are defined as “shell181” elements, the ring stiffener elements are “beam181” elements and the loaded edge elements are “surf156” elements (See Appendix D). The resulting model had a total of 7374 nodes and 7198 elements.

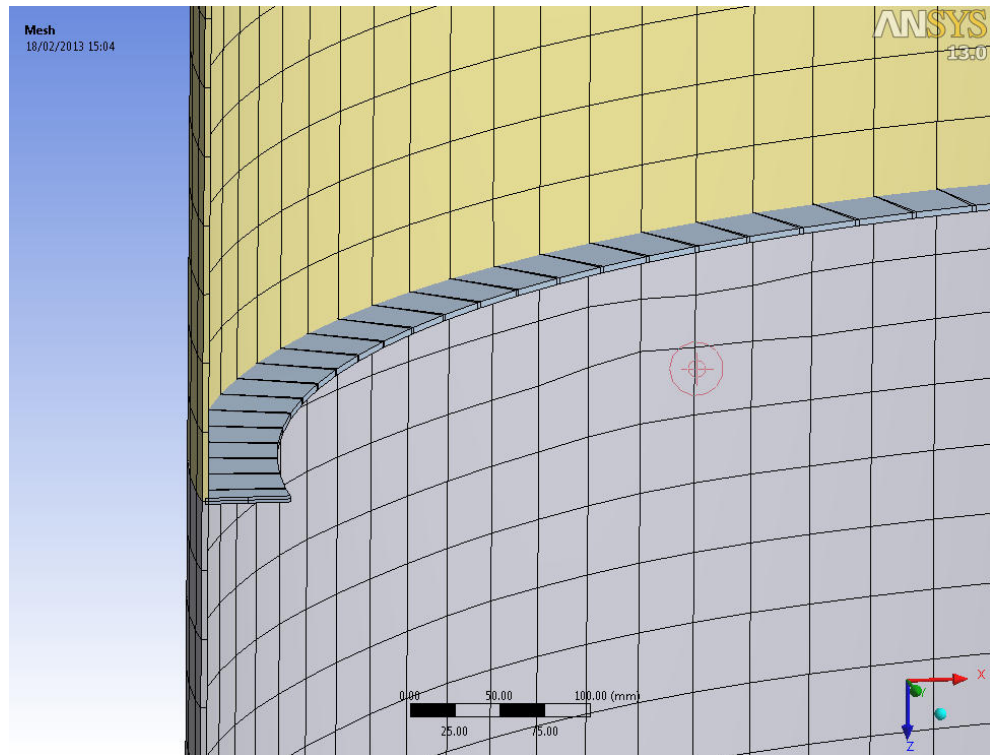


Figure 6.4: Cylinder IC1 - Junction between two shell segments and a ring stiffener

Loading:

A vertical compressive load of 1 kN was applied to the top edge of the cylinder in a static-structural pre-analysis. This pre-analysis is a prerequisite for the linear buckling analysis which determines the load multiplier. The load multiplier is the value that the load defined in the pre-analysis must be factored by in order to initiate linear buckling of the structure. For cylinder IC1 the determined load multiplier was 10354 (see Figure: 6.5) which means that linear buckling occurs at a load of $1000 \times 10354 = 10354000N$.

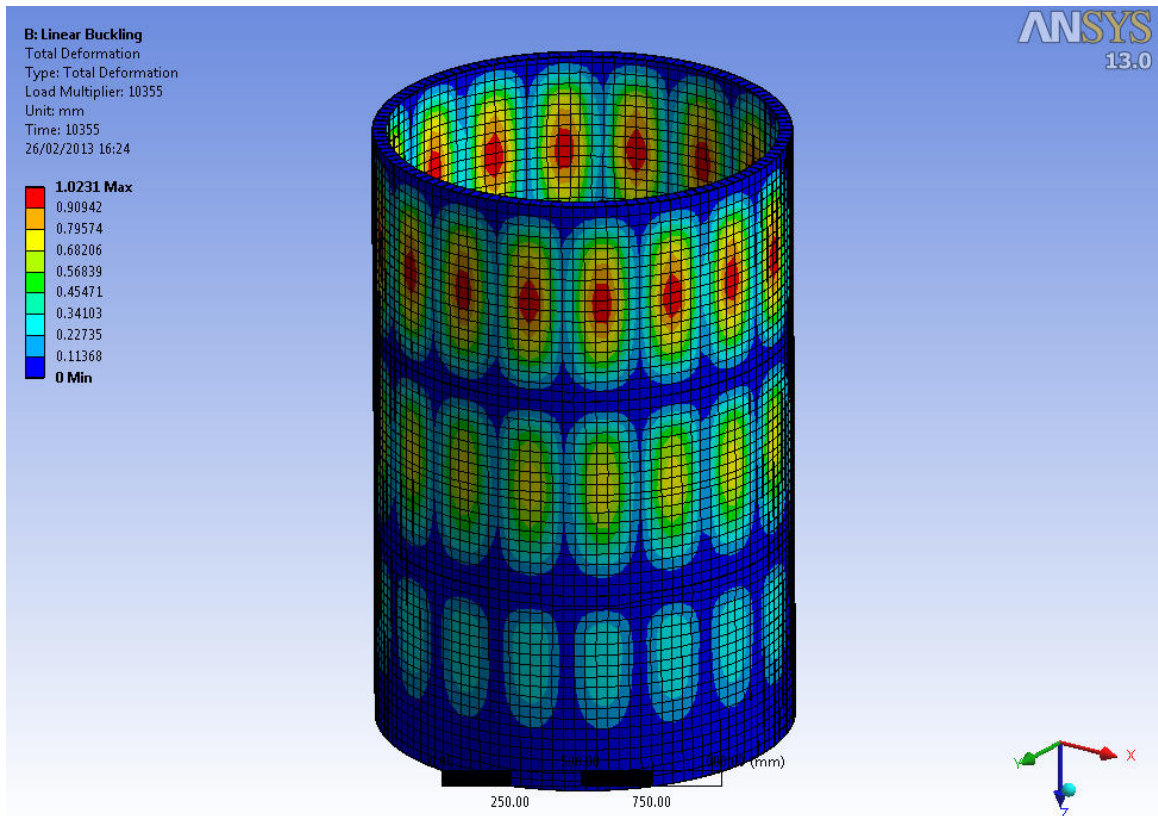


Figure 6.5: Cylinder IC-1 - Linear axial buckling

The area of upon which this load was applied is the top edge of the cylindrical wall, this area is defined as:

$$2\pi r t = 16580.97 \text{ mm}^2$$

The elastic buckling stress is determined by dividing the critical buckling load over the loaded area:

$$R_{cr} = \frac{10355000}{16580} = 624.55 \text{ N/mm}^2$$

It can also be seen that the first eigenmode buckled shape matches the expected buckled shape, that is one half wave between the stiffeners as (see Figure: 3.1). However, the buckling stress due to axial loading is 624.55 N/mm^2 as opposed to the theoretically determined stress, which is:

$$\sigma_{cr} = 0.605 \frac{Et}{r} = 582.32 \text{ N/mm}^2$$

This difference may be attributed to the influence of the ring stiffener structural properties,

which were included in the linear buckling analysis, or it may be a result of too large a mesh, or possibly a combination of both.

A mesh sensitivity analysis was performed setting the element face size to 10mm, this resulted in a model with 49398 nodes and 48940 elements. The load multiplier from the linear buckling analysis for this case was 9738 resulting a buckling load of $587.3N/mm^2$. The computation time for the denser mesh was 1165 seconds compared to the less dense mesh that had a computation time of 5 seconds; which is an increase of 1160 seconds. As there was such an increase in computation time, it was considered reasonable to use the less dense mesh size as a finer mesh in the non-linear analyses would cause impractically long computation times for the study¹. As such, a compromise was made between computation time and the accuracy of results.

Table 6.1: Cylinder IC-1 - Ansys Linear Buckling

Mode 1		
Load multiplier	10355	
Buckling load	10355000	N
Buckling stress, R_{cr}	624.55	N/mm^2

Using the same model but changing the load from a vertical compressive load of 1 N to a uniform external pressure load of 1 Pa, another linear buckling analysis was performed.

¹By changing the value of the elastic buckling resistance the influence on further characteristic buckling resistances was small. For instance, the characteristic buckling resistance from the LBA/MNA analysis using an elastic buckling resistance of $624.55N/mm^2$ was $185.78N/mm^2$ where as if an elastic buckling resistance of $587.3N/mm^2$ had been used, the LBA/MNA resistance would be $180.96N/mm^2$. This is a 2.7% difference in results

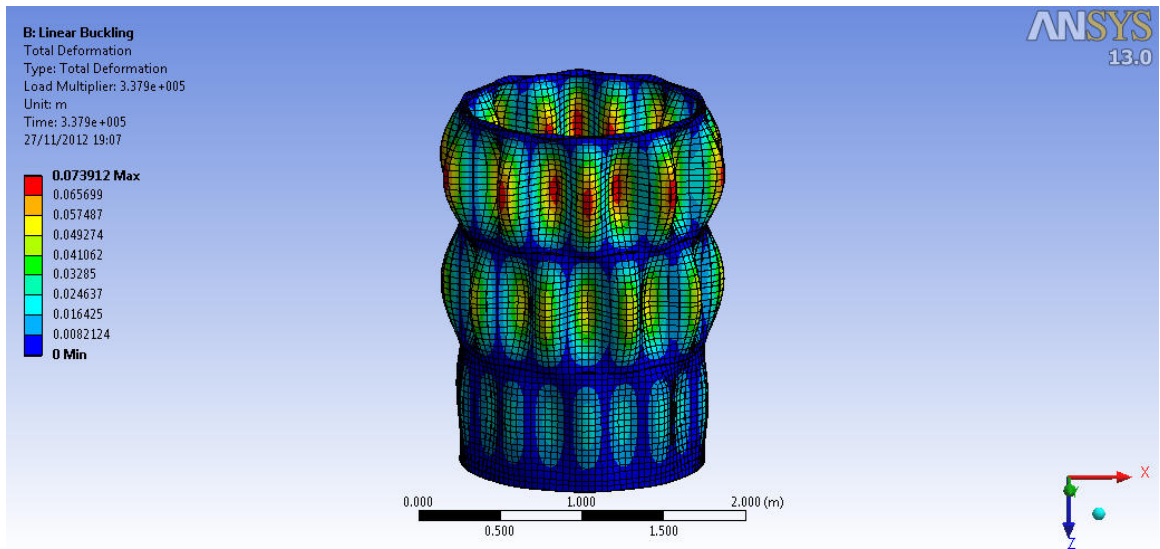


Figure 6.6: Cylinder IC-1 - External pressure buckling

For this loadcase the load multiplier was determined as 3.3795e+05, which means linear buckling occurs at a uniform external pressure of 337950 Pa.

Converting Pascals to N/mm^2 , the critical external buckling pressure is:

$$\text{Critical Pressure} = \frac{337950}{1e + 06} = 0.338 \text{ N/mm}^2$$

Table 6.2: Cylinder IC-1 - Ansys Linear External Pressure Buckling

Linear Buckling - Pressure Load		
Load multiplier	3.379e+005	
Buckling load	337950	Pa
Buckling pressure	0.338	N/mm^2

6.1.1.1 Introduction of imperfections and first GMNIA analysis

Non-linear analyses were only performed using the axial loading loadcase. The following procedure details how the imperfections were included and the GMNIA procedure for Cylinder IC1 specifically for Ansys as was performed in this study.

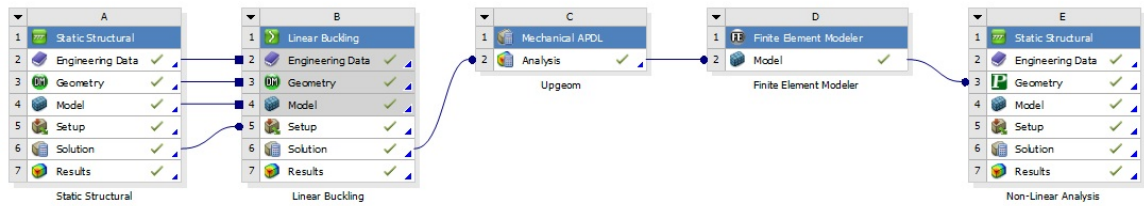


Figure 6.7: Introduction of analyses and GMNIA modules

Geometry:

The first eigenbuckled shape was exported from the linear buckling analysis of cylinder IC1 under axial loading using the APDL “upgeom” command. For the first case, the eigenbuckled shape was scaled to a factor of 1, so the deformed shape matches that given in Figure 6.5. This eigenbuckled shape has a maximum imperfection amplitude, a of 1.0231mm. Following this the model was imported into the finite element modeller which allows the prebuckled shape to be converted to a parasolid file for further analysis. This parasolid geometry was then imported into a new “static structural” module, in which the non-linear (GMNIA) analysis was performed.

Supports:

By exporting the eigenbuckled shape the separation between shell segments is lost as the “finite element modeller” module skin detection tool stitches the entire shell surface together. This procedure removes the ring supports of the structure, as such the simplification was made that the nodes at the locations of the ring stiffeners of cylinder IC1 were infinitely radially stiff (As seen in Figure: 6.3). These nodes were selected, constrained and coupled using APDL commands. The result is that the nodes at the elevations of the ring stiffeners were unable to translate laterally, but were coupled in vertical translation so that they moved in unison.

The nodes at the base of the cylinder were constrained in the same manner as the linear analysis, that is that translation was constrained in the x-, y- and z-directions making the base a “pinned” support. Once again, the top nodes of the cylinder were radially constrained. Lateral translation (x- and y- directions) was constrained but the nodes were not restrained in the vertical (z) direction.

Mesh:

The mesh used for the non-linear analysis was a quadrilateral mesh with a face size of 25mm. The shell elements used were "shell181" with 5 integration points to account for material plasticity. The resulting model had a total of 6726 nodes and 6608 elements.

Loading:

The loading for all non-linear analyses was displacement controlled. For this analysis a displacement of -20mm was applied to the top nodes of the cylinder which would compress the cylinder. The reaction force from the base of the cylinder was used to determine the equivalent force applied.

Steps and Substeps:

For this analysis an applied displacement of -20mm was set at load step 1. This load step was then further subdivided into 100 substeps. The result is an incremental displacement increase of 0.2mm per substep.

Solution process:

The non-linear analysis was analysed using the full Newton-Raphson method with sparse matrix direct solver and the convergence criteria used was an L2-norm (Weisstein; n.d.) of force (and moment) tolerance equal to 0.5%.

Solution:

The solution of this analysis took 316 seconds with a total of 118 iterations to reach the final solution.

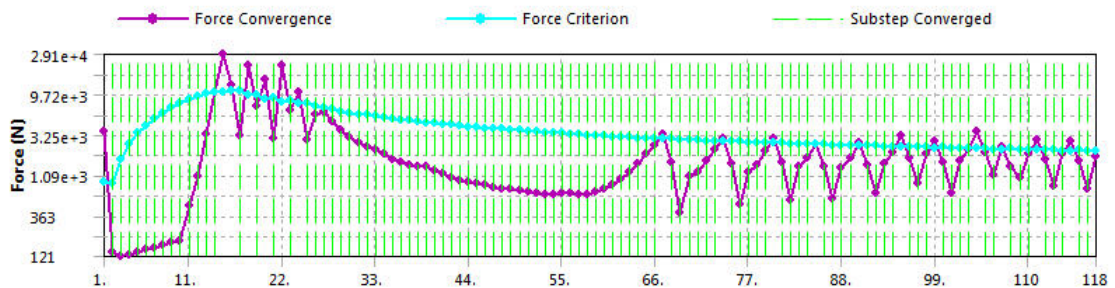


Figure 6.8: Cylinder IC-1 - Force convergence for first analysis

The resultant reaction force for each substep can be used to determine the buckling stresses by dividing the reaction forces by the area over which the force was applied.

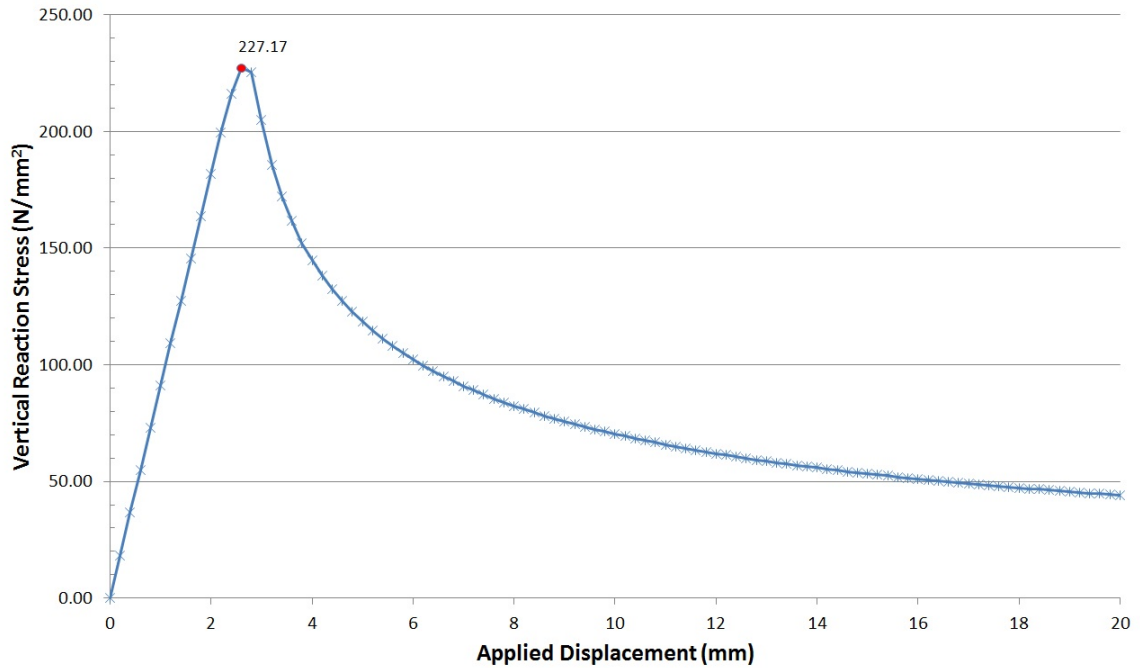


Figure 6.9: Cylinder IC-1 - Deformation vs. Reaction stress for first analysis

From this graph it can be seen that the buckling resistance is $227.17N/mm^2$ (which it can be seen is equivalent to ‘C2’ from Figure 4.8).

The maximum equivalent stress diagram shows that cylinder IC-1 exhibits elastic behaviour and plastic behaviour (see Figure: 6.10) which is as expected as it was seen in the analytical analysis (see Section: 5.1.1.1) that the relative slenderness of the cylinder lies between the squash limit slenderness and the plastic limit slenderness, i.e that $\bar{\lambda}_0 \leq \bar{\lambda}_x \leq \bar{\lambda}_p$. As such elastic-plastic behaviour is expected (see Figure: 7.3 later).

The result of this analysis could then be graphed non dimensionally by plotting the non-dimensional imperfection amplitude on the x-axis, this is the maximum imperfection amplitude from the prebuckled shape (a) divided by the thickness of the shell wall (t):

$$\frac{a}{t} = \frac{1}{3.52} = 0.28$$

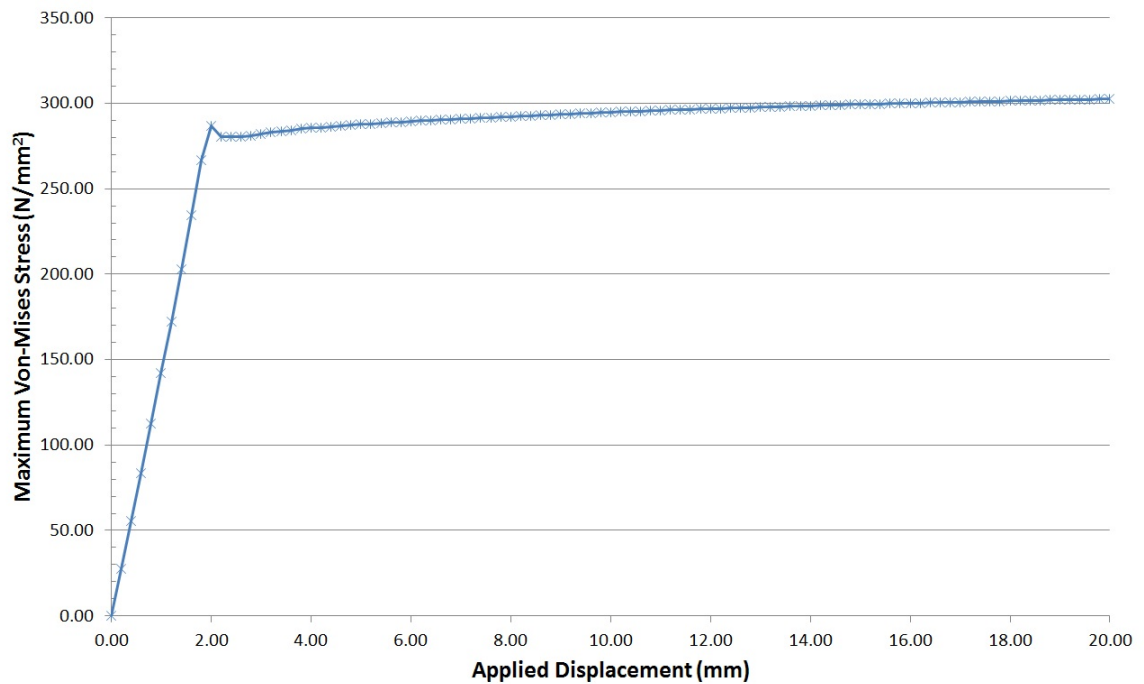


Figure 6.10: Cylinder IC-1 - Maximum equivalent (Von-mises) stress for first analysis

This was plotted against $N_{cr}/N_{cr,perfect}$ (or R_{GMNIA}/R_{GMNA})² to give the ratio of buckling resistance of the structure with the given magnitude of imperfection to the buckling resistance of the structure without included imperfections.

$$\frac{R_{GMNIA}}{R_{GMNA}} = \frac{N_{cr}}{N_{cr,perfect}} = \frac{227.17}{263.07} = 0.86$$

This procedure was then repeated, however for the next analyses rather than scaling the initial pre-buckled shape by a factor of 1, it was scaled to a factor of 5. This resulted in analysing a cylinder with a maximum geometric imperfection amplitude of:

$$1 \times 5 = 5mm$$

² R_{GMNA} was determined by an identical procedure as the one described here except that the imperfect prebuckled shape was not imported, but rather the perfect geometry with no included imperfections was analysed instead

which results in a non dimensional amplitude of:

$$\frac{a}{t} = \frac{5}{3.52} = 1.42$$

resulting in a buckling resistance (R_{GMNIA}) of $218.38N/mm^2$, so:

$$\frac{R_{GMNIA}}{R_{GMNA}} = \frac{N_{cr}}{N_{cr,perfect}} = \frac{218.38}{263.07} = 0.83$$

and so forth.

Table 6.3: Cylinder IC-1 - Amplitude vs. Buckling pressure

Deformation Factor	Amplitude (a/t)	Buckling ($N_{cr}/N_{cr,perfect}$)
1	0.28	0.86
5	1.42	0.83
10	2.84	0.68
15	4.26	0.62
20	5.68	0.60

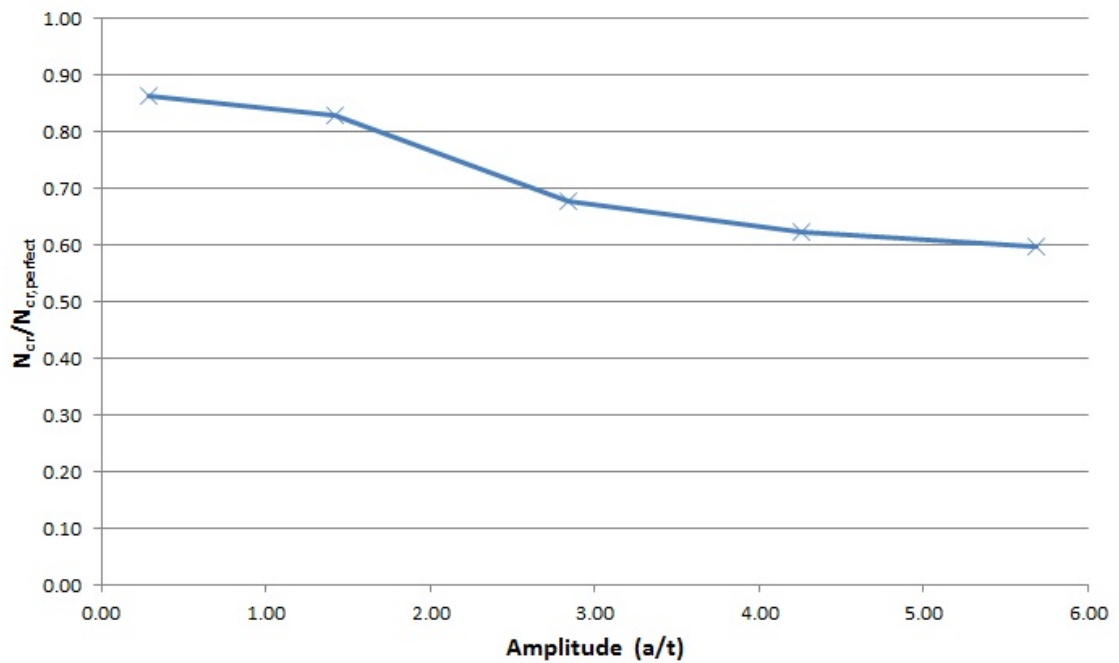


Figure 6.11: Cylinder IC-1 - Amplitude vs. Buckling pressure

6.1.1.2 EN 1993-1-6 Eurocode MNA/LBA Method

For this first example the equations will be written but for further examples only the key values will be given.

The plastic reference resistance is taken from an ANSYS analysis. The analysis performed to obtain this plastic reference resistance is identical to the procedure to obtain R_{GMNA} (The analysis described above without the inclusion of imperfections) apart from the following changes:

- Large deflection effects are not included
- No plastic hardening effects are included in the analysis

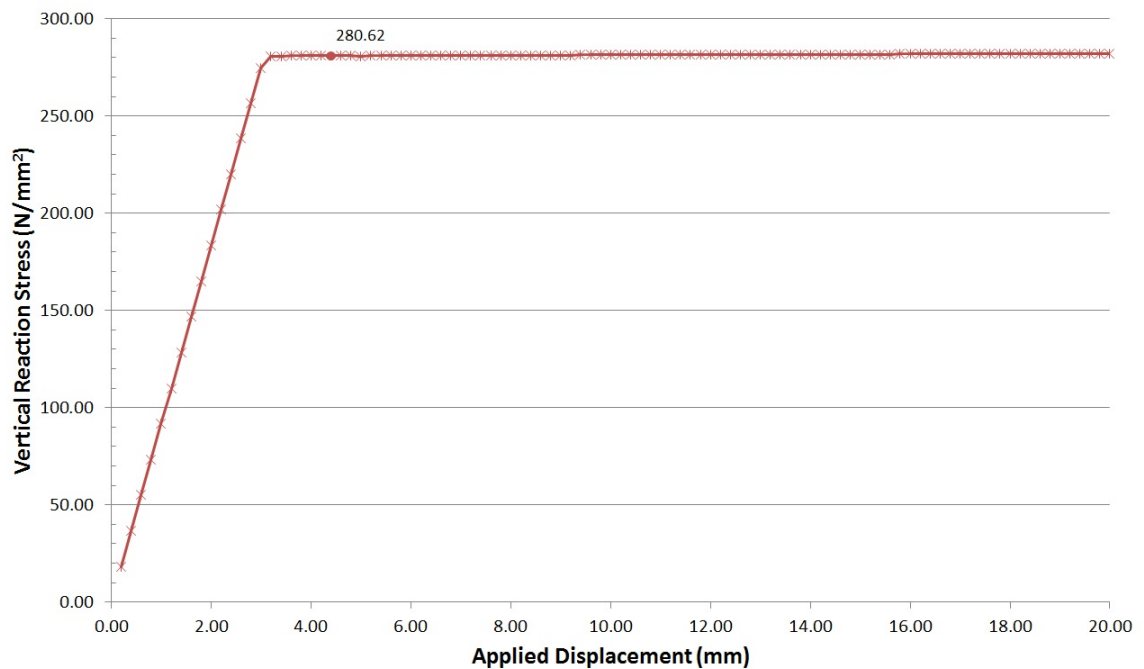


Figure 6.12: Cylinder IC-1 - Plastic reference resistance, R_{pl}

This allows determination of the plastic reference resistance:

$$R_{pl} = 280.62 \text{ N/mm}^2$$

Relative slenderness:

$$\lambda_{ov} = \sqrt{R_{pl}/R_{cr}}$$

$$\lambda_{ov} = \sqrt{280.62/624.55} = 0.67$$

The characteristic imperfection amplitude:

$$\Delta w_k = \frac{1}{Q} \sqrt{\frac{r}{t}} t$$

$$\Delta w_k = \frac{1}{40} \sqrt{\frac{749.7}{3.52}} 3.52 = 1.28$$

For all Eurocode analyses it was assumed that the fabrication quality, Q , was excellent resulting in a value of $Q=40$.

The meridional elastic imperfection factor:

$$\alpha_x = \frac{0.62}{1 + 1.91(\Delta w_k/t)^{1.44}}$$

$$\alpha_x = \frac{0.62}{1 + 1.91(1.28/3.52)^{1.44}} = 0.43$$

Overall buckling reduction factor:

$$\chi_{ov} = 1 - \beta_{ov} \left[\frac{\lambda_{ov} - \lambda_{ov,0}}{\lambda_{ov,p} - \lambda_{ov,0}} \right]^{\eta_{ov}} \quad \text{when} \quad \lambda_{ov,0} \leq \lambda_{ov} \leq \lambda_{ov,p}$$

Where for meridional buckling:

$$\lambda_{ov,0} = 0.2 \quad \beta_{ov} = 0.6 \quad \eta_{ov} = 1$$

so;

$$\chi_{ov} = 1 - 0.6 \left[\frac{0.67 - 0.2}{1.03 - 0.2} \right]^1 = 0.66$$

The characteristic buckling resistance is then determined as:

$$R_k = \chi_{ov} R_{pl}$$

$$R_k = 0.66 \times 280.62 = 185.77 \quad N/mm^2$$

And the design buckling resistance:

$$R_d = R_k / \gamma_{M1}$$

$$R_d = 185.77 / 1.1 = 168.88 \quad N/mm^2$$

6.1.1.3 EN 1993-1-6 Eurocode GMNIA Method

For the buckling design by global numerical GMNIA analysis a required amplitude of the adopted equivalent geometric imperfection form, $\Delta w_{0,eq}$, was determined from the larger of:

$$\begin{aligned}\Delta w_{0,eq,1} &= l_g U_{n1} \\ \Delta w_{0,eq,2} &= n_i t U_{n2}\end{aligned}$$

where:

l_g is the relevant gauge length
 n_i is a multiplier to achieve an appropriate tolerance level
 ($n_i = 25$ is recommended)
 U_{n1} and U_{n2} are the dimple imperfection factors given in Table 4.6:

Which for Cylinder IC-1 resulted in an amplitude of the adopted geometric imperfection of $\Delta w_{0,eq} = 2.0548mm$. From this the imperfect elastic-plastic buckling resistance, R_{GMNIA} , was interpolated from the non-linear analyses of various imperfection amplitudes (Figure 6.11). As the amplitude of the adopted geometric imperfection is 2.0548mm, the equivalent (a/t) is:

$$2.0548/3.52 = 0.584$$

As this falls between the first and second data points in Table 6.3 the equation for this line is taken; this is:

$$y = -0.0294x + 0.8719$$

where x is 0.584, so:

$$y = -0.0294(0.584) + 0.8719 = 0.8547$$

The y-axis is $N_{cr}/N_{cr,perfect}$ (or R_{GMNA}/R_{GMNIA}), so to determine the equivalent R_{GMNIA} for the Eurocode amplitude of the adopted geometric imperfection the buckling resistance of the perfect cylinder ($R_{GMNA} = 263.07N/mm^2$) is multiplied by 0.855:

$$R_{GMNA} = 263.07 \times 0.855 = 224.85 \quad N/mm^2$$

The characteristic buckling resistance was then taken to be:

$$R_k = k_{GMNIA} R_{GMNIA} = 224.95 \quad N/mm^2$$

where k_{GMNIA} was taken to be 1, which will be further discussed in the comparison.

This results in a design buckling resistance for the GMNIA analysis as:

$$R_d = R_k/\gamma_{M1} = 204.5 \quad N/mm^2$$

6.1.2 Cylinder 1

Ring stiffened cylinder subject to hydrostatic pressure only. The stiffeners of this structure are located externally.

6.1.2.1 Linear Buckling Analyses

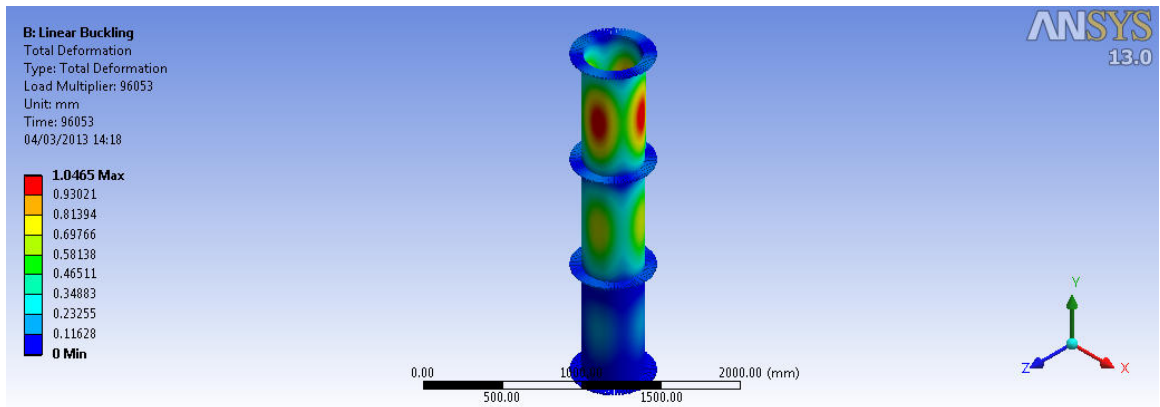


Figure 6.13: Cylinder 1 - Linear axial buckling

Table 6.4: Cylinder 1 - Ansys linear axial buckling

Linear Buckling - Axial Load		
Load multiplier	96053	
Buckling load	96053000	N
Buckling stress, R_{cr}	6167.212	N/mm^2

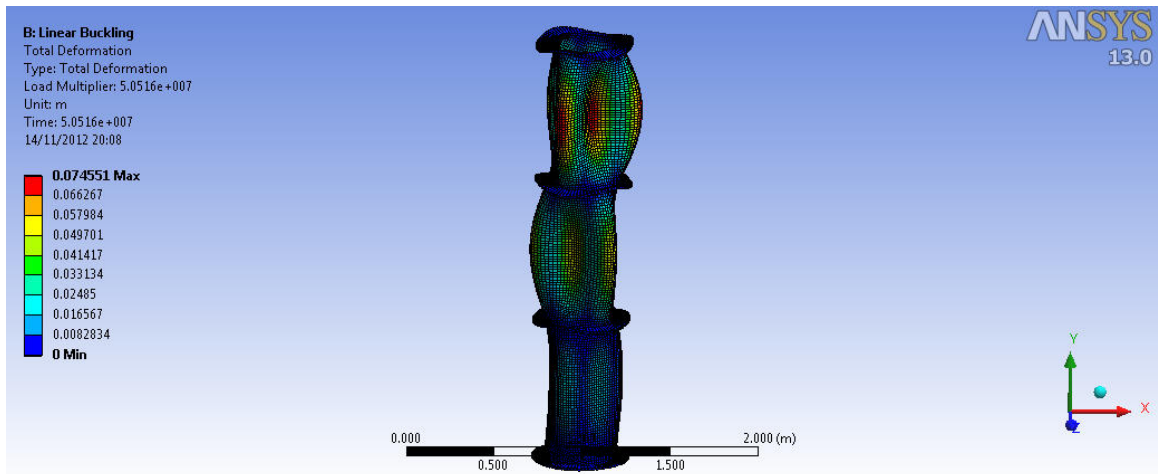


Figure 6.14: Cylinder 1 - External pressure buckling

Table 6.5: Cylinder 1 - Ansys external pressure buckling

Linear Buckling - Pressure Load		
Load multiplier	5.15E+07	
Buckling load	51526000	Pa
Buckling pressure	51.53	N/mm^2

6.1.2.2 Non-Linear Buckling Analyses

Table 6.6: Cylinder 1 - Amplitude vs. Buckling pressure

Deformation Factor	Amplitude (a/t)	Buckling ($N_{cr}/N_{cr,perfect}$)
1	0.08	1.00
10	0.80	0.95
25	1.99	0.84
50	3.98	0.68

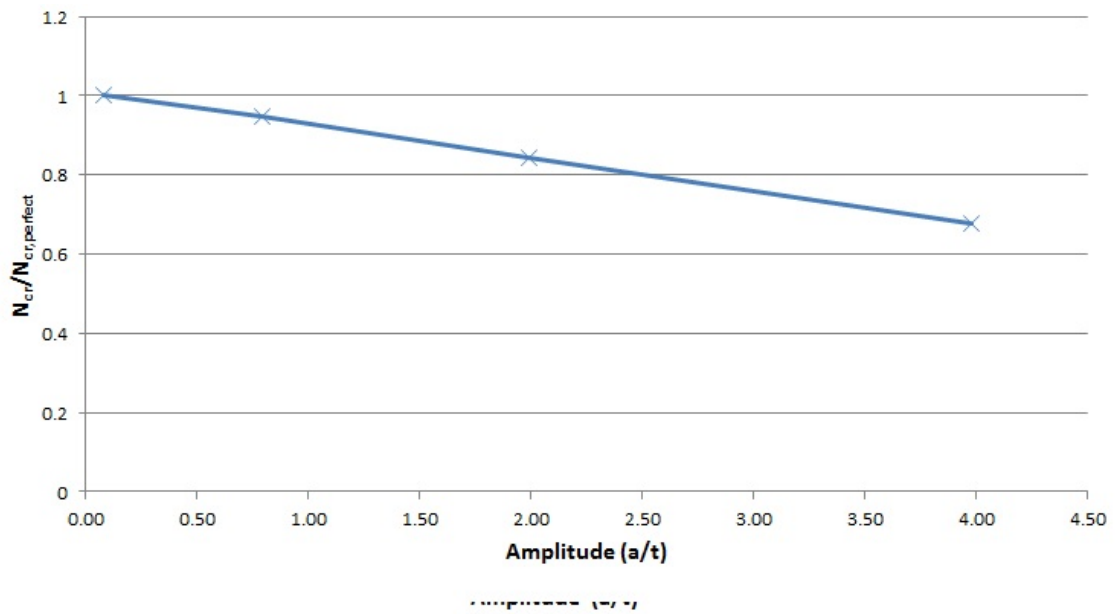


Figure 6.15: Cylinder 1 - Amplitude vs. Buckling pressure

6.1.2.3 EN 1993-1-6 Eurocode MNA/LBA Method

Plastic reference resistance is taken from an ANSYS analysis:

$$R_{pl} = 300.70 \text{ N/mm}^2$$

Relative slenderness:

$$\lambda_{ov} = 0.22$$

The characteristic imperfection amplitude:

$$\Delta w_k = 1.244 \text{ mm}$$

The meridional elastic imperfection factor:

$$\alpha_x = 0.58$$

Overall buckling reduction factor:

$$\chi_{ov} = 0.99$$

Characteristic buckling resistance:

$$R_k = 296.97 \text{ N/mm}^2$$

Design buckling resistance:

$$R_d = 269.97 \text{ N/mm}^2$$

6.1.2.4 EN 1993-1-6 Eurocode GMNIA Method

Amplitude of the adopted equivalent geometric imperfection form:

$$\Delta w_{0,eq} = 3.1425 \text{ mm}$$

Interpolated imperfect elastic-plastic buckling resistance:

$$R_{GMNIA} = 299.19 \text{ N/mm}^2$$

Calibration factor:

$$k_{GMNIA} = 1$$

The characteristic buckling resistance was then taken to be:

$$R_k = 297.21 \text{ N/mm}^2$$

Design buckling resistance for the GMNIA analysis:

$$R_d = 270.19 \text{ N/mm}^2$$

6.1.3 Cylinder 6.1 - First Eigenmode

Ring stiffened cylinder subject to combined radial pressure and axial loading.

6.1.3.1 Linear Buckling Analyses

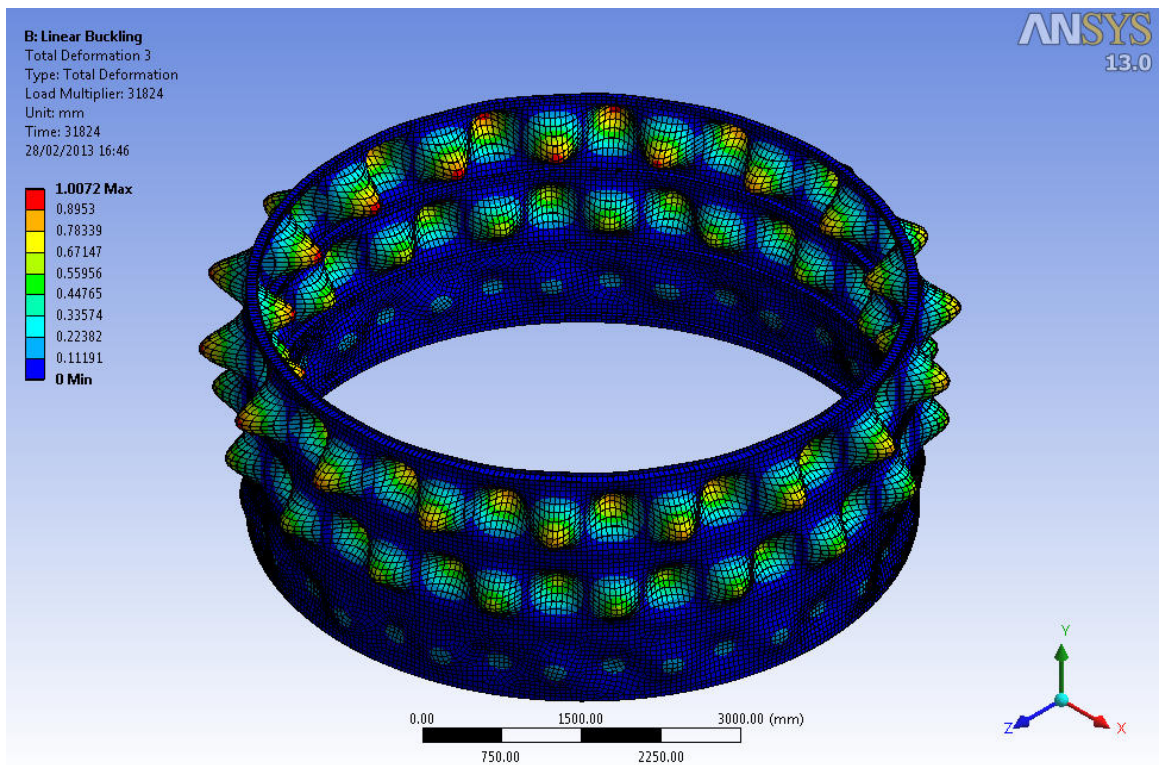


Figure 6.16: Cylinder 6.1 - Linear axial buckling

Table 6.7: Cylinder 6.1 - Ansys linear axial buckling

Linear Buckling - Axial Load		
Load multiplier	31706	
Buckling load	31706000	N
Buckling stress, R_{cr}	250.29	N/mm^2

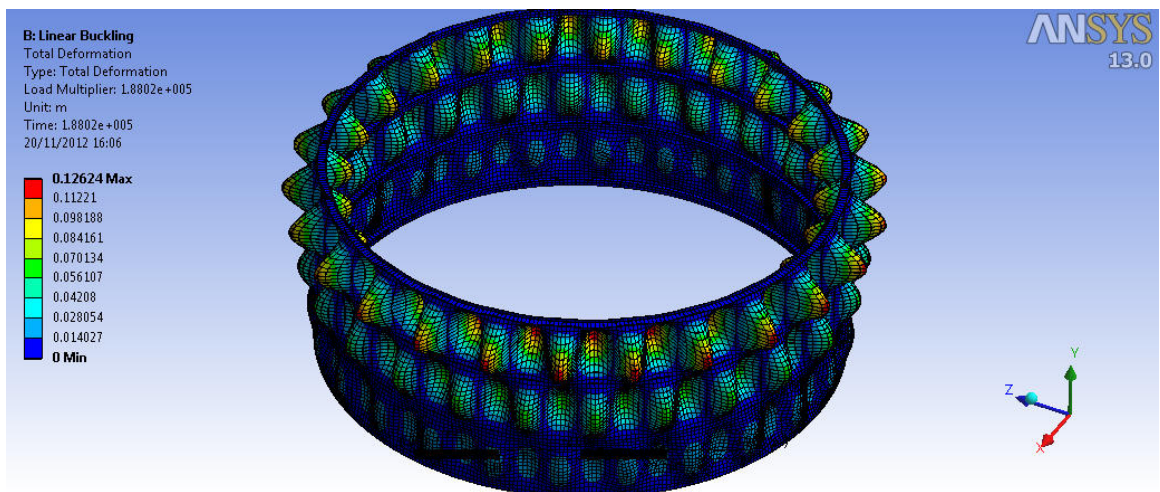


Figure 6.17: Cylinder 6.1 - External pressure buckling

Table 6.8: Cylinder 6.1 - Ansys Linear External Pressure Buckling

Linear Buckling - Pressure Load		
Load multiplier	1.88E+05	
Buckling load	188020	Pa
Buckling pressure	0.188	N/mm^2

6.1.3.2 Non-Linear Buckling Analyses

Table 6.9: Cylinder 6.1 - Amplitude vs. Buckling pressure

Deformation Factor	Amplitude (a/t)	Buckling ($N_{cr}/N_{cr,perfect}$)
1	0.16	1.00
5	0.79	1.00
15	2.36	1.00
20	3.15	1.00
50	7.88	0.99

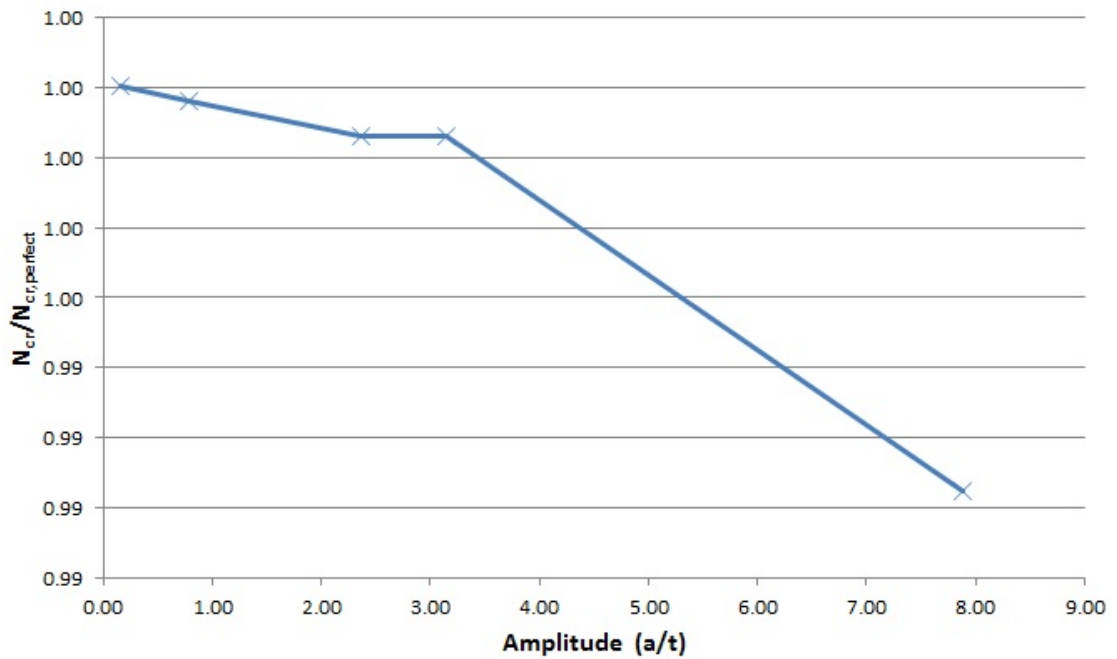


Figure 6.18: Cylinder 6.1 - Amplitude vs. Buckling pressure (first eigenmode)

6.1.3.3 EN 1993-1-6 Eurocode MNA/LBA Method

Plastic reference resistance is taken from an ANSYS analysis:

$$R_{pl} = 241.34 \text{ N/mm}^2$$

Relative slenderness:

$$\lambda_{ov} = 0.98$$

The characteristic imperfection amplitude:

$$\Delta w_k = 3.55 \text{ mm}$$

The meridional elastic imperfection factor:

$$\alpha_x = 0.34$$

Overall buckling reduction factor:

$$\chi_{ov} = 0.35$$

Characteristic buckling resistance:

$$R_k = 84.95 \quad N/mm^2$$

Design buckling resistance:

$$R_d = 77.23 \quad N/mm^2$$

6.1.3.4 EN 1993-1-6 Eurocode GMNIA Method

Amplitude of the adopted equivalent geometric imperfection form:

$$\Delta w_{0,eq} = 5.68mm$$

Interpolated imperfect elastic-plastic buckling resistance:

$$R_{GMNIA} = 186.73 \quad N/mm^2$$

Calibration factor:

$$k_{GMNIA} = 1$$

The characteristic buckling resistance was then taken to be:

$$R_k = 186.73 \quad N/mm^2$$

Design buckling resistance for the GMNIA analysis:

$$R_d = 169.75 \quad N/mm^2$$

6.1.4 Cylinder 6.1 - Second Eigenmode

The GMNIA analysis was performed using another eigenmode as the analysis above was very imperfection insensitive.

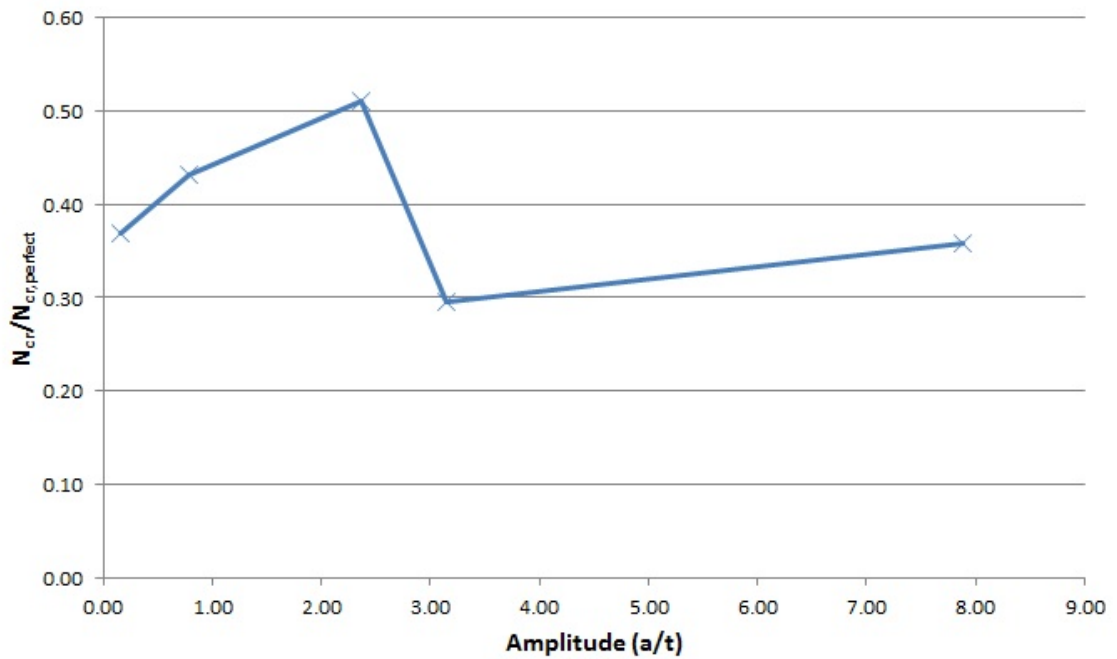


Figure 6.19: Cylinder 6.1 - Amplitude vs. Buckling pressure (second eigenmode)

6.1.4.1 EN 1993-1-6 Eurocode GMNIA Method

Amplitude of the adopted equivalent geometric imperfection form:

$$\Delta w_{0,eq} = 5.68mm$$

Interpolated imperfect elastic-plastic buckling resistance:

$$R_{GMNIA} = 81.95 \text{ N/mm}^2$$

Calibration factor:

$$k_{GMNIA} = 1$$

The characteristic buckling resistance was then taken to be:

$$R_k = 81.95 \text{ N/mm}^2$$

Design buckling resistance for the GMNIA analysis:

$$R_d = 74.5 \text{ N/mm}^2$$

6.2 Ring and Stringer Stiffened Cylinders

6.2.1 Cylinder IC6

Axial force alone.

6.2.1.1 Linear Buckling Analyses

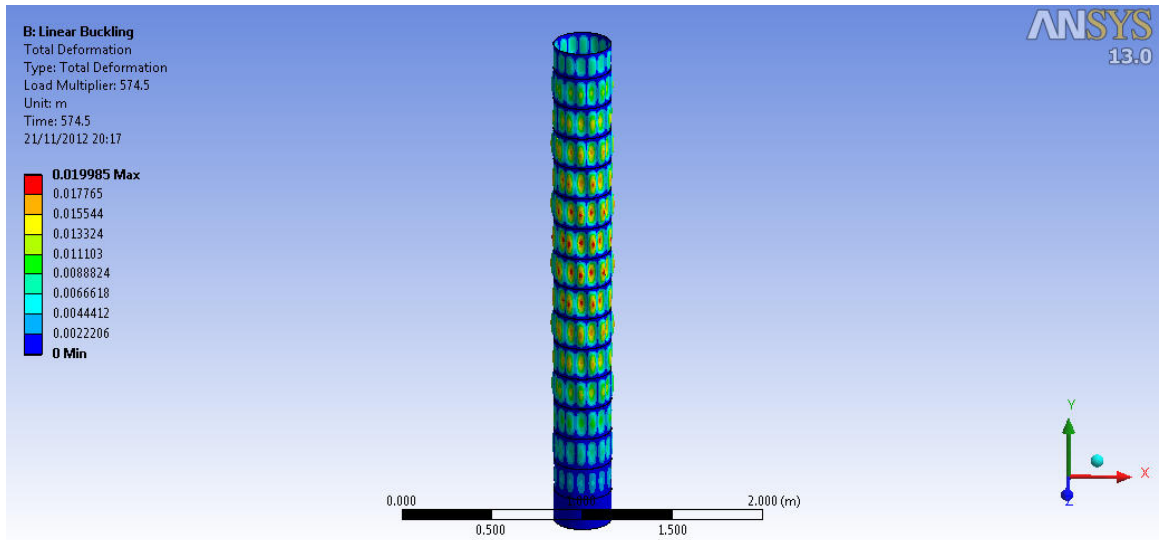


Figure 6.20: Cylinder IC6 - Linear buckling axial loading

Table 6.10: Cylinder IC6 - Ansys linear axial buckling

Linear Buckling - Axial Load		
Load multiplier	574.5	
Buckling load	574500	N
Buckling stress, R_{cr}	680.32	N/mm^2

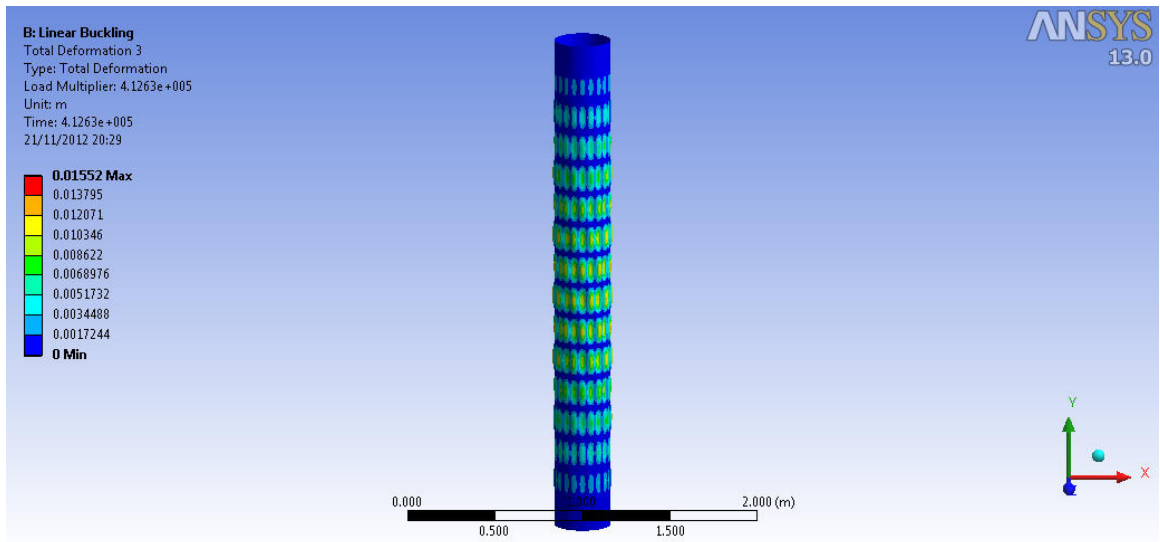


Figure 6.21: Cylinder IC6 - External pressure buckling

Table 6.11: Cylinder IC6 - Ansys external pressure buckling

Linear Buckling - External pressure		
Load multiplier	4.11E+05	
Buckling load	411160	Pa
Buckling pressure	0.412	N/mm ²

6.2.1.2 Non-Linear Buckling Analyses

Table 6.12: Cylinder IC6 - Amplitude vs. Buckling pressure

Deformation Factor	Amplitude (a/t)	Buckling ($N_{cr}/N_{cr,perfect}$)
1	1.19	1.02
5	5.95	0.90
10	11.90	0.53
20	23.81	0.53

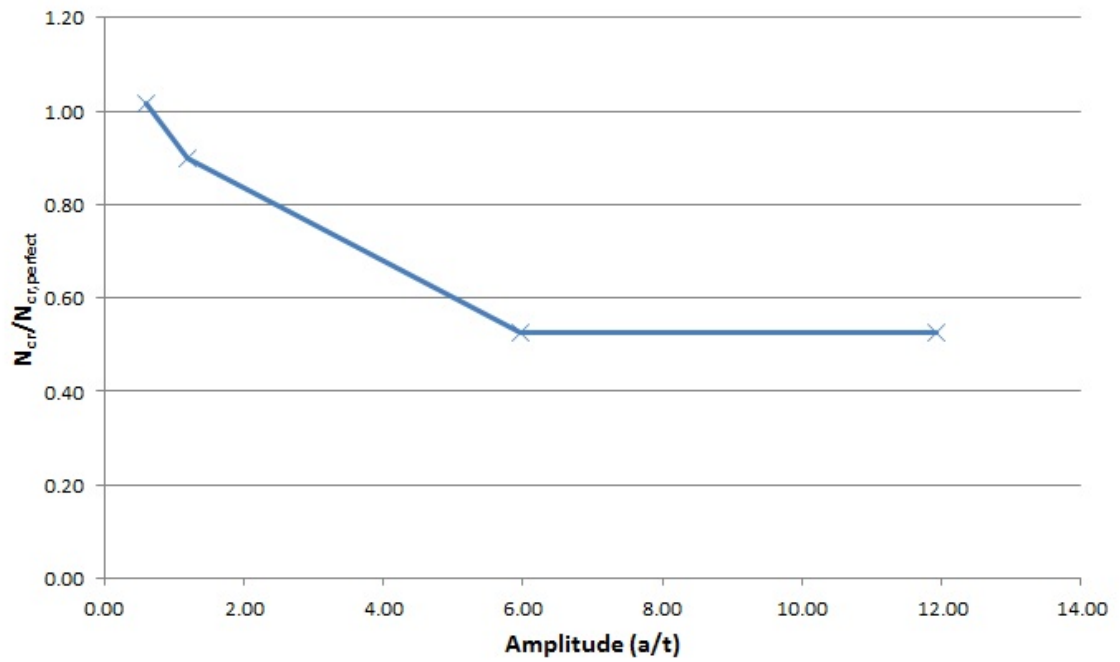


Figure 6.22: Cylinder IC6 - Amplitude vs. Buckling pressure

6.2.1.3 EN 1993-1-6 Eurocode MNA/LBA Method

Plastic reference resistance is taken from an ANSYS analysis:

$$R_{pl} = 339.38 \text{ N/mm}^2$$

Relative slenderness:

$$\lambda_{ov} = 0.71$$

The characteristic imperfection amplitude:

$$\Delta w_k = 0.29 \text{ mm}$$

The meridional elastic imperfection factor:

$$\alpha_x = 0.44$$

Overall buckling reduction factor:

$$\chi_{ov} = 0.46$$

Characteristic buckling resistance:

$$R_k = 217.73 \quad N/mm^2$$

Design buckling resistance:

$$R_d = 197.94 \quad N/mm^2$$

6.2.1.4 EN 1993-1-6 Eurocode GMNIA Method

Amplitude of the adopted equivalent geometric imperfection form:

$$\Delta w_{0,eq} = 0.46mm$$

Interpolated imperfect elastic-plastic buckling resistance:

$$R_{GMNIA} = 333.09 \quad N/mm^2$$

Calibration factor:

$$k_{GMNIA} = 1$$

The characteristic buckling resistance was then taken to be:

$$R_k = 333.05 \quad N/mm^2$$

Design buckling resistance for the GMNIA analysis:

$$R_d = 302.77 \quad N/mm^2$$

6.2.2 Cylinder 2-1C

Radial pressure alone.

6.2.2.1 Linear Buckling Analyses

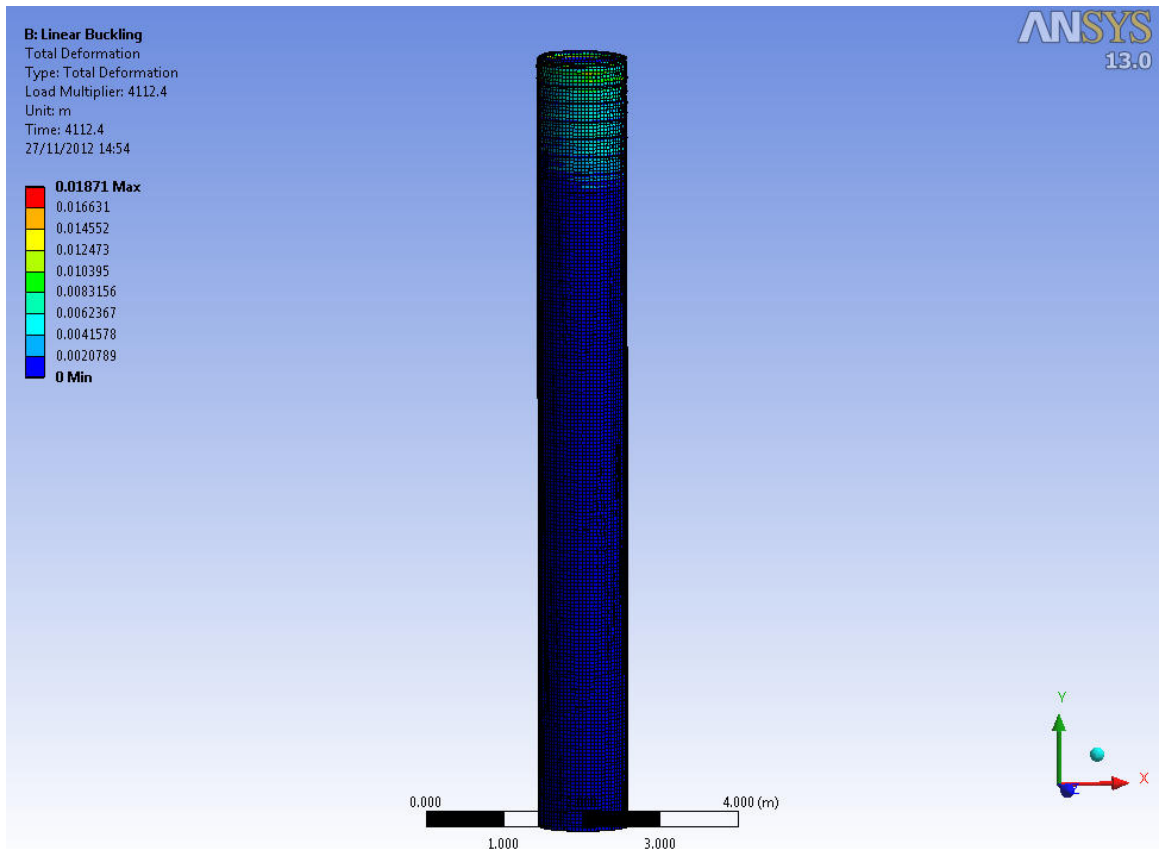


Figure 6.23: Cylinder 2-1C - Linear axial buckling

Table 6.13: Cylinder 2-1C - Ansys linear axial buckling

Linear Buckling - Axial Load		
Load multiplier	4112.4	
Buckling load	4112	N
Buckling stress, R_{cr}	584.41	N/mm^2

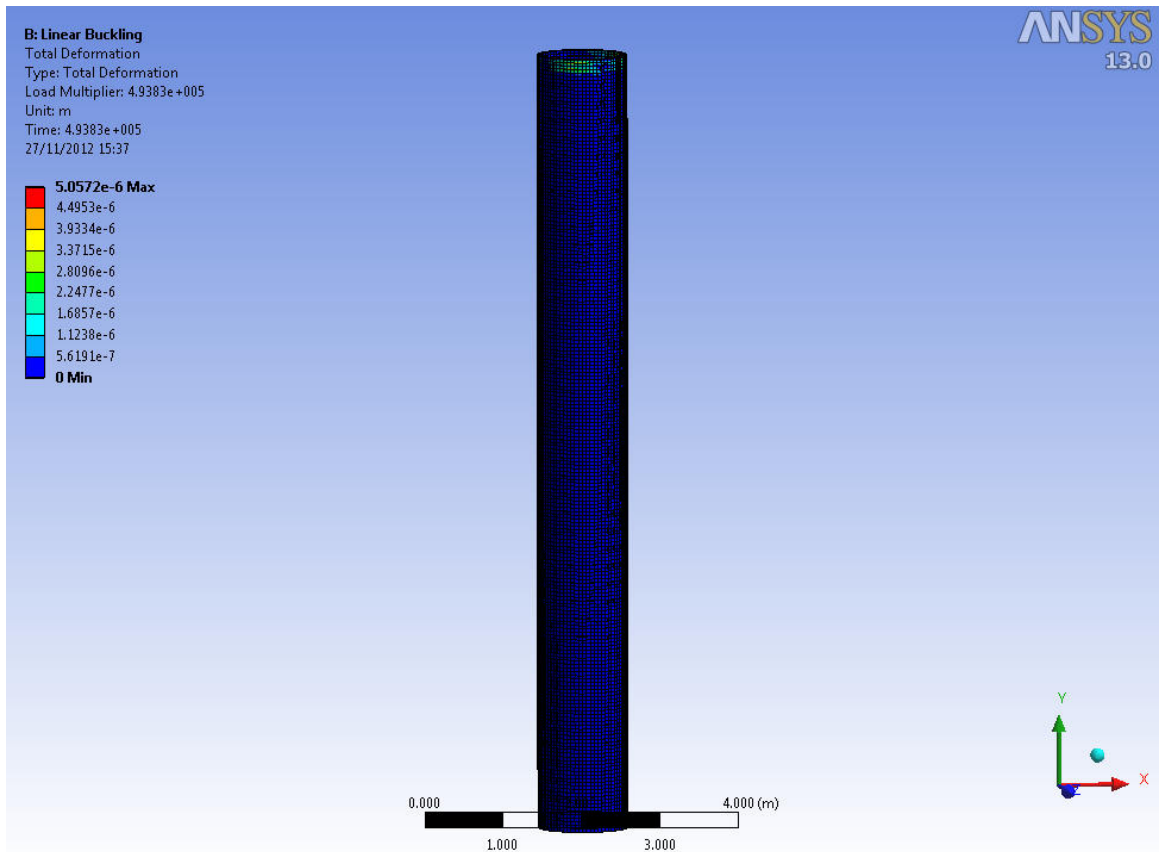


Figure 6.24: Cylinder 2-1C - External pressure buckling

Table 6.14: Cylinder 2-1C - Ansys external pressure buckling

Linear Buckling - External pressure		
Load multiplier	4.94E+05	
Buckling load	493950	Pa
Buckling pressure	0.494	<i>N/mm²</i>

Table 6.15: Cylinder 2-1C - Amplitude vs. Buckling pressure

Deformation Factor	Amplitude (a/t)	Buckling ($N_{cr}/N_{cr,perfect}$)
0.5	0.26	0.64
1	0.51	0.76
5	2.55	0.65
10	5.10	0.19
20	10.20	0.15

6.2.2.2 Non-Linear Buckling Analyses

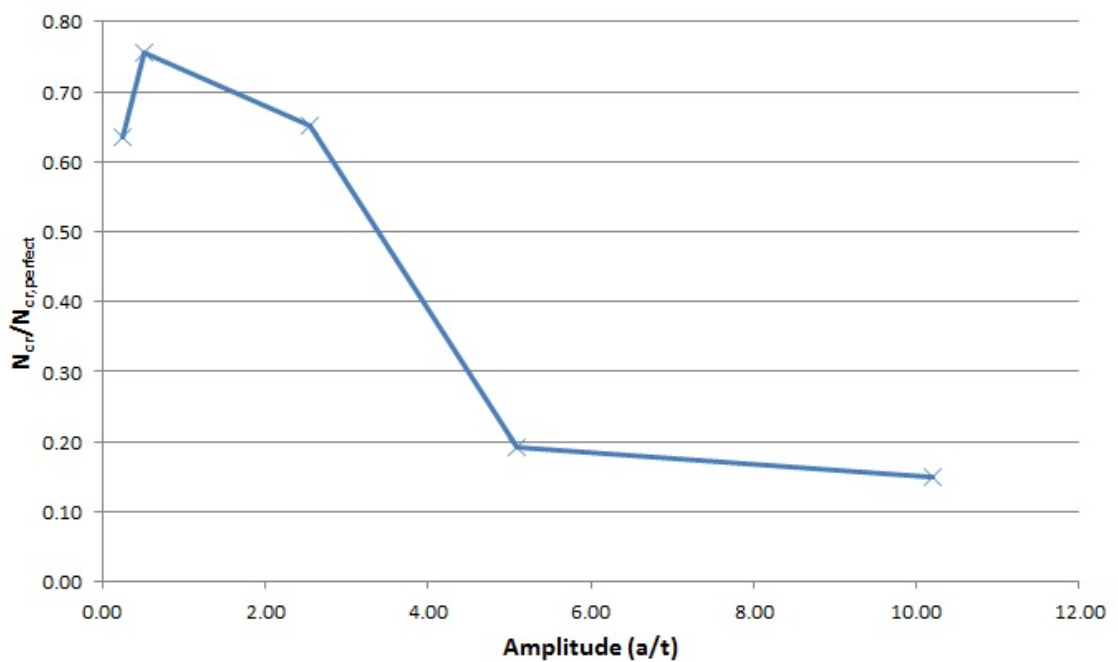


Figure 6.25: Cylinder 2-1C - Amplitude vs. Buckling pressure

6.2.2.3 EN 1993-1-6 Eurocode MNA/LBA Method

Plastic reference resistance is taken from an ANSYS analysis:

$$R_{pl} = 293.72 \text{ N/mm}^2$$

Relative slenderness:

$$\lambda_{ov} = 0.71$$

The characteristic imperfection amplitude:

$$\Delta w_k = 0.84mm$$

The meridional elastic imperfection factor:

$$\alpha_x = 0.40$$

Overall buckling reduction factor:

$$\chi_{ov} = 0.62$$

Characteristic buckling resistance:

$$R_k = 181.13 \text{ N/mm}^2$$

Design buckling resistance:

$$R_d = 164.66 \text{ N/mm}^2$$

6.2.2.4 EN 1993-1-6 Eurocode GMNIA Method

Amplitude of the adopted equivalent geometric imperfection form:

$$\Delta w_{0,eq} = 1.34mm$$

Interpolated imperfect elastic-plastic buckling resistance:

$$R_{GMNIA} = 79.65 \text{ N/mm}^2$$

Calibration factor:

$$k_{GMNIA} = 1$$

The characteristic buckling resistance was then taken to be:

$$R_k = 187.64 \text{ N/mm}^2$$

Design buckling resistance for the GMNIA analysis:

$$R_d = 170.58 \text{ N/mm}^2$$

6.2.3 Cylinder 2-1B

Combined loading of radial pressure and axial load.

6.2.3.1 Linear Buckling Analyses

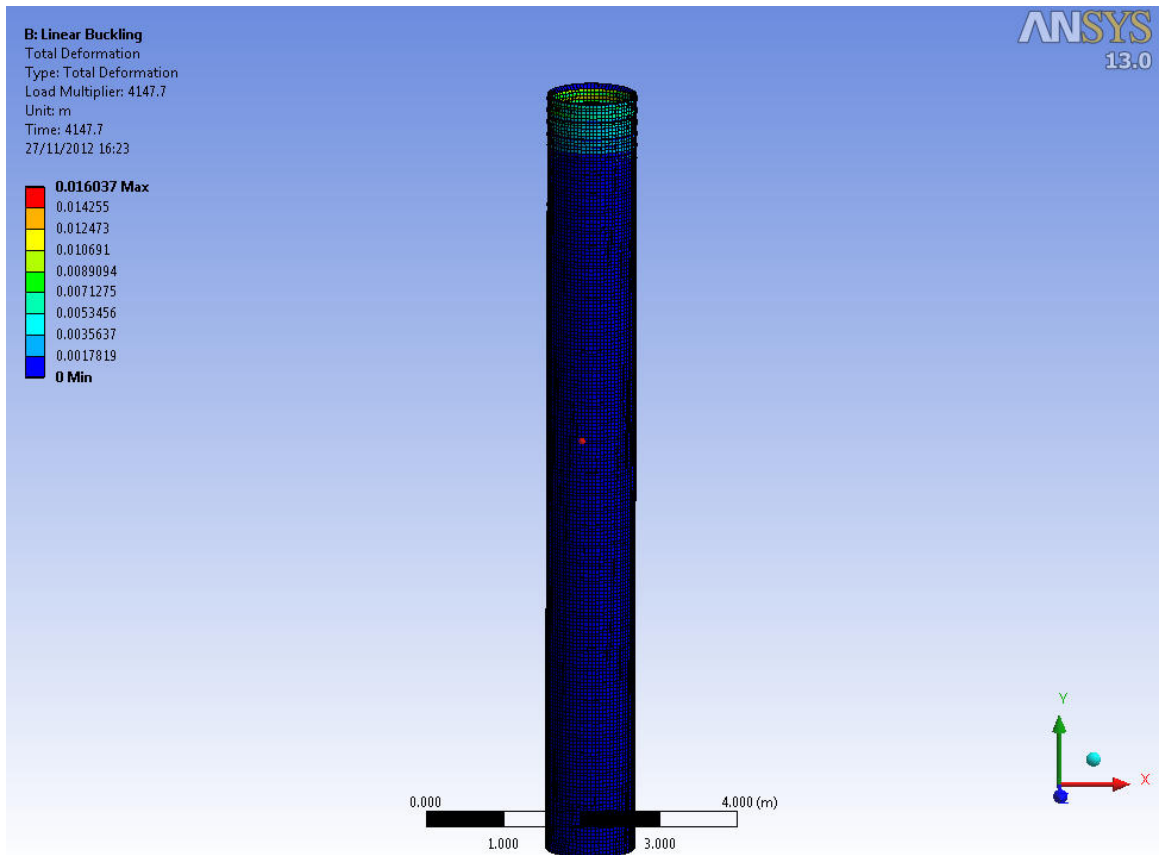


Figure 6.26: Cylinder 2-1B - Linear axial buckling

Table 6.16: Cylinder 2-1B - Ansys linear axial buckling

Linear Buckling - Axial Load		
Load multiplier	4147.7	
Buckling load	4147700	N
Buckling stress, R_{cr}	586.74	N/mm^2

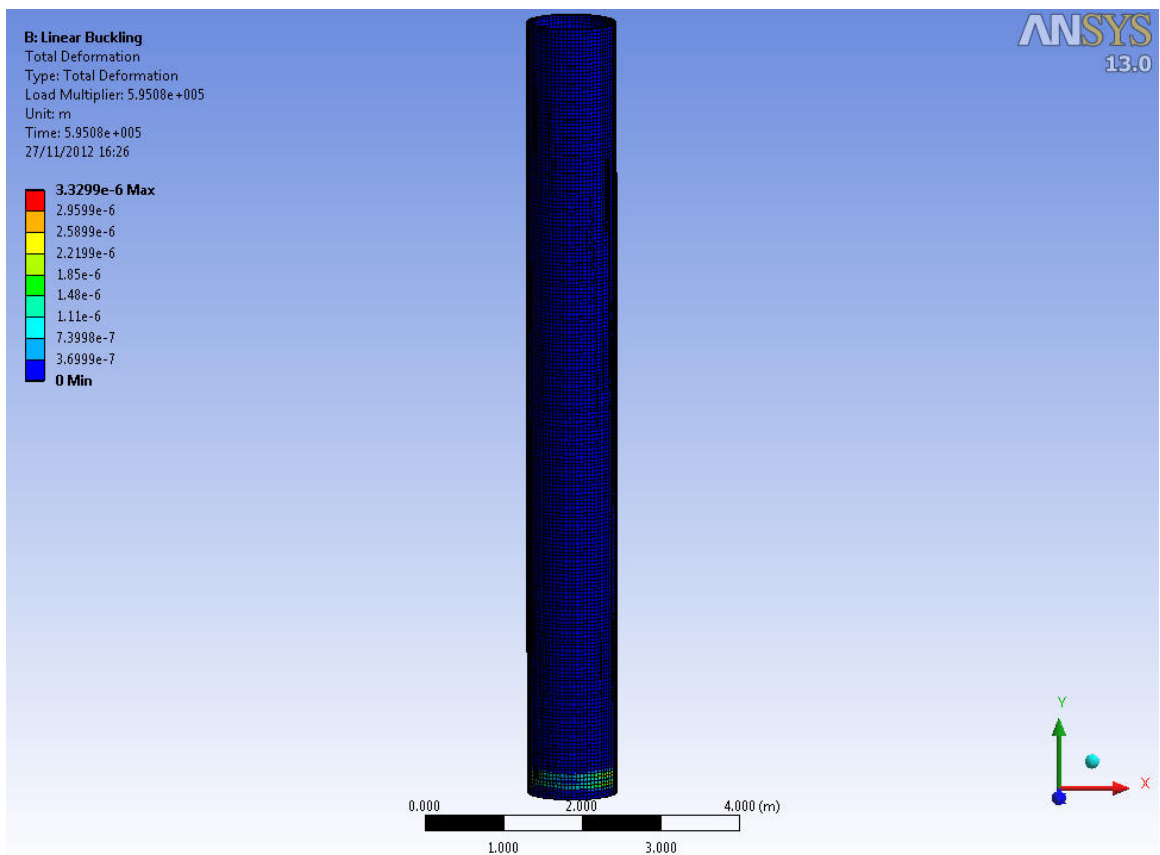


Figure 6.27: Cylinder 2-1B - External pressure buckling

Table 6.17: Cylinder 2-1B - Ansys external pressure buckling

Linear Buckling - External pressure		
Load multiplier	5.95E+05	
Buckling load	595080	Pa
Buckling pressure	0.595	N/mm^2

6.2.3.2 Non-Linear Buckling Analyses

Table 6.18: Cylinder 2-1B - Amplitude vs. Buckling pressure

Deformation Factor	Amplitude (a/t)	Buckling ($N_{cr}/N_{cr,perfect}$)
0.5	0.25	0.72
1	0.51	0.78
5	2.54	0.60
10	5.08	0.59
15	7.61	0.60

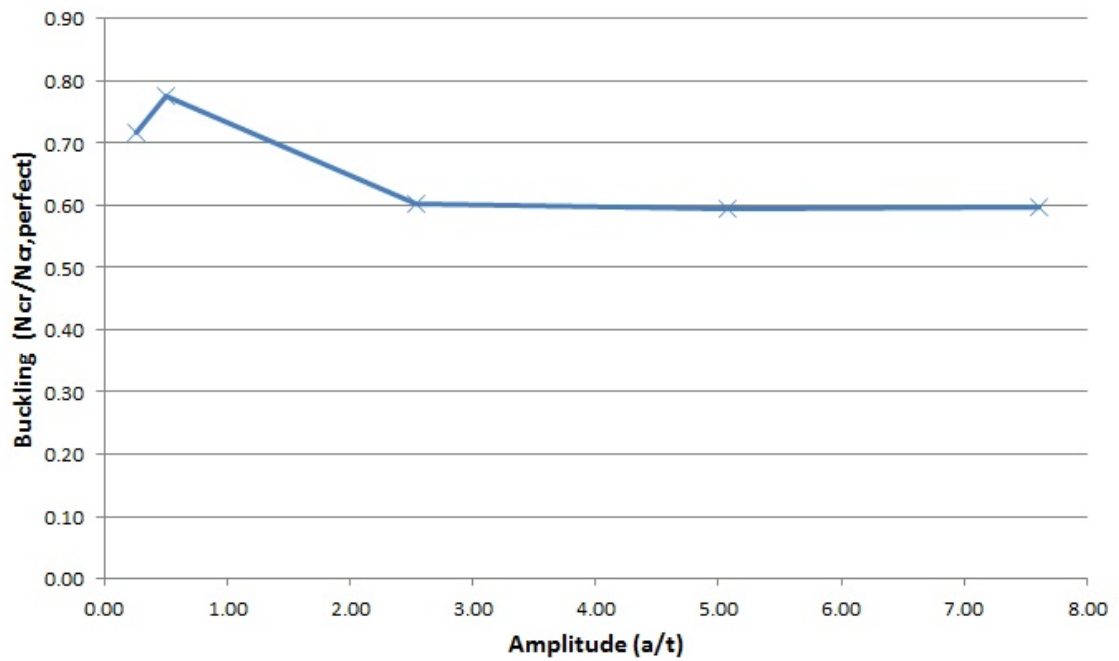


Figure 6.28: Cylinder 2-1B - Amplitude vs. Buckling pressure

6.2.3.3 EN 1993-1-6 Eurocode MNA/LBA Method

Plastic reference resistance is taken from an ANSYS analysis:

$$R_{pl} = 395.9 \text{ N/mm}^2$$

Relative slenderness:

$$\lambda_{ov} = 0.82$$

The characteristic imperfection amplitude:

$$\Delta w_k = 0.84mm$$

The meridional elastic imperfection factor:

$$\alpha_x = 0.40$$

Overall buckling reduction factor:

$$\chi_{ov} = 0.53$$

Characteristic buckling resistance:

$$R_k = 210.76 \quad N/mm^2$$

Design buckling resistance:

$$R_d = 191.60 \quad N/mm^2$$

6.2.3.4 EN 1993-1-6 Eurocode GMNIA Method

Amplitude of the adopted equivalent geometric imperfection form:

$$\Delta w_{0,eq} = 1.34mm$$

Interpolated imperfect elastic-plastic buckling resistance:

$$R_{GMNIA} = 252.69 \quad N/mm^2$$

Calibration factor:

$$k_{GMNIA} = 1$$

The characteristic buckling resistance was then taken to be:

$$R_k = 252.69 \quad N/mm^2$$

Design buckling resistance for the GMNIA analysis:

$$R_d = 229.72 \quad N/mm^2$$

6.2.4 Mesh Sensitivity

A mesh sensitivity analysis was not performed on the numerical analyses, however it is stated in Eglitis et al. (2009) that an element size to shell radius ratio of 1/20 was sufficient for their simulations. This ratio was met by all analyses.

7 COMPARISON

In this chapter the analytical and numerical methods for approaching shell design will be discussed. The results of the design code method and computational method chapters have been compiled here in Tables 7.1 and 7.2 for easy reference.

Table 7.1: Compiled axial loading results

Ring Stiffened				
Cylinder	IC1	1	6.1	
EN 1993-1-6	181.11	291.56	81.73	N/mm^2
ABS	175.14	293.03	60.2	N/mm^2
MNA/LBA	185.78	296.97	84.95	N/mm^2
GMNIA	224.85	297.21	81.95*	N/mm^2
Ring- and Stringer Stiffened				
Cylinder	IC6	2-1C	21-B	
EN 1993-1-6	215.38	175.06	177.55	N/mm^2
EN 1993-4-1	107.62	142.17	143.16	N/mm^2
ABS	327.25	383.63	386.16	N/mm^2
MNA/LBA	217.73	181.13	210.76	N/mm^2
GMNIA	333.05	187.64	252.69	N/mm^2

Table 7.2: Compiled external pressure loading results

Ring Stiffened				
Cylinder	IC1	1	6.1	
EN 1993-1-6	44.91	260.04	58.99	N/mm^2
ABS	53.14	235.23	61.72	N/mm^2
Ring- and Stringer Stiffened				
Cylinder	IC6	2-1C	21-B	
EN 1993-1-6	50.37	91.62	93.25	N/mm^2
EN 1993-4-1	39.99	68.66	71.06	N/mm^2
ABS	126.49	184.28	188.92	N/mm^2

* The value for the second eigenmode is shown here

7.1 Analytical Comparison

7.1.1 Ring Stiffened Cylinders

Firstly looking at the ring stiffened cylinder the characteristic axial buckling resistances are very similar when the Eurocode and the ABS code are compared. For cylinder IC1 the ABS code is 3.3% lower than the Eurocode, for cylinder 1 the ABS is 0.5% higher with the exception being cylinder 6.1 in which the ABS buckling resistance is 25.4% lower than the Eurocode.

The Eurocode and the ABS code both approach the design of non-stringer stiffened cylindrical shells similarly, i.e. the ABS takes the classical buckling stress and reduces it by a lower bound knock down factor dependent, where as the Eurocode determines the slenderness of the structure and knocks down the yield stress with a reduction factor. Though both methods are based on the same parameters, their implementation is slightly different. For instance, the ABS uses the traditional Batdorf parameter z which is replaced by the dimensionless length parameter ω in the Eurocode. The advantages of ω are that it is a non-dimensional length that increases linearly with increasing cylinder length and normalises the length relative to the characteristic dimensions that control the shell behaviour. As opposed to the Batdorf parameter which depends weakly on Poisson's ratio (Rotter; 2008).

$$z = \sqrt{1 - \nu^2}(l^2\sqrt{rt}) = \omega^2\sqrt{1 - \nu^2}$$

The length dependent factor, denoted C in the ABS and C_x in the Eurocode is required as the classical buckling stress for cylinders without it is valid for medium length cylinders. For short cylinders the length dependent parameter will increase the buckling resistance as when a cylinder length decreases, the model becomes increasing like an infinitely wide plate strip, whereas for long cylinders the buckling behaviour is closer to that of an Euler column (Timoshenko and Gere; 1961, p465-467). Interestingly, there are only two length domains in the ABS code with regard to C , the length dependent coefficient, which could be categorised as 'short' and 'medium'. The Eurocode states that once the cylinder becomes long enough that flexural buckling is dominant the procedures listed in EN 1993-1-6 and EN 1993-4-1 are no longer sufficient as flexural buckling is not covered and length dependant factor is limited to a maximum of 0.6 causing a plateau in the buckling strength as the length increases. In this case the designer is to consult the flexural buckling section in EN 1993-1-1. It can be seen in Figure: 7.1 that this Euler flexural buckling behaviour is also

not covered by the ABS code.

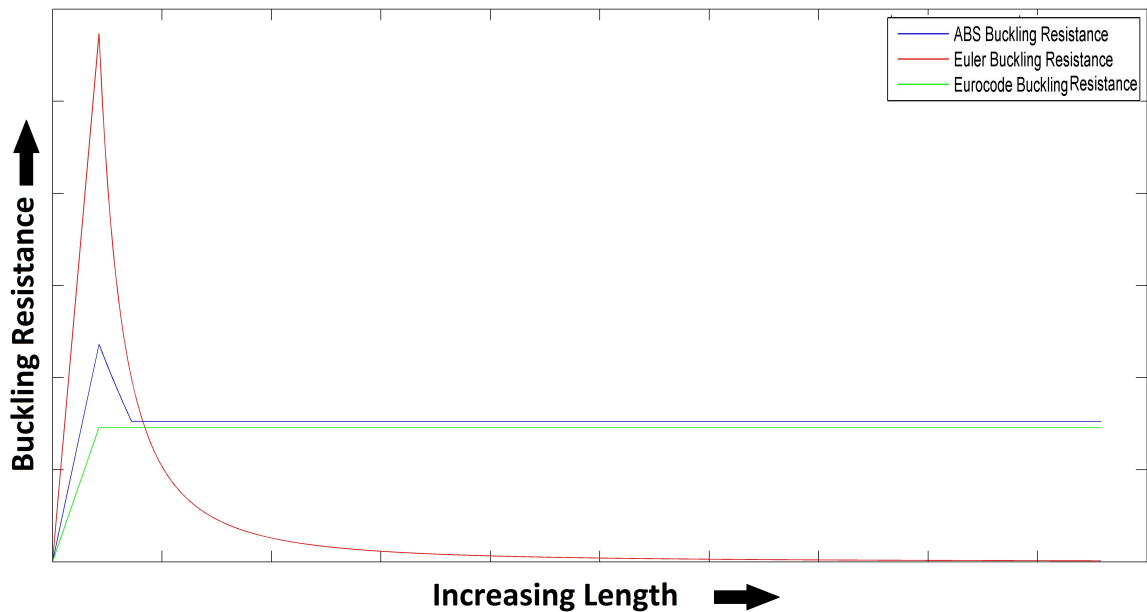


Figure 7.1: Buckling resistance vs. Increasing length

With regards to the difference between the Eurocode and the ABS code analytically determined buckling resistance for cylinder 6.1, the ABS code determines the buckling resistance to be 25.4% lower than that of the Eurocode value. Cylinder 6.1 is the most slender of the cylinders studied (see Figure: 8.9) so it is possible that the ABS code determines more conservative buckling resistances for more slender structures. However, this is one other difference between how the Eurocode and the ABS code analytical methods determine the buckling resistance, and that is the influence of the support conditions.

The Eurocode boundary conditions are absolutely defined as various degrees of fixed, pinned or free (see Table: 4.1) as opposed to the ABS code which takes the properties of the stiffeners into account. With the ABS code there are checks to ensure that the second moment of area of the stiffeners is sufficient, something that is not as rigorously defined within the Eurocode. For a chapter on cylindrical shells with ring stiffeners under external pressure the “Buckling of Steel Shells - European Design Recommendations” (2008, p331-347) uses the rules from the Deutscher Ausschluß für Stahlbau (Richtlinie; n.d.). As restraint of flexural buckling of the ring stiffeners is crucial in controlling the global buckling check of a

stiffened steel shell (ECCS, 2008) it is advisable for the Eurocode to adopt clearer and more stringent design requirements for the minimum stiffness of stiffeners. For example, the minimum stiffness of the stiffeners is clearly defined in the ABS code as follows:

The moment of inertia of the ring stiffeners, I_r , together with the effective length of shell plating, l_{eo} , should not be less than that given by the following equation:

$$I_r = \frac{\sigma_x(1 + \delta)tr_e^4}{500el} + \frac{\sigma_\theta r_e^2 lt}{2EK_\theta} \left(1 + \frac{z_e}{100r} \frac{E}{\eta\sigma_0 - \sigma_{\theta R}}\right)$$

where:

σ_x	=	compressive stress in longitudinal direction
σ_θ	=	compressive hoop stress midway between adjacent ring stiffeners
$\sigma_{\theta R}$	=	compressive hoop stress at outer edge of ring flange
δ	=	A_s/st
i_r	=	moment of inertia of the ring stiffeners with associated effective shell length, l_{eo}
l_{eo}	=	$1.56\sqrt{rt} \leq l$
r_e	=	radius to the centroid of ring stiffener, accounting for the effective length of shell plating
z_e	=	distance from inner face of ring flange to centroid of ring stiffener, accounting for the effective length of shell plating
K_θ	=	coefficient to account for the effect of ring stiffener
t	=	thickness of cylindrical shell
E	=	modulus of elasticity
σ_0	=	specified minimum yield point
A_s	=	cross sectional area of stringer stiffener
s	=	shell plate width between adjacent stringers
η	=	maximum allowable strength utilization factor for stiffened cylindrical shells subjected to external pressure

The moment of inertia of the stringer stiffeners, is, with effective breadth of shell plating, s_{em} , is not to be less than:

$$i_o = \frac{st^3}{12(1 - \nu^2)} \gamma_0$$

where:

$$\begin{aligned}\gamma_0 &= (2.6 + 4.0\delta)\alpha^2 + 12.4\alpha - 13.2\alpha^{1/2} \\ \alpha &= 1/s \\ \nu &= \text{Poisson's ratio}\end{aligned}$$

Using this ABS check, the ratio of the actual ring-stiffener stiffness, I_{rs} , to the minimum required ring-stiffener stiffness, I_r is tabled in Table: 7.3 where any value > 1 denotes that the stiffener meets the minimum stiffness requirements.

Table 7.3: Ring stiffener stiffness check

Cylinder	I_{rs}/I_r
IC1	24.2
1	0.88
6.1	0.29

It can be seen that cylinder 6.1 falls well below the minimum stiffness requirements for the ABS code but as the stiffness of the ring stiffener is not taken into account in the formulation of the buckling resistance for ring-stiffened cylinders under axial loading, it can be concluded that the ABS code determines more conservative buckling resistances for more slender cylinders.

The elastic-plastic stability interaction is dealt with in different ways in both codes, where the ABS defines a piecewise function that alters the critical buckling stress over a certain proportional limit of the yield stress. The Eurocode accounts for this in the formulation of the stability reduction factor χ , through determining the relative slenderness of the shell structure.

The relative slenderness is defined as a ratio of the plastic buckling resistance to the elastic buckling resistance. In the analytical case the plastic buckling resistance is taken as the yield stress of the material. The elastic buckling resistance is easily determined by the classical elastic buckling resistance equations, so:

$$\lambda = \sqrt{\frac{f_{y,k}}{\sigma_{R,cr}}}$$

The relative slenderness of a shell structure can fall within three ranges according to the Eurocode. The first range is when the slenderness is below the squash limit slenderness, λ_0 .

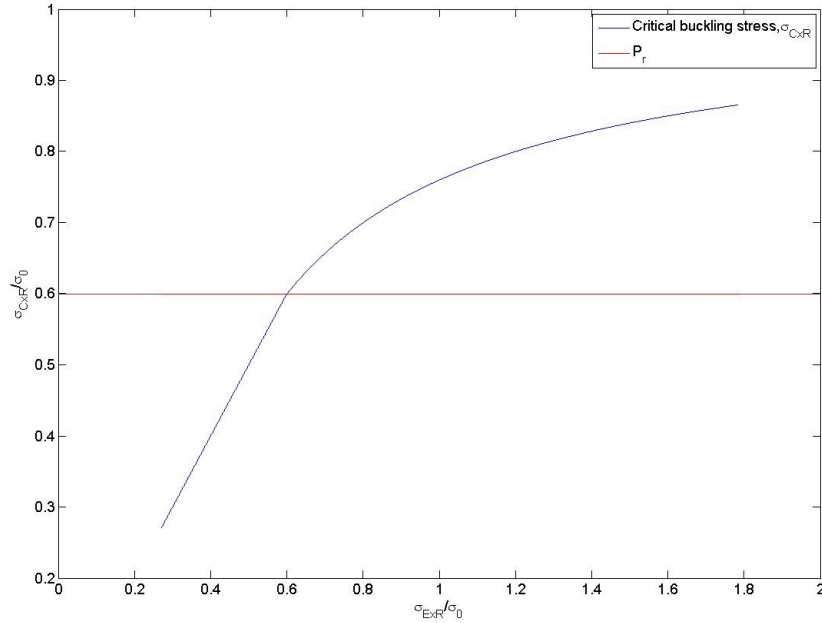


Figure 7.2: Effect of plasticity on critical buckling stress in ABS codes

In this range the reduction factor $\chi = 1$. In this range purely plastic behaviour is expected from the shell structure.

The next range that the relative slenderness may fall into is between the squash limit slenderness and the plastic limit slenderness, $\lambda_0 \leq \lambda \leq \lambda_p$. Within this range the structure is expected to show elastic, and plastic behaviour. In this range the reduction factor is determined by not only the plastic limit slenderness, λ_p , and the squash limit slenderness λ_0 , but also by the plastic range factor, β , and the interaction exponent, η .

The last region into which the relative slenderness may fall is when the relative slenderness is greater than the plastic limit slenderness, $\lambda_p \leq \lambda$. Within this region the structure behaves purely elastically. The most important and critical parameter for the reduction factor in this region is the elastic imperfection slenderness, α , known as the “knock-down” factor.

These parameters are experimentally determined and define the curve of the reduction factor (see Figure: 7.3). These factors are given for basic buckling cases in Annex D of EN 1993-1-6 and they may be altered adjusted based on other data but it is recommended that conservative values are used if they cannot be evaluated formally for the global system

under the loading types that may be featured in the design (Rotter; 2008, p.105). However, all these factors apart from the elastic imperfection factor may also be determined computationally (see Rotter 2005) allowing their use to become more case specific.

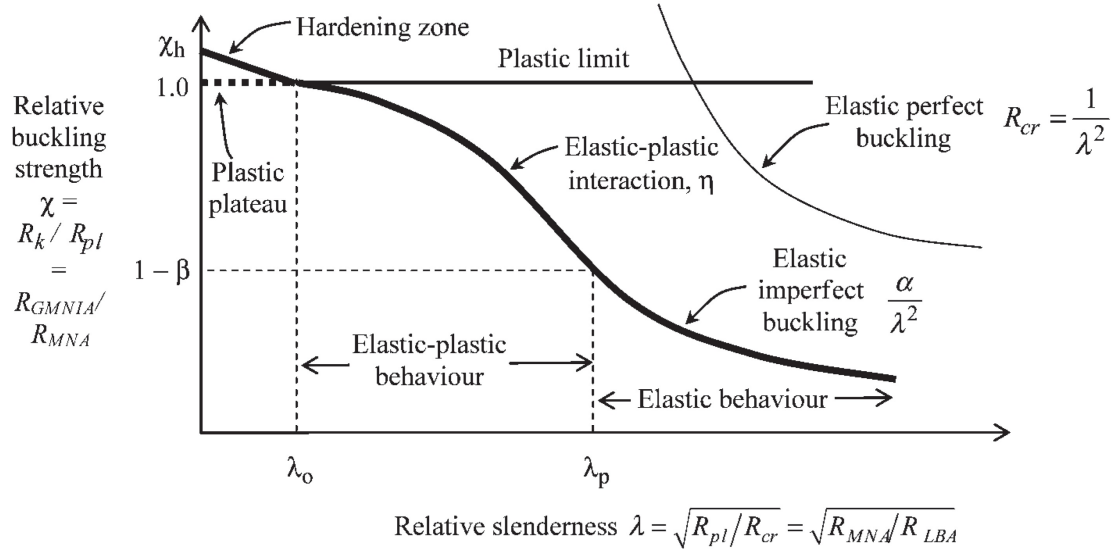


Figure 7.3: Capacity curve and parameters α , β , λ_0 and η (Rotter; 2007)

For the ring stiffened cylinder examples the ABS critical buckling stress for external pressure is also quite close to the Eurocode characteristic buckling resistance under external pressure. For cylinder IC1 the Eurocode buckling resistance is 15.5% lower than that of the ABS code, for cylinder 1 the Eurocode resistance is 9.5% higher and for cylinder 6.1 the Eurocode resistance is 4.4% lower.

This is interesting as both codes take different approaches. On the one hand the ABS derives an elastic hoop buckling stress for an imperfect cylindrical shell that is dependent on loading conditions (radial or hydrostatic pressure), length and slenderness parameters but also dependent on the strengthening effect of the ring stiffener which is determined by the structural properties of the stiffener. This is then knocked down by a constant lower-bound knock down factor. Similarly the derivation of this buckling stress is also a piecewise function to take into account the effects of plasticity.

The Eurocode on the other had uses the classical buckling stress of a cylinder subject to external pressure which is also adjusted dependent on a non-dimensional length, in this case ω , but also dependent on clearly defined boundary conditions. So as opposed to defining the stiffness of the ring stiffeners dependent on their structural properties they are categorised

as either; free, pinned, radially pinned, fixed etc. (See Table: 4.1).

The similarity of the buckling resistances under this loading condition is interesting as despite the fact that the ABS code takes into account the structural properties of the ring stiffeners but the Eurocode doesn't. Also, as can be seen in Table: 7.3 the minimum stiffness is not met by cylinder 1 and cylinder 6.1. The correlation of the results is due to the fact that despite the stiffness of the ring stiffener not being sufficient, the length between the ring stiffeners is large enough that the influence of these stiffeners does not come into effect. That is to say that the distance between the stiffeners is larger than the half wave length of the buckle. This is can be shown by examining the determination of the factor K_θ , which is the factor taking into account the ring stiffeners:

$$K_\theta = 1 - \frac{1 - k\nu}{1 + t(t_w + l\bar{\omega})/\bar{A}_R} G_\alpha$$

$$\bar{A}_R = A_R \left(\frac{r}{r_R}\right)^2$$

$$\bar{\omega} = \frac{\cosh 2\alpha - \cos 2\alpha}{\alpha(\sinh 2\alpha + \sin 2\alpha)}$$

$$\alpha = \frac{l}{1.56\sqrt{rt}}$$

$$G_\alpha = 2 \frac{\sinh \alpha \cos \alpha + \cosh \alpha \sin \alpha}{\sinh 2\alpha + \sin 2\alpha} \geq 0$$

$k = N_x/N_\theta$ for lateral pressure
 $= N_x/N_\theta + 0.5$ for hydrostatic pressure
 $A_R =$ cross sectional area of ring stiffener
 $N_x =$ axial load per unit length
 $N_\theta =$ circumferential load per unit length
 $r_R =$ radius to centroid of ring stiffener
 $t =$ thickness of cylindrical shell
 $t_w =$ stiffener web thickness
 $l =$ length between adjacent ring stiffeners (unsupported)

So, in order for $G_\alpha \geq 0$ then α must be less than $2.4l$. Which can only occur if the length between ring stiffeners is less than 2.4 times the theoretical half-wave length for external

pressure buckling. So, provided $1.56\sqrt{rt} < 2.4l$ the structural properties of the ring stiffeners have no influence.

7.1.2 Ring- and Stringer Stiffened Cylinders

Significant differences in the critical buckling resistances of the structures occur when ring-stiffeners and stringer stiffeners are present. The procedure to calculate the buckling resistance in the ABS code was mentioned previously in the methodology chapter, however the Eurocode states that for ring- and stringer-stiffened silo structures the cylindrical wall should be designed by the same criteria as the unstiffened wall or by the global analysis procedure in EN 1993-6-1 provided the spacing of the stringer stiffeners is greater than $2\sqrt{rt}$ (Clause 5.3.3.3 (1) EN 1993-4-1 *Eurocode 3 - Design of steel structures - Part 4-1: Silos* (2007)), which is the case for the three stringer stiffened structures studied.

It can be seen that the differences in buckling resistance is quite large if the stringer stiffened method in the ABS code is compared against the unstiffened Eurocode method. Alternative approaches are suggested in the Eurocode such as carrying the axial compression in the stiffeners alone, thus not taking into account the membrane action of the shell wall which is not of interest for this study. As such, another approach which is modified from the methods described in clauses 5.3.4.3.3(3) and 5.3.4.5(4) of EN 1993-1-4 was studied. These Eurocode methods are theoretical methods based on differential equations which take into account the structural properties of the stiffeners. These two clauses detail similar procedures for determining the meridional buckling resistance and the external pressure buckling resistance (Section: 4.2).

The results of the modified Eurocode method, which takes into account the geometrical properties of the stiffeners, were studied (labelled EN 1993-4-1 in Tables: 7.1 and 7.2). The buckling resistances under axial compression and uniform external pressure are reasonable, yet conservative, values. No examples of their use could be found so the results of the calculations performed were verified by calculating and comparing the ω values from the two different Eurocode axial loading methods (Equations: 4.1 and 4.30). As these values matched it was deemed that the calculations were performed correctly and that the results are correct.

The Eurocode states that when vertical stiffeners are present and the spacing of the stiffeners is less than $2\sqrt{rt}$ then the cylinder is to be designed in the same manner as an unstiffened

shell or through the global analysis procedures of EN 1993-1-6, however, the fundamental theory is there to allow the development of an analytical process to determine the buckling resistance of ring and stringer stiffened cylindrical shells.

A similar method to the modified Eurocode approach taken in this study is used in Rotter (2008, p.353-363) to determine the buckling resistance of cylindrical shells under longitudinal compression but which does not take into account the effect of the ring stiffeners. The range of applicability of the method adopted in the “*Buckling of Steel Shells - European Design Recommendations*” 2008 limits the degree of stiffening to:

$$\frac{A_s}{bt} \leq 2$$

$$\frac{I_s}{bt^3} \leq 15$$

$$\frac{I_{ts}}{bt^3} \leq 2.4$$

where:

- A_s is the area of the stringer stiffener
- b is the separation between stiffener centres
- I_{ts} is the uniform torsion constant (Saint-Venant’s torsion) of a stiffener
- t is the thickness of the cylindrical shell

It is also stated that “for shells that are more heavily stiffened than [these conditions] there do not appear to be enough test results to formulate precise rules” (Rotter; 2008). In comparison, the ABS method which is semi-empirical is based around theoretical buckling stresses but has indeed been calibrated using experimental data. So, some experimental data required to make such rules for the Eurocode does exist, but it may be possible that the Eurocode committee deemed this data to be insufficient. Regardless, it seems as though the development of an analytical approach that takes the stringer stiffeners into account would be a useful addition to the Eurocode.

7.2 Computational Comparison

7.2.1 Ring-stiffened Cylinders

Comparing the results of the computational analyses to that of the design codes we see that there is quite a close correlation when examining the cylinders without stringer stiffeners. The characteristic buckling resistances determined from both the LBA/GMNA and the GMNIA analyses tend to be slightly higher values than those obtained in the codes.

The MNA/LBA analysis are between 1.8% and 3.8% higher than the Eurocode analytical methods for determining the buckling resistance. This increase in buckling resistance is unexpected as the MNA/LBA method is virtually identical to the Eurocode analytical method apart from the fact that using the MNA/LBA method the relative slenderness is obtained computationally. If it is recalled that;

$$\lambda = \sqrt{\frac{f_{y,k}}{\sigma_{R,cr}}}$$

and numerically:

$$\lambda = \sqrt{\frac{R_{pl}}{R_{cr}}}$$

and it was seen in Section: 6.1.1 that with a sparser mesh the classical elastic buckling resistance, R_{cr} , derived from the numerical analysis is higher than that of the classical theory, $\sigma_{R,cr}$. So, as R_{pl} is very close to the yield stress of the material, $f_{y,k}$ it can be concluded that the relative slenderness that was determined numerically is slightly lower than that of the analytical method, resulting in a slightly higher reduction factor (i.e. less of a reduction) and therefore a slightly higher numerically determined characteristic buckling resistance.

A large discrepancy in the numerical buckling resistance results can be seen with the GMNIA analysis for cylinder 6.1's first eigenmode where the GMNIA buckling resistance is much higher than any other method, in fact it is 128.5% higher the Eurocode analytically determined buckling resistance. This could well be due to the apparent imperfection insensitivity of cylinder 6.1. It is possible that if the calibration factor k was used in this study the value would be outside the accepted range ($0.8 < k_{GMNIA} < 1.2$), thereby deeming the analysis invalid.

This result is considerably different than any other resistance determined for the same struc-

ture so there is little confidence that this is the correct characteristic buckling resistance. It should be noted that cylinder 6.1 falls into the elastic relative slenderness range i.e. the overall slenderness of this structure is greater than the plastic limit relative slenderness λ_p meaning its behaviour is within the heavily knocked down elastic imperfect buckling range. As such, another study was performed using geometric imperfections based around another eigenmode. The results of this second analysis are much closer to the analytical buckling resistances and 56.1% lower than the first eigenmode buckling resistance which reiterates how important it is to make sure that the most detrimental geometrical imperfection is used and illustrates the importance of having an expectation of the behaviour of your structure before it is computationally analysed.

7.2.2 Ring- and Stringer-stiffened Cylinders

The computational buckling resistances become quite different to the design code resistance once stringer stiffeners are introduced. The ABS code resistances are much higher than those of the computational models or the Eurocode as neither the ANSYS models nor the Eurocode incorporated the stringer stiffeners into their buckling resistance formulation. So the numerical analyses can only be compared to the Eurocode analytical method. Once again we see that the MNA/LBA determined buckling resistances are higher than the Eurocode analytically determined buckling resistance, as there have been no other changes this difference is still likely due to the reason given above.

Table 7.4: Numerical buckling resistance comparison table

Cylinder	IC6	2-1C	21-B	
Eurocode	215.38	175.06	177.55	N/mm^2
MNA/LBA	217.73	181.13	210.76	N/mm^2
GMNIA	333.09	187.67	252.69	N/mm^2

The GMNIA analyses buckling resistances do not correspond so well for these 3 case study cylinders. In fact for cylinder IC6 the GMNIA result is 54.7% higher than the Eurocode analytical method and for cylinder 21-B the GMNIA result is 42.3% higher. This is likely due to the same reason that a higher buckling resistance was found for cylinder

6.1, that is that the imperfection modelled was not as detrimental as the real imperfections used in the determination of the lower-bound knock-down factor. Given more time it would have been appropriate to analyse more imperfections types.

8 DISCUSSION

8.1 General Discussion

It can be said that there are two approaches to shell design. One in which a shell structure is designed to be purely functional, the other in which the shell structure is optimised. Taking the Eurocode approach to analytically designing the stringer stiffened cylindrical shells for instance; this approach is purely functional. The potential buckling resistance of a ring and stringer stiffened shell is drastically under estimated in comparison to the buckling resistance which can be derived by the American Bureau of Shipping code. To design a structure around this conservative resistance is under utilising the potential load resistance of the structure. Though the design may be safer, the result is a conservative design with an inefficient usage of materials with probable higher costs. In terms of more geometrically complex structures this underestimation of the strength could potentially increase the cost of the project significantly as the scale of the structure could be much larger. As such, an alternative to purely functional design would be recommended.

Such an alternative is optimised design. This method would utilise complex analyses, such as the Eurocode GMNIA method to design shell structures. The significant disadvantage of using complex numerical methods to optimise the design of shell structures, however, is the computational time required. As seen from this study, incorrectly modelling of imperfections can result in overestimating the buckling resistance of shell structures. In order to get an accurate representation of the buckling resistance of the shell structure numerous imperfection studies must be performed. If structural elements (such as supports) were then to be repositioned in the model in order to determine the most optimal support configuration then these imperfection studies must be run for each configuration further increasing the computation time and further more imperfection sensitivity analyses should be run for each type of imperfection. It can be seen that more the design is to be optimised, the greater the number of analyses that must be run (see Figure: 8.1 as the number of support configurations go from 1 to j , the number of imperfection types go from 1 to k and the number of amplitudes analysed go from 1 to n the complexity of the computational design approach

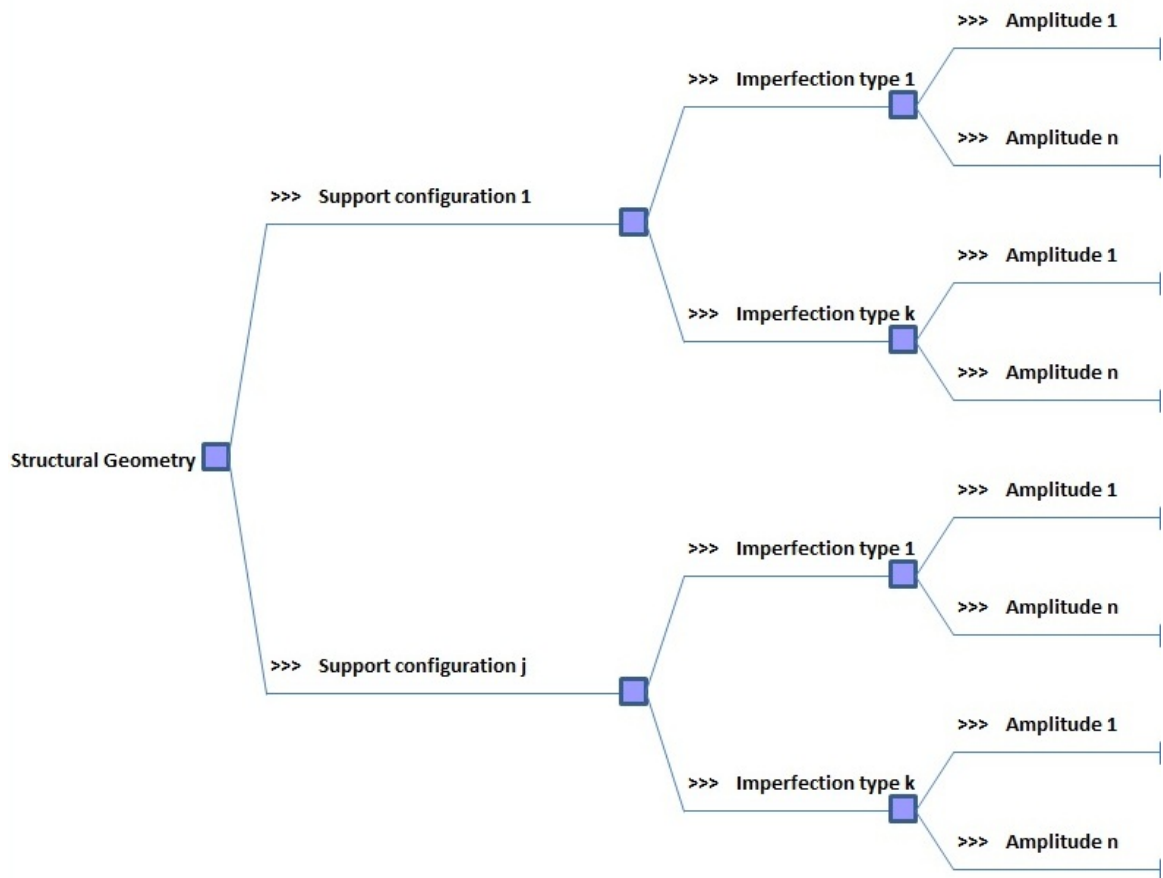


Figure 8.1: Analysis tree for optimised design

significantly increases). With such potential increases in computation time the decision to optimise the design of a structure must be justified. This justification can be based on:

- Economics or;
- Consequence of failure

If the structure, for example a silo, is to be mass produced then it may be prudent to optimise the design so that the cost per unit is as low as possible while still meeting the safety criteria. This would result in a lower net financial cost for the production of this structure. Alternatively if the shell structure contains hazardous materials and people or the environment may be at risk then it is logical to accurately determine the resistance of the structure so that this resistance will not be exceeded. Similarly, if a geometrically complex shell structure were to have people inside the structure and if their lives were to be at risk if the

structure fails then it would be wise to design the structure in such a way that the buckling resistance is accurately known, and that the expected loading conditions will not exceed this resistance.

The time required to design a shell structure optimally may be reduced by experience. Say for instance if the designer knows what method a structure will fail and the approximate critical load at which failure occurs prior to running a numerical analysis. In this case, a numerical analysis is more of a tool to confirm the suspected failure mode and to give a more accurate critical buckling load. This approach is best illustrated using cylinder 6.1 as an example. The initial full GMNIA procedure that was run using the first eigenmode as a pre-deformed shape resulted in a characteristic buckling resistance of $186.73N/mm^2$. However, when looking at the characteristic buckling stresses determined by the design codes which are based on experimental data we get values of $81.73N/mm^2$ and $60.2N/mm^2$ from the Eurocode and ABS code respectively. These values are 44% of and 32% of the finite element analysis determined buckling stress which is quite a significant difference. Similarly, the characteristic buckling resistances for cylinder IC6 and cylinder 21-B were higher than expected in the GMNIA analyses when compared to the analytical analyses. The numerical analyses performed to obtain the critical buckling stresses were the full analysis including material non-linearity and geometric imperfections and, had it not been known to expect a lower value, an inexperienced engineer may make the error of using this higher characteristic buckling load. In reality an engineer should double check that the obtained characteristic buckling load from the numerical analysis is the lowest critical value by running multiple analyses but it may also be the case that familiarity breeds complacency as in each of the other finite element analyses run on ring stiffened cylinders, the first eigenmode was sufficient.

The Eurocode includes a check to ensure that these errors do not occur by using the calibration factor, k . This calibration factor was described previously but to reiterate the numerical critical buckling stress is to be compared to the known buckling stress of a similar structure and if this ratio falls outside the range of $0.8 < k < 1.2$ the numerical result is deemed invalid. This calibration factor is a good check for simple shells upon which many experiments have been performed, but when analysing more geometrically complex shell structures where there may be no precedent its usefulness comes into question. The computational model may be compared to scale model tests, but then the question arises as to whether the scale model tests accurately describe the structural behaviour of the full

size structure. The necessary load combinations, imperfections, supports may be far more accurately modelled computationally as opposed to modelled by a scaled down structure. This leads to the second approach to designing shell structures; rigorously designing the structures computationally.

The experience built up from this study of singly curved cylindrical steel shells structures has provided a foundation upon which the design of more complex shells can be based. The critical aspects of simple shell design must be fully understood before the designer can confidently approach the design of more complex cases. As well as this the designer must also become competent with the computational programs required to perform the numerical analyses. It could be said that the understanding of shell behaviour and the competency with finite element programs go hand in hand as in order to have confidence in the numerically determined results, there is a certain amount of experience required to interpret if these results are correct.

8.2 Computational Method Discussion

8.2.1 The MNA/LBA Method

The usefulness of the MNA/LBA method in this study was limited, this is due to the geometry and the load case examined. The aspect that separates the MNA/LBA analysis apart from the Eurocode analytical method is that the relative slenderness is determined numerically. In the case of a uniformly compressed, axially loaded cylinder, the elastic buckling stress is easy to determine through theory and the plastic buckling stress in this study was typically found to be approximately the buckling stress. As such, the MNA/LBA analysis had no benefits over the Eurocode analytical approach and was in fact, more time consuming.

The MNA/LBA analysis becomes useful in the case when the elastic buckling load or plastic buckling load are not so easy to determine, such as asymmetric loading or more complicated geometry. The buckling parameters used in the determination of the reduction factor also open the MNA/LBA analysis up to more complex shapes provided that these buckling parameters have been determined for such geometry. With more complex or freeform geometry the numerical method would be required to determine the elastic and plastic buckling resistances and from these the relative slenderness could be determined.

Assuming the buckling parameters are already known for the structure or structural ele-

ment being analysed, this means that only two numerical analyses are required; one for the elastic resistance, the other for the plastic resistance. Comparing this to the GMNIA method, this is a great reduction in the required computation time.

The critical point regarding the applicability of the MNA/LBA analysis is that the buckling parameters must be pre-defined. This makes this method suitable for the mass production of particular shells or shell panels. If the manufacturer mass produces certain shells or panels, then it would be interesting if there was a standardisation in the determination of the buckling parameters. If this were the case, the buckling parameters could be supplied by the manufacturer to the design engineer to simplify the analysis process and to save computation time. With these buckling parameters at hand, the design engineer would not be required to resort to GMNIA analyses if it is not felt that such time consuming analyses are justified.

Knowing the buckling parameters and being able to determine the relative slenderness also has advantages of its own.

8.2.1.1 Relative Slenderness

The determination of the relative slenderness in the Eurocode method is a useful tool in determining the expected buckling behaviour of the shell structure. Taking cylinder 1, which is the least slender cylinder out of those studied, and cylinder 6.1, which is the most slender the expected buckling behaviour can be shown through the non-linear finite element analysis.

Cylinder 1 has a relative slenderness, λ_{ov} , of 0.22. This places it very close to the squash limit relative slenderness λ_0 of 0.2. As such, we expect to a significant influence of plasticity and stresses equal to or higher than (due to plastic strain hardening) the yield stress of $301N/mm^2$. This is illustrated graphically in Figures 8.3 and 8.2.

Buckling in these shell structures occurs when the analysis fails to converge, so the characteristic buckling stress is between the second last data point and the next increment. Convergence is lost before the stress of this next increment can be determined causing the graph to go to 0 at the end of the load step.

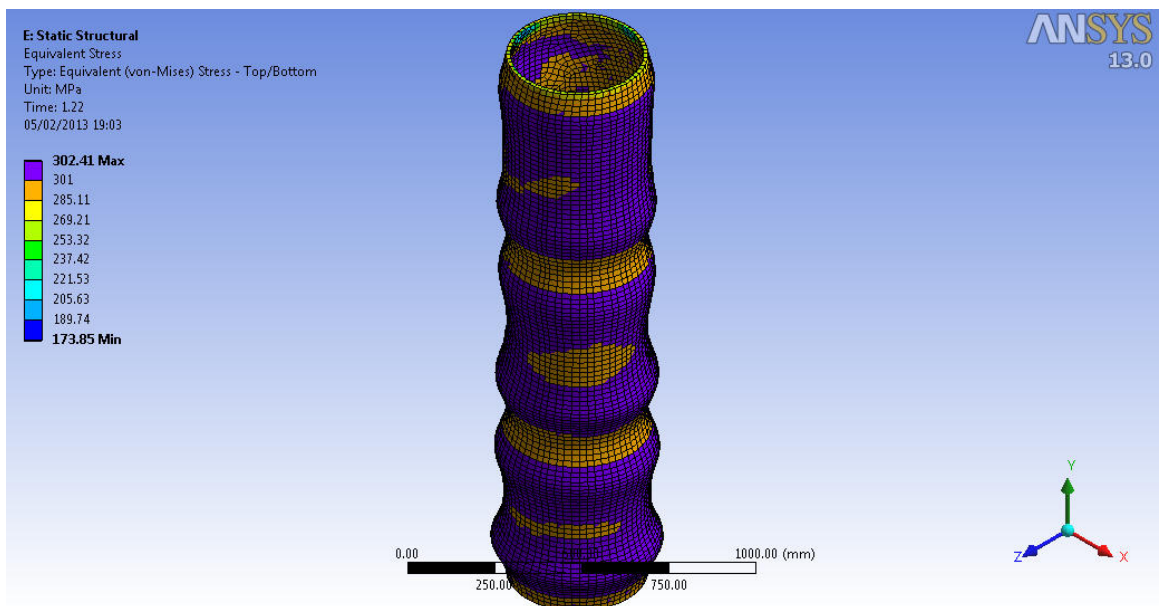


Figure 8.2: Cylinder 1 - Stress distribution before buckling

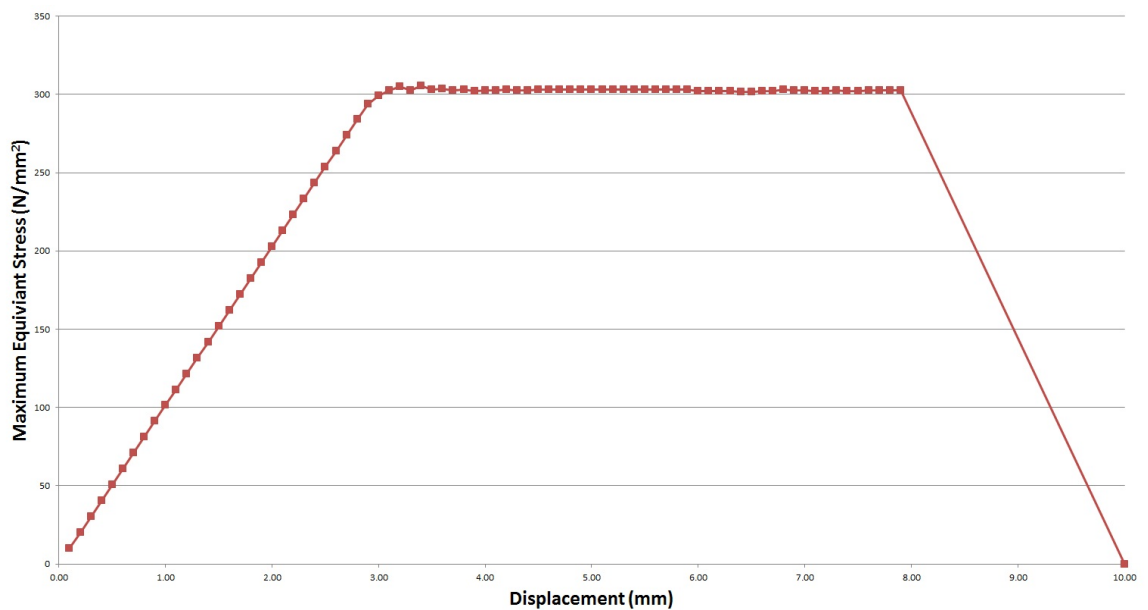


Figure 8.3: Cylinder 1 - Stress vs. Applied displacement

Cylinder 6.1 has a relative slenderness, λ_{ov} , of 0.98. This places it past the plastic limit relative slenderness λ_0 of 0.92 for this cylinder in the heavily knocked down elastic-imperfect buckling region. As such, plasticity is not expected and buckling is expected to be quite

sudden. The yield stress for this cylinder is 276N/mm^2 . This is illustrated graphically in Figures 8.5 and 8.4.

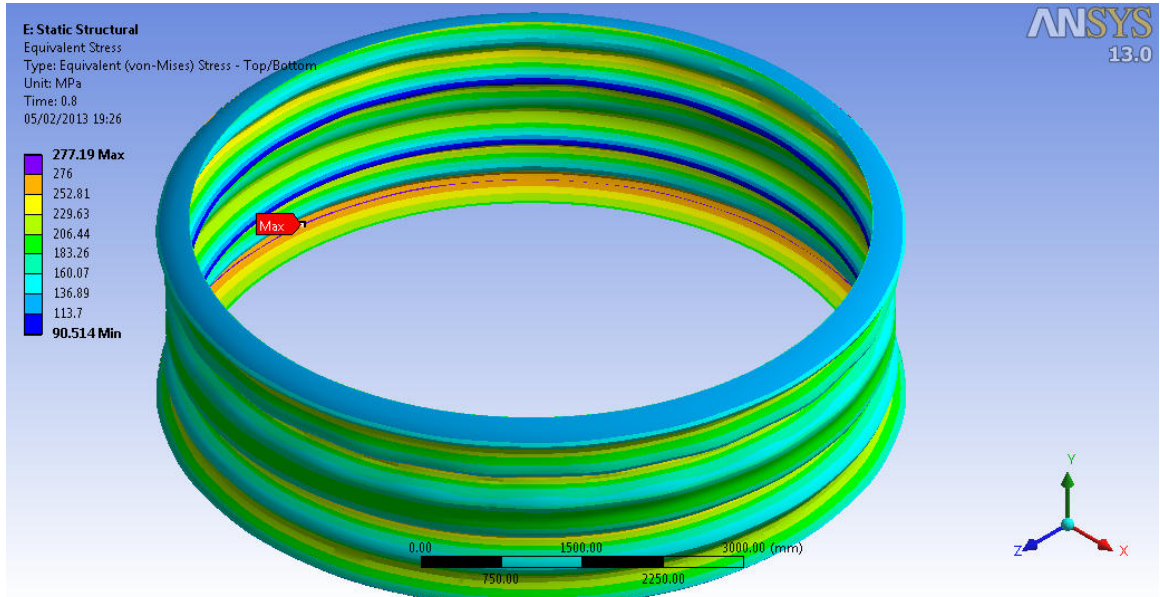


Figure 8.4: Cylinder 6.1 - Stress distribution before buckling

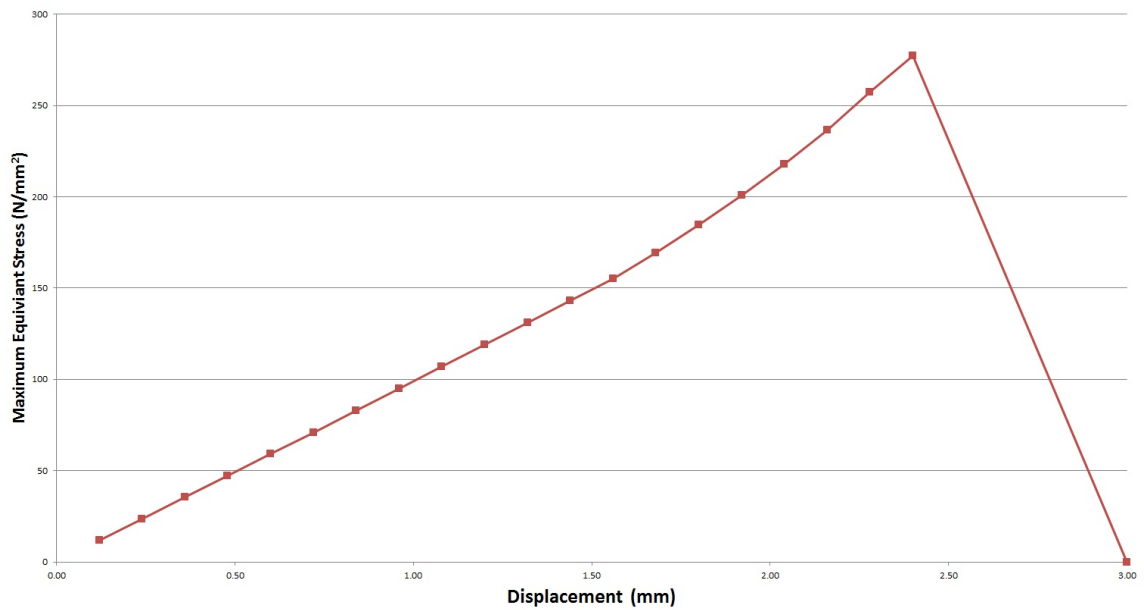


Figure 8.5: Cylinder 6.1 - Stress vs. Applied displacement

These examples show that the relative slenderness of a structure is a useful guide in deter-

mining the ductility of the structure. For low slenderness values the structure will behave more plastically resulting in plastic deformations before failure. Where as for slender structures the buckling behaviour will be sudden and brittle. This is further illustrated by the load deformation Figures 8.7 and 8.6.

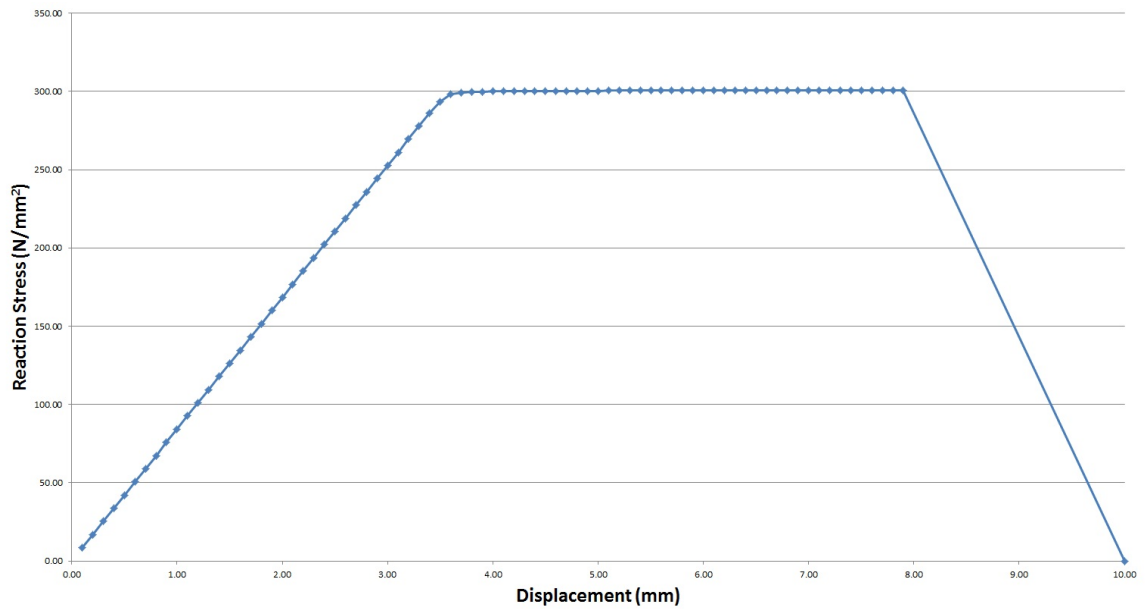


Figure 8.6: Cylinder 1 - Reaction stress vs. Applied displacement

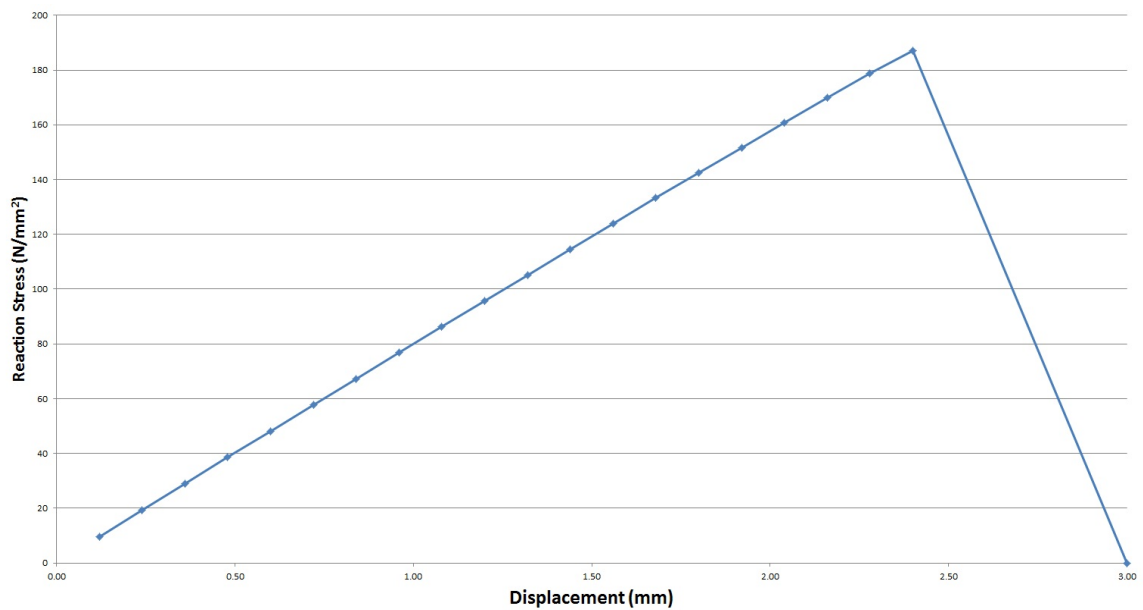


Figure 8.7: Cylinder 6.1 - Reaction stress vs. Applied displacement

The ability to quickly be forewarned of the buckling behaviour of a structure or structural element without the requirement of running GMNIA analyses is a useful tool in designing for ductile failure. Knowing the relative slenderness that causes the structure to fail suddenly and elastically allows the designer to exert a measure of control on the expected failure of a shell structure or shell element.

A level of risk can be associated with the relative slenderness of a structure if its behaviour can be predicted. This may allow the determination of a financial cost for insurance, or a fee for the structural consultants. As the slenderness increases, so the risk of failure may increase and as the risk for failure increases, the time and skill required to design the structure safely increases.

8.2.2 The GMNIA method

The GMNIA method is the most complex approach to numerical design. As there is no experimentally determined knock-down factor the determination of the buckling resistance using this method is a purely numerical design approach. A major consequence of such a complex method is the time required to run the required analyses as has been previously discussed. The advantage of the GMNIA method, however, is that it opens up the prospect of running very complex analyses; multiple loadcases, asymmetric loading, complex geome-

try etc. As a result the GMNIA analysis can become a tool for analysing very case specific structures. If the structure being designed has no precedent, then the GMNIA method is an excellent approach in determining its buckling resistance.

A word of warning is that the GMNIA method is not without its pitfalls. The GMNIA

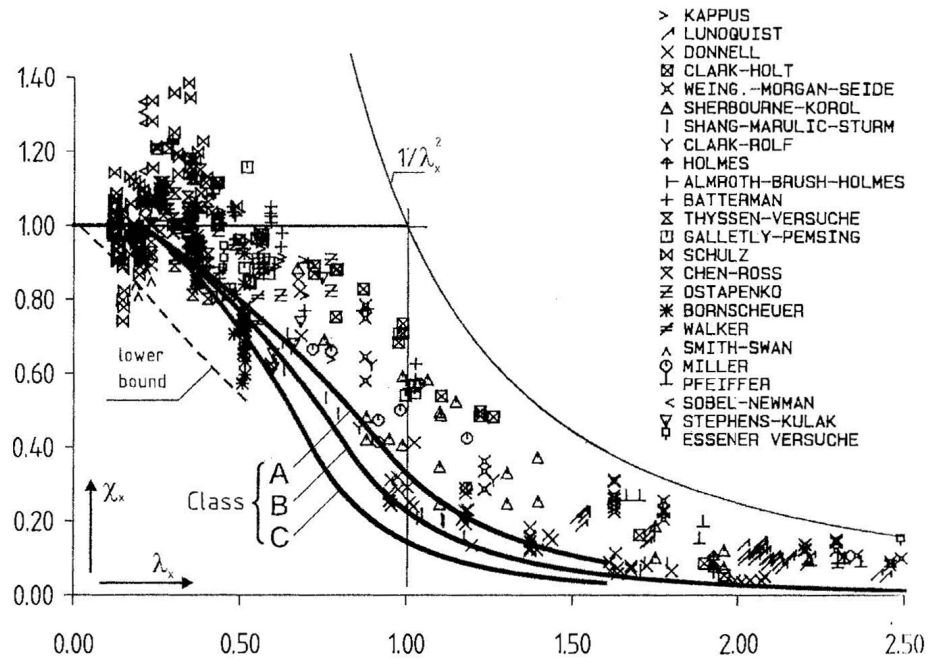


Figure 8.8: Results of a “reliable” selection of published axial compression cylinder tests, compared to the EN buckling curves (Rotter; 2008)

method can, theoretically, determine everything that the structural engineer needs to know from the model input into the program. The problem with this is how accurately the model may reflect reality and how these results are interpreted as the interpretation may vary from one program user to the next.

8.2.2.1 Interpretation of GMNIA results

The potential difficulties with the interpretation of the results is best illustrated using the case study cylinders in which the GMNIA analysis determined a much higher characteristic buckling load than then analytical analyses. So cylinders IC6, 2-1B and the first eigenmode of cylinder 6.1; in these cases if there were no other analyses to give the GMNIA a base comparison, then the numerically determined buckling resistances could be interpreted as correct.

Determining the relative slenderness of a structure is an excellent measure to decide how imperfection sensitive the structure is and how cautious the designer should be in interpreting the results. The relative slenderness may also be used as a guide to determine how rigorous the designer should be with modelling of different types of imperfections and ensuring that the modelled imperfection does not over-estimate the strength of the structure. This is illustrated through Figures 8.8 and 8.9. It can be seen from the experimental data in Figure 8.8 that as the slenderness goes up, the reduction factor becomes more influential in the reduction of the buckling resistance, comparing this to cylinders studied (Figure 8.9) it can be decided which cylinders to be more cautious with, cylinder 6.1 being a prime example as its relative slenderness lies above the plastic limit slenderness in the heavily knocked down elastic range.

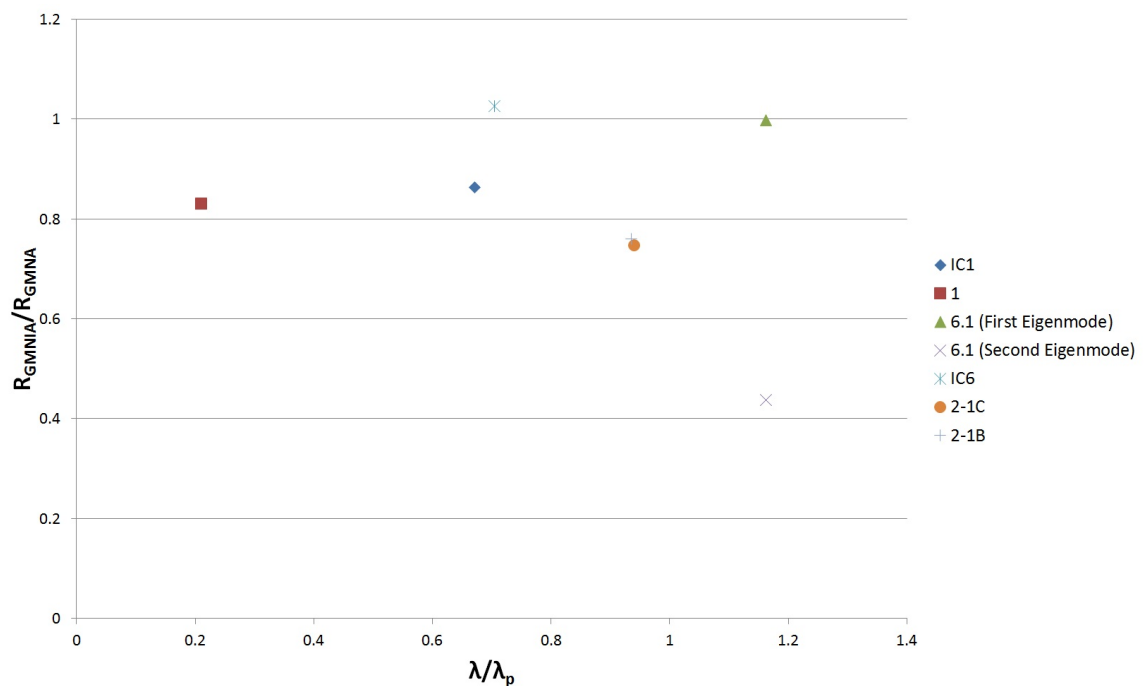


Figure 8.9: Buckling resistance vs. non-dimensional slenderness

8.2.2.2 Difficulties Modelling the GMNIA Analysis

An example of the potential modelling difficulties for the GMNIA analyses is the simplification that had to be made in this study due to the use of the pre-eigenbuckled shape.

In this study there was no difficulty in the solution or post-processing phases of the analysis

process but a modelling problem was encountered in the pre-processing phase, that is the modelling of the structural geometry. In order for the ring and stringer stiffeners to be introduced to the model the shell surface had to be split at the junction of their intersection (see Figure: 6.4). This was possible provided that no pre-eigenbuckled shape was imported however, once the pre-eigenbuckled shape was exported it was as a contiguous shell surface with no edges where the supports should be included. A simplification could be made with regard to the ring stiffeners, but unfortunately no simplification could be justified for the stringer stiffeners, the result of which being the stringer stiffeners were not modelled in the GMNIA analyses.

A number of other geometry modelling programs were used in an effort to split the surfaces but it was found that it was either impossible, or beyond the capabilities of a user with limited experience in these programs. The geometry modeller that is integrated in Ansys workbench was also found to have limited capabilities when it came to more complex geometry. This raises the question as to whether using the pre-eigenbuckled shape is an appropriate method to introduce imperfections into the model.

Though imperfections were introduced to the case study cylinders they were not representative of the realistic imperfections to be expected in such structures. As well as this, the introduction of these imperfections came at the cost of properly modelling the structural geometry. The end result in using the pre-eigenbuckled shape to introduce imperfections was that the full analytical capabilities of the finite element analysis were not utilised in analysing the real structural geometry. Had other methods of introducing imperfections been used it may have been the case that the stiffeners could be added to the structure resulting in a potentially more realistic determination of the buckling resistance.

It can be speculated that this modelling problem would introduce great difficulties if the shell geometry is modelled by a party other than the designers who will be doing the finite element analysis. For example, if the shell geometry was defined by an architectural firm and this geometry was sent to structural engineers for analysis and optimisation the surface would have to be pre-split where the stiffeners are expected to be so that they could be introduced and modelled. It is likely that the location and orientation of these stiffeners would not be decided upon before beginning numerical analyses. In order to manipulate the given geometry, it would be a requirement that the structural engineering consultants and the architectural firm have compatible software.

9 CONCLUSIONS AND RECOMMENDATIONS FOR FURTHER STUDY

A study was performed on the Eurocode and American Bureau of Shipping (ABS) methods of determining the buckling resistance of 6 axially compressed steel shell cylinders. A comparison was made between the analytical approaches to determining the buckling resistance of these cylinders and also a comparison was made of the numerical methods to determine the buckling resistance of these same structures. A minor objective of this study was to make recommendations as to how these methods could be adopted or adapted to aid in the design of geometrically complex steel shell structures. Based on this study the following conclusions have been made:

- By not taking into account the stringer stiffeners the Eurocode analytical method for determining the buckling resistance of steel shell structures is 34% to 54% lower than that of the buckling resistance of the same structures determined by the American Bureau of Shipping Guideline to Buckling of Offshore Structures code.
- The Eurocode MNA/LBA numerical method to determine the buckling resistance of shell structures shows excellent potential for reducing computation time provided that the required buckling parameters to determine the reduction factor have already been pre-determined. As these buckling parameters can be determined through numerical GMNIA analyses, the most time consuming analyses of the numerical approach would not have to be repeated.
- The introduction of different imperfection types can have a significant affect on the numerically determined GMNIA buckling resistance of a steel shell structure. For instance, the buckling resistance of cylinder 6.1 with a second eigenmode pre-buckled shape was 56% lower than when the pre-buckled shape used was the first eigenmode with the same maximum imperfection amplitude. So, in circumstances where there is sufficient experimental data to perform an analytical determination of the buckling resistance, such as simple geometry under simple loading, complex GMNIA analyses

are unnecessary and may in fact result in unconservative buckling resistances if the incorrect imperfection type is modelled.

- The computational time required to design accurately by the GMNIA method can be so long that its use may not be warranted in cases where an alternative design approach would be sufficient. The usage of this method could be justified by other external factors such as economics or consequences of failure.
- Utilisation of the pre-eigenbuckled shape to introduce imperfections into the GMNIA analyses resulted in simplifications being made to the structural geometry of the case study cylinders and as a result of such simplifications the minor stiffeners were not modelled computationally. For example, the numerical GMNIA buckling resistance for cylinder 2-1C was 51% lower than the analytically determined ABS buckling stress for the same structure.

9.1 Recommendations for Further Study

Based on this study it was found that there are potential topics for further research. Recommendations for the further study of these topics are given below:

- Further research is warranted into the Eurocode buckling parameters. As their use can reduce computation time, simplify numerical analyses procedures and give insight into the expected behaviour of shell structures a greater understanding of these parameters is justified. Research could be done into how the scale of a structure influences these parameters, whether the parameters can be interpolated between different geometric shapes or sizes. Research can be done in trying to determine the influence of the addition of stiffeners on these parameters. The significance of such research could be that a geometrically complex structure the buckling parameters could be determined for a set geometry under the expected loading conditions, then if these buckling parameters do not change a significant amount for changes in stiffener size or orientation then the computation time for each design iteration could be significantly reduced. Another advantage of this research is that manufacturers could supply these buckling parameters to designers for their products in a similar way that the structural properties and resistances of I-sections are readily available to the structural engineer. This would cut out the requirement for GMNIA analyses for the structural

Conclusions and Recommendations for Further Study

engineer, and these analyses would become the responsibility of the manufacturer.

- The significance of imperfections in shell design is well known to researchers of shell structures. This study also illustrated their significance for very simple shell geometry and as shell geometry gets more complicated, the influence of imperfections is less easy to determine. The affect of imperfections on simple shell geometry has been determined through physical experimentation and lower-bound curve fitting but the capabilities of complex computational analysis have also been made clear in this study. It is proposed that further research be done into numerically determining the influence of imperfections as opposed to this being done through physical experimentation. Through programming it becomes a simple, automated process to run a large number of pre-defined analyses and save the results for comparison. The computational analyses could then be benchmarked against physical experimentation. The potential of these numerical studies is a much more cost efficient approach to imperfections studies. As opposed to materials being purchased and shell structures being constructed a model could be computationally built and structural properties assigned.
- As there are significant differences between the Eurocode and ABS code analytically determined buckling resistances for the ring and stringer stiffened cylinders it is recommended that the Eurocode includes a method of incorporating a method to analytically determine the buckling resistance of such structures. It was found that there has been sufficient theory developed to form such methods and their implementation in the Eurocode could result in less-conservative and more economical structures being designed.

REFERENCES

- American Bureau of Shipping - Commentary on the guide for buckling and ultimate Strength assessment for offshore structures* (2005). American Bureau of Shipping (ABS).
- American Bureau of Shipping - Guide for buckling and ultimate strength assessment for offshore structures* (2004). American Bureau of Shipping (ABS).
- Baruch, M. and Singer, J. (1963). Effect of eccentricity of stiffeners on the general instability of stiffened cylindrical shells under hydrostatic pressure, *Journal of Mechanical Engineering Science* **5**(1): 23–27.
- Batdorf, S. B. (1947). A simplified method of elastic-stability analysis for thin cylindrical shells I: Donnell's equation, *Technical Report NACA-TN-1341*, NASA, Langley Research Center.
- Bathe, K. and Dvorkin, E. (1986). A formulation of general shell elements the use of mixed interpolation of tensorial components, *International Journal for Numerical Methods in Engineering* **22**(3): 697–722.
- Das, P., Thavalingam, A. and Bai, Y. (2003). Buckling and ultimate strength criteria of stiffened shells under combined loading for reliability analysis, *Thin-walled structures* **41**(1): 69–88.
- Donnell, L. H. (1933). Stability of thin-walled tubes under torsion., *Technical Report NACA-TN-179*, NASA, Langley Research Center.
- Dvorkin, E. (1984). *On nonlinear finite element analysis of shell structures*, PhD thesis, Massachusetts Institute of Technology.
- Dvorkin, E. and Bathe, K. (1984). A continuum mechanics based four-node shell element for general non-linear analysis, *Engineering computations* **1**(1): 77–88.
- Eglītis, E., Kalniņš, K. and Ozoliņš, O. (2009). Experimental and numerical study on buckling of axially compressed composite cylinders, *Scientific Journal of Riga Technical University. Construction Science* **10**(10): 33–49.

- Eurocode 3 - Design of steel structures - Part 1-6: Strength and stability of shell structures* (2007). Comité Européen de Normalisation (CEN).
- Eurocode 3 - Design of steel structures - Part 4-1: Silos* (2007). Comité Européen de Normalisation (CEN).
- Faculty of Civil and Geodetic Engineering, University of Ljubljana (n.d.). The European Steel Design Education Programme (ESDEP) Course notes, <http://www.fgg.uni-lj.si/kmk/esdep/master/wg08/10700.htm>. Accessed: 12/12/2012.
- Forasassi, G. and Frano, R. (2006). Buckling of imperfect thin cylindrical shell under lateral pressure, *Journal of Achievements in Materials and Manufacturing Engineering* **18**(1-2): 287–290.
- Gerard, G. and Becker, H. (1957). Handbook of structural stability part III: buckling of curved plates and shells (naca, washington, dc) technical note, 3783.
- Lee, P. and Bathe, K. (2004). Development of MITC isotropic triangular shell finite elements, *Computers & structures* **82**(11): 945–962.
- Mahfouz, S. (1999). *Design optimization of structural steelwork*, PhD thesis, University of Bradford, UK.
- Miller, C. D. (1977,). Buckling of axially compressed cylinders, *Journal of the Structural Division, ASCE* **103**(ST3): 695 – 721.
- Rajakumar, C. and Rogers, C. (1991). The lanczos algorithm applied to unsymmetric generalized eigenvalue problem, *International journal for numerical methods in engineering* **32**(5): 1009–1026.
- Richtlinie, D. (n.d.). 017: Beulsicherheitsnachweise für schalen–spezielle fälle–. entwurf 1992. deutscher ausschuß für stahlbau, *Stahlbau-Verlagsgesellschaft* .
- Rotter, J. (1998). Shell structures: the new european standard and current research needs, *Thin-walled structures* **31**(1-3): 3–23.
- Rotter, J. (2005). The practical design of shell structures exploiting different methods of analysis, *Shell Structures: Theory and Applications* pp. 71–86.

-
- Rotter, J. (2007). Recent advances in the philosophy of the practical design of shell structures, implemented in eurocode provisions, *Proc. SEMC* .
- Rotter, John Michael Schmidt, H. (2008). *Buckling of Steel Shells - European Design Recommendations*, number 125, 5th edn, ECCS European Convention for Constructional Steelwork.
- Schneider, W. and Brede, A. (2005). Consistent equivalent geometric imperfections for the numerical buckling strength verification of cylindrical shells under uniform external pressure, *Thin-Walled Structures* **43**(2): 175 – 188.
- The EN Eurocodes* (n.d.). <http://eurocodes.jrc.ec.europa.eu/>. Accessed: 05/02/2013.
- Timoshenko, S. and Gere, J. (1961). *Theory of elastic stability*, McGraw-hill New York.
- Timoshenko, S. and Woinowsky-Krieger, S. (1959). *Theory of plates and shells*, Vol. 2, McGraw-hill New York.
- V.I. Weingarten, E.J. Morgan, P. S. (1965). Elastic stability of thin-walled cylindrical and conical shells under axial compression, *American Institute of Aeronautics and Astronautics Journal(AIAAJ)* pp. pp.500–505.
- Weingarten, V., Seide, P. and Peterson, J. (1968). Buckling of thin-walled circular cylinders. nasa sp 8007, *Space Vehicle Design Criteria (Structures)* .
- Weisstein, E. W. (n.d.). L^2 -Norm. From Mathworld - A Wolfram Web Resource, <http://mathworld.wolfram.com/L2-Norm.html>. Accessed: 31/01/2013.

LIST OF FIGURES

1.1	Yas Hotel Bridge, Abu Dhabi	2
1.2	Stable postbuckling curve	4
1.3	Unstable postbuckling curve	5
1.4	Limit load buckling	5
1.5	Stiffened panel failure levels	6
1.6	Buckling modes of stiffened cylindrical shells	7
1.7	Steel plate girder	9
1.8	First buckling mode of flat plate - deformed shape and stress	11
1.9	ANSYS - First buckling mode flat plate and buckling stress	12
1.10	Wave number vs. Buckling coefficient	13
1.11	First buckling mode of curved panel - deformed shape and stress	13
1.12	Types of shell analysis	15
2.1	Yas hotel link bridge stiffeners	19
3.1	First and second modal shapes	21
3.2	A geometric imperfection illustrated as a crease in a cylinder	26
3.3	4-noded quadrilateral shell element	27
3.4	4 node shell	28
4.1	Eurocode defined boundary conditions	29
4.2	Wireframe model	44
4.3	Separation of surfaces	44
4.4	Axial loading	46
4.5	External pressure loading	46
4.6	Computational analysis procedure	47
4.7	Steps in buckling strength assessment using design by global numerical MNA/LBA analysis	50
4.8	Definition of buckling resistance from global GMNIA analysis	51
4.9	Example interpolation of the R_{GMNIA} for the amplitude of the adopted equivalent geometric imperfection	53
6.1	Cylinder IC1 AutoCAD model	68
6.2	Cylinder IC1 - Cross section of ring stiffeners	69
6.3	Cylinder IC1 - Radial constraints on top nodes	70
6.4	Cylinder IC1 - Junction between two shell segments and a ring stiffener	71
6.5	Cylinder IC-1 - Linear axial buckling	72
6.6	Cylinder IC-1 - External pressure buckling	74
6.7	Introduction of analyses and GMNIA modules	75

6.8	Cylinder IC-1 - Force convergence for first analysis	76
6.9	Cylinder IC-1 - Deformation vs. Reaction stress for first analysis	77
6.10	Cylinder IC-1 - Maximum equivalent (Von-mises) stress for first analysis	78
6.11	Cylinder IC-1 - Amplitude vs. Buckling pressure	79
6.12	Cylinder IC-1 - Plastic reference resistance, R_{pl}	80
6.13	Cylinder 1 - Linear axial buckling	83
6.14	Cylinder 1 - External pressure buckling	84
6.15	Cylinder 1 - Amplitude vs. Buckling pressure	85
6.16	Cylinder 6.1 - Linear axial buckling	87
6.17	Cylinder 6.1 - External pressure buckling	88
6.18	Cylinder 6.1 - Amplitude vs. Buckling pressure (first eigenmode)	89
6.19	Cylinder 6.1 - Amplitude vs. Buckling pressure (second eigenmode)	91
6.20	Cylinder IC6 - Linear buckling axial loading	92
6.21	Cylinder IC6 - External pressure buckling	93
6.22	Cylinder IC6 - Amplitude vs. Buckling pressure	94
6.23	Cylinder 2-1C - Linear axial buckling	96
6.24	Cylinder 2-1C - External pressure buckling	97
6.25	Cylinder 2-1C - Amplitude vs. Buckling pressure	98
6.26	Cylinder 2-1B - Linear axial buckling	100
6.27	Cylinder 2-1B - External pressure buckling	101
6.28	Cylinder 2-1B - Amplitude vs. Buckling pressure	102
7.1	Buckling resistance vs. Increasing length	106
7.2	Effect of plasticity on critical buckling stress in ABS codes	109
7.3	Extended capacity curve and parameters α , β , λ_0 and η	110
8.1	Analysis tree for optimised design	118
8.2	Cylinder 1 - Stress distribution before buckling	122
8.3	Cylinder 1 - Stress vs. Applied displacement	122
8.4	Cylinder 6.1 - Stress distribution before buckling	123
8.5	Cylinder 6.1 - Stress vs. Applied displacement	123
8.6	Cylinder 1 - Reaction stress vs. Applied displacement	124
8.7	Cylinder 6.1 - Reaction stress vs. Applied displacement	125
8.8	Results of a “reliable” selection of published axial compression cylinder tests, compared to the EN buckling curves	126
8.9	Buckling resistance vs. non-dimensional slenderness	127

LIST OF TABLES

4.1	Parameter C_{xb} for the effect of boundary conditions on the critical meridional buckling stress in long cylinders	30
4.2	Values of fabrication quality parameter Q	31
4.3	Values of α_θ based on fabrication quality	32
4.4	External pressure buckling factors for medium-length cylinders C_θ	33
4.5	External pressure buckling factors for short cylinders C_{θ_s}	33
4.6	Recommended values for dimple imperfection parameters	53
5.1	Ring stiffened shell geometry	54
5.2	Cylinder IC-1 - Axial	58
5.3	Cylinder IC1 - External Pressure	63
5.4	Cylinder 1 - Axial	63
5.5	Cylinder 1 - External Pressure	63
5.6	Cylinder 6.1 - Axial	64
5.7	Cylinder 6.1 - External Pressure	64
5.8	Ring and stringer stiffened cylinders geometry	64
5.9	Cylinder IC6 - Axial	65
5.10	Cylinder IC6 - External pressure	65
5.11	Cylinder IC6 - Alternative Eurocode	65
5.12	Cylinder 2-1C - Axial	65
5.13	Cylinder 2-1C - External pressure	66
5.14	Cylinder 2-1C - Alternative Eurocode	66
5.15	Cylinder 2-1B - Axial	66
5.16	Cylinder 2-1B - External pressure	66
5.17	Cylinder 2-1B - Alternative Eurocode	67
6.1	Cylinder IC-1 - Ansys Linear Buckling	73
6.2	Cylinder IC-1 - Ansys Linear External Pressure Buckling	74
6.3	Cylinder IC-1 - Amplitude vs. Buckling pressure	79
6.4	Cylinder 1 - Ansys linear axial buckling	83
6.5	Cylinder 1 - Ansys external pressure buckling	84
6.6	Cylinder 1 - Amplitude vs. Buckling pressure	84
6.7	Cylinder 6.1 - Ansys linear axial buckling	87
6.8	Cylinder 6.1 - Ansys Linear External Pressure Buckling	88
6.9	Cylinder 6.1 - Amplitude vs. Buckling pressure	88
6.10	Cylinder IC6 - Ansys linear axial buckling	92
6.11	Cylinder IC6 - Ansys external pressure buckling	93
6.12	Cylinder IC6 - Amplitude vs. Buckling pressure	93
6.13	Cylinder 2-1C - Ansys linear axial buckling	96

6.14	Cylinder 2-1C - Ansys external pressure buckling	97
6.15	Cylinder 2-1C - Amplitude vs. Buckling pressure	98
6.16	Cylinder 2-1B - Ansys linear axial buckling	100
6.17	Cylinder 2-1B - Ansys external pressure buckling	101
6.18	Cylinder 2-1B - Amplitude vs. Buckling pressure	102
7.1	Compiled axial loading results	104
7.2	Compiled external pressure loading results	104
7.3	Ring stiffener stiffness check	108
7.4	Numerical buckling resistance comparison table	115

Appendix A

```

clear all;
clc;

% Buckling of axially loaded singly curved plates

E=2*10^5; % Modulus of Elasticity (N/mm^2)
nu=0.3; % Poisson ratio
t=5; % Plate thickness (mm)
b=1000; % Plate length
r=500; % Radius of curvature

Area=t*pi*r; % Loaded Area (mm^2)

for j=1:50;

    % nwav=zeros(1,length(j));
    nwav(j)=0+j;

    %lambda=zeros(1,length(j));
    lambda(j)=(pi*r)/nwav(j);

    %beta=zeros(1,length(j));
    beta(j)=b/lambda(j);

    zb=(b^2/(r*t))*sqrt(1-nu^2);

    A(j)=((nwav(j)^2+beta(j)^2)^2/beta(j)^2);
    B(j)=((12*zb^2*beta(j)^2)/(pi^4*(nwav(j)^2+beta(j)^2)^2));

    kc(j)=A(j)+B(j);

    n_wav=find(kc==min(kc));

    n=n_wav;
end
plot(kc)

lambda=(pi*r)/n;
beta=b/lambda;

A=((n^2+beta^2)^2/beta^2);
B=((12*zb^2*beta^2)/(pi^4*(n^2+beta^2)^2));

kc=A+B;

sigma=((pi^2*E)/(12*(1-nu^2)));
sigmacr=kc*sigma*(t/b)^2;

fprintf('Critical Buckling Stress for curved plate is: %.2f N/mm^2',sigmacr)

force=sigmacr*Area;
fprintf('\nCritical Buckling Force for curved plate is: %.2f N',force)

```

Appendix B


```

% Critical Buckling Stress due to External Pressure (Section 4 - 3.5)
%%%%%%%%%%%%%%%%%%%%%%%%%%%%%%%%%%%%%%%%%%%%%%%%%%%%%%%%%%%%%%%%%%%%%%%%

% The critical buckling stress for an unstiffened or ring-stiffened
% cylindrical shell subjected to external pressure may be taken as:

% Nominal or lower bound knock-down factor to allow for shape imperfections
rho_thetaR=0.8;

% K_theta
if (N_theta>0)
pressure=menu('Loading from:', 'Radial Pressure', 'Hydrostatic Pressure');
switch pressure
case 1
k=(N_x/N_theta); % For lateral pressure ((N_x/N_theta)+0.5 for
hydrostatic pressure)
k1=0; % 0 for lateral pressure, 0.5 for hydrostatic
pressure
case 2
k=(N_x/N_theta)+0.5;
k1=0.5; % 0 for lateral pressure, 0.5 for hydrostatic
pressure
end
elseif (N_theta==0)
k=0;
k1=0; % 0 for lateral pressure, 0.5 for hydrostatic
pressure
end
alpha=1/(1.56*sqrt(r*t));

% Code says it must be greater than or equal to 0 which wasn't adhered
% to in some examples in the ABS commentary document
if
2*((sinh(alpha)*cos(alpha)+cosh(alpha)*sin(alpha))/(sinh(2*alpha)+sin(2*alpha)
))>=0
G_alpha=2*((sinh(alpha)*cos(alpha)+cosh(alpha)*sin(alpha))/(sinh(2*alpha)+sin
(2*alpha)));
else
G_alpha=0;
end

omegabar=(cosh(2*alpha)-
cos(2*alpha))/(alpha*(sinh(2*alpha)+sin(2*alpha)));
Abar_R=(A_R)*(r/r_R)^2;

K_theta=1-(((1-k*nu)/(1+(t*(t_w+1*omegabar)/Abar_R)))*G_alpha;

% Elastic buckling pressure (N/mm^2)
A_L=((sqrt(z))/(1-nu^2)^(1/4))-1.17+1.068*k1;
C_p=(A_L)/(r/t);

```

```

if (A_L<=2.5)
    q_CEthetaR=((1.27*E)/(A_L^(1.18)+0.5))*(t/r)^2;
elseif (2.5<A_L && A_L<=0.208*(r/t))
    q_CEthetaR=((0.92*E)/A_L)*(t/r)^2;
elseif (0.208*(r/t)<A_L && A_L<=2.85*(r/t))
    q_CEthetaR=(0.836*C_p^(-1.061)*E)*(t/r)^3;
else
    q_CEthetaR=0.275*E*(t/r)^3;
end

% Elastic hoop buckling stress for an imperfect cylindrical shell (N/mm2)
sigma_EthetaR=rho_thetaR*((q_CEthetaR*(r+(0.5*t)))/t)*K_theta;

DELTA=sigma_EthetaR/sigma_0;

% Plasticity reduction factor
if (DELTA<=0.55)
    PHI=1;
elseif (0.55<DELTA && DELTA<=1.6)
    PHI=(0.45/DELTA)+0.18;
elseif (1.6<DELTA && DELTA<=6.25)
    PHI=1.31/(1+(1.15*DELTA));
else
    PHI=1/DELTA;
end

sigma_CthetaR=PHI*sigma_EthetaR;

fprintf('\n\nThe critical buckling stress for an unstiffened or ring-stiffened
cylindrical shell subjected to external pressure\n\n')
fprintf('sigma_CthetaR= %.2f N/mm^2 \n',sigma_CthetaR)

%% 5 Curved Panels

%%%%%%%%%%%%%%%%%%%%%%%%%%%%%%%%%%%%%%%%%%%%%%%%%%%%%%%%%%%%%%%%%%%%%%%%
%%%%%%%%%%%%%%%%%%%%%%%%%%%%%%%%%%%%%%%%%%%%%%%%%%%%%%%%%%%%%%%%%%%%%%%%
% Critical Buckling Stress for Axial Compression or Bending Moment (Section
4 - 5.3)
%%%%%%%%%%%%%%%%%%%%%%%%%%%%%%%%%%%%%%%%%%%%%%%%%%%%%%%%%%%%%%%%%%%%%%%%
%%%%%%%%%%%%%%%%%%%%%%%%%%%%%%%%%%%%%%%%%%%%%%%%%%%%%%%%%%%%%%%%%%%%%%%%

% z_s
z_s=sqrt(1-nu^2)*(s^2/(r*t));

% KxP
if (z_s<=11.4)
    K_xP=4+((3*z_s^2)/pi^4);
else
    K_xP=0.702*z_s;
end

% Nominal or lower bound knock-down factor to allow for shape imperfections
if (z_s<=11.4)
    rho_xP=1-(0.019*z_s^(1.25))+((0.0024*z_s)*(1-(r/(300*t))));

```

```

else
    rho_xP=0.27+(1.5/z_s)+(27/z_s^2)+(0.008*sqrt(z_s)*(1-(r/(300*t))));
end

% Classical buckling stress for a perfect curved panel between adjacent
stringer stiffeners (N/mm2)
sigma_CExP=K_xP*((pi^2*E)/(12*(1-nu^2)))*(t/s)^2;

% Lambda_n
lambda_n=sqrt(sigma_0/(rho_xP*sigma_CExP));

% Factor compensating for the lower bound nature of rho_xP (Bias factor)
if (lambda_n<=1)
    B_xP=1+(0.15*lambda_n);
else
    B_xP=1.15;
end

% Elastic buckling stress for an imperfect curved panel (N/mm^2)
sigma_ExP=B_xP*rho_xP*sigma_CExP;

if (sigma_ExP<=P_r*sigma_0)
    sigma_CxP=sigma_ExP;
else
    sigma_CxP=sigma_0*(1-P_r*(1-P_r)*(sigma_0/sigma_ExP));
end
fprintf('\n\nThe critical buckling stress of a curved panel subjected to axial
compression\n')
fprintf('sigma_CxP = %.2f N/mm^2 \n',sigma_CxP)

%%%%%%%%%%%%%%%%%%%%%%%%%%%%%%%%%%%%%%%%%%%%%%%%%%%%%%%%%%%%%%%%%%%%%%%%
% Critical Buckling Stress under External Pressure (Section 4 - 5.5)
%%%%%%%%%%%%%%%%%%%%%%%%%%%%%%%%%%%%%%%%%%%%%%%%%%%%%%%%%%%%%%%%%%%%%%%%

% The critical buckling stress for curved panels bounded by adjacent
% pairs of ring and stringer stiffeners subjected to external pressure
% may be taken as:

% Circumferential wave number starting at 0.5Ns and increasing until a
% minimum value of qCE?P is attained
alpha_2=(pi*r)/l;
if (N_s<1)
for j=1:50;
    wav(j)=0+j;

% Elastic buckling pressure (N/mm^2)
q_minCEthetaP(j)=(((E*t)/r)/wav(j)^2+(k*alpha_2^2)-
1)*(((wav(j)^2+alpha_2^2-1)^2/(12*(1-
nu^2)))*(t/r)^2)+(alpha_2^4/(wav(j)^2+alpha_2^2)^2));

n_wav=find(q_minCEthetaP==min(q_minCEthetaP));

n=wav(n_wav);

```

```

end
elseif (N_s>=1)
    vec_j=0.5*N_s:50;
    for j=1:length(vec_j);
        wav(j)=vec_j(j);

% Elastic buckling pressure (N/mm^2)
    q_minCEthetaP(j)=((E*t)/r)/(wav(j)^2+k*alpha_2^2-
1))*(((wav(j)^2+alpha_2^2-1)^2/(12*(1-
nu^2)))*(t/r)^2+(alpha_2^4/(wav(j)^2+alpha_2^2)^2));

    n_wav=find(q_minCEthetaP==min(q_minCEthetaP));

    n=wav(n_wav);
    end
end
% Elastic buckling pressure (N/mm^2)
    q_CEthetaP=(((E*t)/r)/(n^2+k*alpha_2^2-1))*(((n^2+alpha_2^2-1)^2/(12*(1-
nu^2)))*(t/r)^2+(alpha_2^4/(n^2+alpha_2^2)^2));

% Elastic hoop buckling stress of imperfect curved panel (N/mm^2)
sigma_EthetaP=((q_CEthetaP*(r+0.5*t))/t)*K_theta;

DELTA2=sigma_EthetaP/sigma_0;

% Plasticity reduction factor
if (DELTA2<=0.55)
    PHI2=1;
elseif (0.55<DELTA2 && DELTA2<=1.6)
    PHI2=(0.45/DELTA2)+0.18;
elseif (1.6<DELTA2 && DELTA2<=6.25)
    PHI2=1.31/(1+(1.15*DELTA2));
else
    PHI2=1/DELTA2;
end

sigma_CthetaP=PHI2*sigma_EthetaP;
fprintf('\nThe critical buckling stress of a curved panel subjected to
external pressure\n')
fprintf('sigma_CthetaP = %.2f N/mm^2 \n',sigma_CthetaP)

%%%%%%%%%%%%%%%%%%%%%%%%%%%%%%%%%%%%%%%%%%%%%%%%%%%%%%%%%%%%%%%%%%%%%%%%
%%%%%%%%%%%%%%%%%%%%%%%%%%%%%%%%%%%%%%%%%%%%%%%%%%%%%%%%%%%%%%%%%%%%%%%%
% Critical Buckling Stress for Axial Compression or Bending Moment (Section
4 - 7.3)
%%%%%%%%%%%%%%%%%%%%%%%%%%%%%%%%%%%%%%%%%%%%%%%%%%%%%%%%%%%%%%%%%%%%%%%%
%%%%%%%%%%%%%%%%%%%%%%%%%%%%%%%%%%%%%%%%%%%%%%%%%%%%%%%%%%%%%%%%%%%%%%%%

% The critical buckling stress of ring and stringer-stiffened cylindrical
% shells subjected to axial compression or bending may be taken as:

% Reduced shell slenderness ratio
lambda_xP=sqrt(sigma_0/sigma_Exp);

```

```

% Reduced effective width of shell (mm)
if (lambda_xP>0.53)
    s_e=(0.53/lambda_xP)*s;
else
    s_e=s;
end

A_s=(d_st*t_st)+(b_st*t_fst);
% Cross sectional area of stringer stiffener (mm^2)

switch stringerstiffener
    case 1
        % Distance from inner surface of shell to centroid of stringer stiffener
        y_st=((d_st+(t_fst/2))*(t_fst*b_st))+((d_st/2)*(t_st*d_st))/(A_s);

        % Moment of inertia of stringer stiffener
        I_s=(1/3)*((t_st*y_st^3)+(b_st*((d_st+t_fst)-y_st)^3)-((b_st-
        t_st)*((d_st+t_fst)-y_st-t_fst)^3));
        z_st=y_st; %r-y_st; % Distance from centerline
        of shell to the centroid of stringer stiffener (mm)

        case 2
            % Distance from inner surface of shell to centroid of stringer stiffener
            y_st=(d_st+t_st)-((t_st*(2*d_st+b_st)+d_st^2))/(2*(d_st+b_st)); % Short edge
            of leg in contact with cylinder
            %y_st=(d_st+t_st)-((t_st*(2*d_st+b_st)+d_st^2))/(2*(d_st+b_st)); % Long edge
            of leg in contact with cylinder

            z_st=y_st; %r-y_st; % Distance from centerline
            of shell to the centroid of stringer stiffener (mm)

            % Moment of inertia of stringer stiffener
            I_s=(1/3)*((t_st*y_st^3)+(b_st*((d_st+t_st)-y_st)^3)-((b_st-
            t_st)*((d_st+t_st)-y_st-t_st)^3));
        end

        % Minimum moment of inertia of stringer stiffeners
        alpha_0=1/s;

        if A_s>0
            delta=A_s/(s*t);
        else
            delta=0;
        end
        gamma_0=((2.6+(4.0*delta))*alpha_0^2)+(12.4*alpha_0)-(13.2*alpha_0^(0.5));

        I_0=((s*t^3)/(12*(1-nu^2)))*gamma_0;

        % Check moment of inertia of stringers
        if (I_0<I_s)
            sufficiency='OK';
        else
            sufficiency='Insufficient';
        end
    end
end

```



```

% Critical Buckling Stress for External Pressure (Section 4 - 7.5)
%%%%%%%%%%%%%%%%%%%%%%%%%%%%%%%%%%%%%%%%%%%%%%%%%%%%%%%%%%%%%%%%%%%%%%%%

% The critical buckling stress for ring and stringer-stiffened
% cylindrical shells subjected to external pressure may be taken as:

% Geometrical parameter
g=2*pi*((l^2*A_s)/(N_s*I_s));

% Effective pressure correction factor
if (g<=500)
    K_p=0.25+((0.85/500)*g);
else
    K_p=1.10;
end

% Collapse pressure of a stringer stiffener plus its associated shell
% plating (N/mm^2)
q_s=(16/(s*l^2))*A_s*abs(z_st)*sigma_0; %(16/(s*l^2))*A_s*abs(z_st-
(t/2))*sigma_0;

% Collapse hoop stress for a stringer stiffener plus its associated
% shell plating (N/mm^2)
sigma_sp=((q_s*(r+0.5*t))/t)*K_theta;

sigma_CthetaB=min((sigma_CthetaR+sigma_sp)*K_p,sigma_0);

fprintf('\nThe critical buckling stress for ring and stringer-stiffened
cylindrical shells subjected to external pressure\n')
fprintf('sigma_CthetaB = %.2f N/mm^2 \n',sigma_CthetaB)

%% Overall Critical Buckling Stress
BUCK=[sigma_CxR,sigma_CthetaR,sigma_CxP,sigma_CthetaP,sigma_CxB,sigma_CthetaB
];
sigma_Cij=min(BUCK);
fprintf('\nOverall Critical Buckling Stress\n')
fprintf('sigma_Cij = %.2f N/mm^2 \n',sigma_Cij)

%% Factors

% Adjustment factor
if (sigma_Cij <= 0.55*sigma_0)
    psi=0.833;
else
    psi=0.629+0.371*(sigma_Cij/sigma_0);
end

beta=(s/t)*sqrt((sigma_0/E)); % Slenderness ratio ('b' has been
replaced by 's', the short length of plate)

eta=1; % 0.8*psi; % Maximum allowable strength
utilization factor of shell buckling (0.6 or 0.8 times psi)

```

```

% NOTE: eta is based on factors of safety given in offshore installation
% rules characterised by loading conditions.
if A_s>0
    delta=A_s/(s*t);
elseif A_s<=0
    delta=0;
end

%% Longitudinal Stress
% Stress due to axial force
sigma_a=P/(2*pi*r*t*(1+delta));

% Stress due to bending moment
sigma_b=M/(pi*r^(2)*t*(1+delta));

% Longitudinal Stress
sigma_x=sigma_a+sigma_b;

%% Hoop Stress

K_thetaR=(1-k*nu)/(1+(Abar_R/(t*(t_w+l*omegabar))));

% The hoop stress may be taken as...
% At midway of shell between adjacent ring stiffeners:
sigma_theta=((q*(r+0.5*t))/t)*K_theta;

% The hoop stress may be taken as...
% At inner face of ring flange:
sigma_thetaR=((q*(r+0.5*t))/t)*(r/r_F)*K_thetaR;

%% Minimum moment of inertia of ring stiffeners
I_r=((sigma_x*(1+delta)*t*r_R^4)/(500*E*l))+(((sigma_theta*r_R^2*l*t)/(2*E*K_
theta))*(1+((y_rs/(100*r))*(E/((eta*sigma_0)-sigma_thetaR)))));

% Check moment of inertia of ring stiffeners
if (I_r<I_rs)
    ringsufficiency='OK';
else
    ringsufficiency='Insufficient';
end
fprintf('\nRing stiffener moment of inertia = %s \n',ringsufficiency)

%% Curved Panel Buckling Unity Check (Section 5.1)
% The buckling limit state of curved panels between adjacent stiffeners can
% be defined by the following equation

% Coefficient to reflect interaction between longitudinal and hoop
% stresses (negative values are acceptable)
phi_p=((0.4*(sigma_CxP+sigma_CthetaP))/sigma_0)-0.8;

```

```

BSL=(sigma_x/(eta*sigma_CxP))^2-
(phi_p*(sigma_x/(eta*sigma_CxP))*((sigma_theta/(eta*sigma_CthetaP))))+(sigma_
theta/(eta*sigma_CthetaP))^2;
fprintf('Curved Panel Buckling State Limit %.2f \n',BSL)

if (BSL<=1)
    Unity_Check='OK';
else
    Unity_Check='Fail';
end
fprintf('Curved Panel Unity Check: %s \n',Unity_Check)

fprintf('\nFor Excel Spreadsheet: Unstiffened/Ring-stiffened\n')
fprintf('Axial\n')
fprintf('Knockdown Factor: %.2f \n',rho_xR)
fprintf('Classical buckling stress (bay in axial compression): %.2f
\n',sigma_CExR)
fprintf('Elastic buckling stress: %.2f \n',sigma_ExR)
fprintf('Critical buckling stress: %.2f \n',sigma_CxR)
fprintf('Pressure\n')
fprintf('Plasticity: %.2f \n',PHI)
fprintf('Elastic hoop stress: %.2f \n',sigma_EthetaR)
fprintf('Critical buckling stress: %.2f (N/mm^2)\n',sigma_CthetaR)

fprintf('\nFor Excel Spreadsheet: Ring- & Stringer-stiffened Axial\n')
fprintf('Axial\n')
fprintf('Knockdown Factor: %.2f \n',rho_xB)
fprintf('Elastic compressive buckling stress of stringer-stiffened shell:
%.2f \n',sigma_s)
fprintf('Elastic buckling stress of column: %.2f \n',sigma_c)
fprintf('Elastic buckling stress: %.2f \n',sigma_ExB)
fprintf('Critical buckling stress: %.2f \n',sigma_CxB)
fprintf('Pressure\n')
fprintf('Plasticity: %.2f \n',DELTA)
fprintf('Critical buckling stress: %.2f (N/mm^2)\n',sigma_CthetaB)

```

Appendix C

```

fprintf('\n -----')
fprintf('\nEUROCODE\n')
fprintf('Axial Buckling to Annex D: EC3, ENV 1993-1-6:1999\n')
fprintf('External Pressure Buckling to Clause 5.3.4.5: EC 3: Design of steel
structures - Silos, EN 1993-4-1')
fprintf('\n ----- \n')

% Material Properties and Safety Factors
f_yk=sigma_0;
gamma_M1=1.1;
alpha_n=0.8;

ro=r+(t/2);
ri=r-(t/2);

A=2*pi*r*t;

% Loading
F_x=P; % Meridional Loading
sigma_xEd=F_x/A; % Meridional Stress
sigma_thetaEd=(q*r)/t; % Hoop Stress

omega=1/sqrt(r*t);
BC1=menu('First boundary condition:', 'Fixed', 'Pinned', 'Free');
BC2=menu('Second boundary condition:', 'Fixed', 'Pinned', 'Free');
Fabricationquality=menu('Fabrication Quality
is:', 'Excellent', 'High', 'Normal');
pressure=menu('The Pressure on the cylinder is:', 'External', 'Internal');

switch Fabricationquality
case 1
    Q=40;
    alpha_theta=0.75;
    alpha_tau=0.75;
case 2
    Q=25;
    alpha_theta=0.65;
    alpha_tau=0.65;
case 3
    Q=16;
    alpha_theta=0.5;
    alpha_tau=0.5;
end

% Boundary Coniditions
if (BC1==1 && BC2==1)
    C_xb=6;
elseif (BC1==1 && BC2==2)
    C_xb=3;
elseif (BC1==2 && BC2==2)
    C_xb=1;
end

if (BC1==1 && BC2==1)
    Case=1;

```

```

elseif (BC1==1 && BC2==2)
    Case=2;
elseif (BC1==2 && BC2==2)
    Case=3;
elseif (BC1==1 && BC2==3)
    Case=4;
elseif (BC1==2 && BC2==3)
    Case=5;
elseif (BC1==3 && BC2==3)
    Case=6;
end
%%%%%%%%%%%%%%%%%%%%%%%%%%%%%%%%%%%%%%%%%%%%%%%%%%%%%%%%%%%%%%%%%%%%%%%%
%% Axial Buckling
%%%%%%%%%%%%%%%%%%%%%%%%%%%%%%%%%%%%%%%%%%%%%%%%%%%%%%%%%%%%%%%%%%%%%%%%

if (1.7<omega && omega<(r/(2*t)))
    C_x=1;
    Cylinderlength='medium';
elseif (omega<1.7)
    C_x=1.36-(1.83/omega)+(2.07/omega^2);
    Cylinderlength='short';
else
    C_x=min((1+((0.2/C_xb)*(1-(2*omega*(t/r))))),0.6);
    Cylinderlength='long';
end

sigma_xRc=0.605*E*C_x*(t/r);           % The elastic critical meridional
buckling stress

deltawk=(1/Q)*sqrt(r/t)*t;             % The characteristic imperfection
amplitude
lambdabar_x=sqrt(f_yk/sigma_xRc);      % Relative shell slenderness in
meridional direction

switch pressure
case 1
    alpha_x=0.62/(1+(1.91*(deltawk/t)^1.44)); % The meridional elastic
imperfection reduction factor
case 2
    alpha_x1=0.62/(1+(1.91*(deltawk/t)^1.44)); % The meridional elastic
imperfection reduction factor
    pbar=(q*r)/(t*sigma_xRc);

    alpha_xpe=alpha_x1+(1-alpha_x1)*(pbar/(pbar+(0.3/alpha_x1^0.5))); %
A factor covering pressure-induced elastic stabilisation

    s=(1/400)*(r/t);

    alpha_xpp=(1-(pbar^2/lambdabar_x^4))*(1-
(1/(1.12+s^1.5)))*((s^2+(1.21*lambdabar_x^2))/(s*(s+1))); % A factor
covering pressure-induced plastic stabilisation

    alpha_xp=min(alpha_xpe,alpha_xpp);
    alpha_x=alpha_xp;
end

```

```

beta_x=0.6; % The plastic range factor
eta_x=1;    % The interaction exponent

lambdabar_x0=0.2; % The meridional squash limit slenderness
lambdabar_xp=sqrt(alpha_x/(1-beta_x)); % Plastic limit relative
slenderness

% Buckling reduction factor
if (lambdabar_x<=lambdabar_x0)
    Chi_x=1;
elseif (lambdabar_x0<lambdabar_x && lambdabar_x<lambdabar_xp)
    Chi_x=1-(beta_x*((lambdabar_x-lambdabar_x0)/(lambdabar_xp-
lambdabar_x0))^eta_x);
elseif (lambdabar_xp<=lambdabar_x)
    Chi_x=alpha_x/(lambdabar_x)^2;
end

sigma_xRk=Chi_x*f_yk; % The characteristic buckling stress

sigma_xRd=sigma_xRk/gamma_M1; % The design buckling resistance

fprintf('\nThe meridional design buckling resistance = %.2f N/mm^2
\n',sigma_xRd)

%%%%%%%%%%%%%%%%%%%%%%%%%%%%%%%%%%%%%%%%%%%%%%%%%%%%%%%%%%%%%%%%%%%%%%%%
%% Circumferential Local Panel Buckling
%%%%%%%%%%%%%%%%%%%%%%%%%%%%%%%%%%%%%%%%%%%%%%%%%%%%%%%%%%%%%%%%%%%%%%%%

% Circumferential buckling satisfaction test
% Cylinders need not be checked against circumferential shell buckling if
they satisfy:

omega2=1/sqrt(r*t);

if (r/t)<=0.21*(sqrt(E/f_yk))
    circcheck='No';
else
    circcheck='Yes';
end

fprintf('\nCircumferential shell buckling check required: %s \n',circcheck)

% C_theta
if Case==1
    C_theta=1.5;
elseif Case==2
    C_theta=1.25;
elseif Case==3
    C_theta=1;
elseif Case==4
    C_theta=0.6;
elseif Case==5
    C_theta=0;

```

```

        elseif Case==6
            C_theta=0;
        end

% Short Cylinder
if (omega2/C_theta)<20
    if Case==1
        C_thetas=1.5+(10/omega2^2)-(5/omega2^3);
    elseif Case==2
        C_thetas=1.25+(8/omega2^2)-(4/omega2^3);
    elseif Case==3
        C_thetas=1+(3/omega2^1.35);
    elseif Case==4
        C_thetas=0.6+(1/omega2^2)-(0.3/omega2^3);
    end

    % Critical circumferential buckling stress
    sigma_thetaRc=0.92*E*(C_thetas/omega2)*(t/r);

% Medium length cylinder
elseif (20<=(omega2/C_theta) && (omega2/C_theta)<=1.63*(r/t))
    if Case==1
        C_theta=1.5;
    elseif Case==2
        C_theta=1.25;
    elseif Case==3
        C_theta=1;
    elseif Case==4
        C_theta=0.6;
    elseif Case==5
        C_theta=0;
    elseif Case==6
        C_theta=0;
    end

    % Critical circumferential buckling stress
    sigma_thetaRc=0.92*E*(C_theta/omega2)*(t/r);

% Long cylinder
elseif (omega2/C_theta)>1.63*(r/t)

% Critical circumferential buckling stress
    sigma_thetaRc=E*(t/r)^2*(0.275+(2.03*((C_theta/omega2)*(r/t))^4));

end
beta_theta=0.6; % The plastic range factor
eta_theta=1;    % The interaction exponent

lambdabar_theta=sqrt(f_yk/sigma_thetaRc); % Relative shell slenderness in
circumferential direction
lambdabar_theta0=0.4; % The circumferential squash limit slenderness
lambdabar_thetap=sqrt(alpha_theta/(1-beta_theta)); % Plastic limit
relative slenderness

if (lambdabar_theta<=lambdabar_theta0)

```

```

Chi_theta=1;
elseif (lambdabar_theta0<lambdabar_theta && lambdabar_theta<lambdabar_thetap)
    Chi_theta=1-(beta_theta*((lambdabar_theta-
lambdabar_theta0)/(lambdabar_thetap-lambdabar_theta0))^eta_theta);
elseif (lambdabar_thetap<=lambdabar_theta)
    Chi_theta=alpha_theta/(lambdabar_theta)^2;
end

sigma_thetaRk=Chi_theta*f_yk;    % The characteristic buckling stress

sigma_thetaRd=sigma_thetaRk/gamma_M1;    % The design buckling resistance

% The following variables are defined in Page 57 1993-4-1 - Silos
% NOTE 1: The above properties for the stiffeners (A, I, It etc.) relate to
the stiffener section alone: no
% allowance can be made for an "effective" section including parts of the
shell wall.

% According to Eurocode: The wall should be designed for the same external
pressure buckling criteria as the unstiffened
% wall unless a more rigorous calculation is necessary.
G=E/(2*(1+nu)); % Shearing Property

% For caluclation of D, the following is assumed.
l1=1000;
l_i=1;    % is the half wavelength of the potential buckle in the
vertical direction
A_r=A_R;    %22.51; %ABS=A_R    % is the cross-sectional area of a
ring stiffener
I_rs=I_rs;    %13.4418; %ABS=I_r    % is the second moment of area of
a ring stiffener about the vertical axis (Changed from I_r to match ABS)
d_r=1; %180; %ABS=1    % is the separation between ring stiffeners
e_r=y_rs;    %+(t/2); %9.0916; %ABS=y_rs+(t/2)% is the outward
eccentricity from the shell middle surface of a ring stiffener
y_st=((d_st+(tfst/2))*(tfst*b_st))+((d_st/2)*(t_st*d_st))/(A_s);
e_s=z_st;    %6.7; %ABS=z_st    % is the outward eccentricity from
the shell middle surface of a stringer stiffener

% Distance from inner surface of shell to centroid of stringer stiffener
y_st=((d_st+(tfst/2))*(tfst*b_st))+((d_st/2)*(t_st*d_st))/(A_s);
A_s=(d_st*t_st)+(b_st*tfst);
z_st=y_st;

C_phi=(E*t);    % is the sheeting stretching stiffness in the axial
direction
C_theta=E*t;    % is the sheeting stretching stiffness in the
circumferential direction
C_phitheta=0.38*E*t;    % is the sheeting stretching stiffness in membrane
shear

D_phi=(1/12)*E*t^3/((1-nu^2));    % (E*Ixx)/(2*pi*r);
%(1/12)*E*t^3/((1-nu^2)); % *(1+(1/4)*pi^2*t^2/l1^2));    % is the
sheeting flexural rigidity in the axial direction

```

```

D_theta=(1/12)*E*t^3/((1-nu^2));          %0.13*E*t^3;          %
(1/12)*E*t^3/((1-nu^2));          % 0.13*E*t^3;          % is the sheeting
flexural rigidity in the circumferential direction
D_phitheta=2*D_theta;          %(G*t^3)/12; %2*dphi % (1/12)*E*t^3/((1-
nu^2)*(1+(1/4)*pi^2*t^2/11^2));          % is the sheeting twisting flexural
rigidity in twisting

vec_l=1:d_r;

C11=C_phi+(E*A_s/d_s);
C12=nu*sqrt(C_phi*C_theta);
C14=(e_s*E*A_s)/(r*d_s);

C22=C_theta+((E*A_r)/(d_r));
C25=(e_r*E*A_r)/(r*d_r);

C33=C_phitheta;

C44=(D_phi+((E*I_s)/(d_s))+((E*A_s*e_s^2)/(d_s)))/r^2;
C45=0; %(nu*sqrt(D_phi*D_theta))/r^2;

C55=(D_theta+((E*I_rs)/d_r)+((E*A_r*e_r^2)/d_r))/r^2;

C66=(D_phitheta+(0.5*((G*I_ts)/d_s)+((G*I_tr)/d_r)))/r^2;

% 5.3.4.5 Buckling under external pressure, partial vacuum or wind
for j=1:20;
    n(j)=0+j;

omega(j)=(pi*r)/(n(j)*l_i);

A1(j)=n(j)^4*(omega(j)^4*C44 + 2*omega(j)^2*(C45+C66) + C55)+ C22 +
2*n(j)^2*C25;
A2(j)=((2*omega(j)^2)*
(C12+C33)*(C22+n(j)^2*C25)*(C12+n(j)^2*omega(j)^2*C14))-
(((omega(j)^2*C11)+C33)*(C22+n(j)^2*C25)^2 )-(omega(j)^2*(C22
+omega(j)^2*C33)*(C12+n(j)^2*omega(j)^2*C14)^2);
A3(j)=((omega(j)^2*C11 + C33)*(C22 + C25 + omega(j)^2*C33))-omega(j)^2*(C12 +
C33)^2;

P_nRcrumin(j)=(1/(r*n(j)^2))*(A1(j)+(A2(j)/A3(j)));
n_wav=find(P_nRcrumin==min(P_nRcrumin));          %
min(P_nRcrumin(P_nRcrumin>0));          %
end
n=n_wav;

circ=2*pi*r;
omega=(pi*r)/(n*l_i);

A1=n^4*(omega^4*C44 + 2*omega^2*(C45+C66) + C55)+ C22 + 2*n^2*C25;
A2=((2*omega^2)* (C12+C33)*(C22+n^2*C25)*(C12+n^2*omega^2*C14))-
(((omega^2*C11)+C33)*(C22+n^2*C25)^2 )-(omega^2*(C22
+omega^2*C33)*(C12+n^2*omega^2*C14)^2);

```

```

A3=((omega^2*C11 + C33)*(C22 + C25 + omega^2*C33))-omega^2*(C12 + C33)^2;

P_nRcru=(1/(r*n^2))*(A1+(A2/A3));
P_nRd=alpha_n*P_nRcru/gamma_M1;

% The critical buckling stress resultant (Meridional Loading)
for k=1:20;
nb(k)=0+k;

omegab(k)=(pi*r)/(nb(k)*l_i);

A1b(k)=nb(k)^4*(omegab(k)^4*C44 + 2*omegab(k)^2*(C45+C66) + C55)+ C22 +
2*nb(k)^2*C25;
A2b(k)=(2*omegab(k)^2)*
(C12+C33)*(C22+nb(k)^2*C25)*(C12+nb(k)^2*omegab(k)^2*C14))-
(((omegab(k)^2*C11)+C33)*(C22+nb(k)^2*C25)^2)-(omegab(k)^2*(C22
+omegab(k)^2*C33)*(C12+nb(k)^2*omegab(k)^2*C14)^2);
A3b(k)=(omegab(k)^2*C11 + C33)*(C22 + C25 + omegab(k)^2*C33))-
omegab(k)^2*(C12 + C33)^2;

n_xRcrmin(k)=(1/(nb(k)^2*omegab(k)^2))*(A1b(k)+(A2b(k)/A3b(k)));

n_wavb=find(n_xRcrmin==min(n_xRcrmin));
end
nb=n_wavb;

circ=2*pi*r;
omegab=(pi*r)/(nb*l_i);

A1b=nb^4*(omegab^4*C44 + 2*omegab^2*(C45+C66) + C55)+ C22 + 2*nb^2*C25;
A2b=((2*omegab^2)*(C12+C33)*(C22+nb^2*C25)*(C12+nb^2*omegab^2*C14))-
(((omegab^2*C11)+C33)*(C22+nb^2*C25)^2)-(omegab^2*(C22
+omegab^2*C33)*(C12+nb^2*omegab^2*C14)^2);
A3b=((omegab^2*C11 + C33)*(C22 + C25 + omegab^2*C33))-omegab^2*(C12 + C33)^2;

n_xRcr=(1/(nb^2*omegab^2))*(A1b+(A2b/A3b));

tm=t+(A_s/s);

lambdaglob=sqrt((tm*sigma_0)/n_xRcr);
n_xRk=lambdaglob*tm*sigma_0;

N_xRk=n_xRk/t;
n_xRd1=alpha_x*n_xRcr/gamma_M1;
n_xRd2=(A_s*sigma_0)/gamma_M1;
n_xRd=min(n_xRd1,n_xRd2);

%%%%%%%%%%%%%%%%%%%%%%%%%%%%%%%%%%%%%%%%%%%%%%%%%%%%%%%%%%%%%%%%%%%%%%%%
% ECCS - Simplified
%%%%%%%%%%%%%%%%%%%%%%%%%%%%%%%%%%%%%%%%%%%%%%%%%%%%%%%%%%%%%%%%%%%%%%%%
phi_eccs=1/(1+(A_s/s*t));
Qeccs=25;
deltawkeccs=(1/Qeccs)*sqrt(r/tm)*tm;

```

```

alpha_xeccs=0.62/(1+(1.91*(deltawkeccs/tm)^1.44));

n_xRcreccs=((pi^2*E*I_se)/(l^2*s))+phi_eccs*tm*alpha_xeccs*sigma_xRc;

lambdaglobeccs=sqrt((tm*sigma_0)/n_xRcreccs);
n_xRkeccs=lambdaglobeccs*tm*sigma_0;

N_xRkeccs=n_xRkeccs/t;

%%%%%%%%%%%%%%%%%%%%%%%%%%%%%%%%%%%%%%%%%%%%%%%%%%%%%%%%%%%%%%%%%%%%%%%%
fprintf('\nFor Excel Spreadsheet: Annex D\n')
fprintf('Knockdown Factor: %.2f \n',Chi_x)
fprintf('Critical elastic buckling stress for meridional loading: %.2f
\n',sigma_xRc)
fprintf('Characteristic buckling stress for meridional loading: %.2f
\n',sigma_xRk)
fprintf('Design buckling resistance for meridional loading: %.2f
\n',sigma_xRd)
fprintf('\nThe characteristic buckling stress for uniform external
pressure:%.2f N/mm^2',sigma_thetaRk)
fprintf('\nThe design buckling resistance for uniform external pressure:%.2f
N/mm^2\n',sigma_thetaRd)

fprintf('\nFor Excel Spreadsheet: Rigorous method')
fprintf('\nThe partial safety factor: %.2f \n',gamma_M1)
fprintf('Imperfection reduction factor: %.2f \n',alpha_n)
fprintf('The critical buckling stress resultant for meridional loading: %.2f
(N/mm)\n',n_xRcr)
fprintf('The characteristic buckling stress resultant for meridional loading:
%.2f (N/mm)\n',n_xRk)
fprintf('The design maximum meridional loading: %.2f (N/mm)\n',n_xRd)
fprintf('\nThe critical buckling stress for uniform external pressure: %.2f
(N/mm^2)\n',P_nRcru)
fprintf('The design maximum external pressure: %.2f (N/mm^2)\n',P_nRd)

fprintf('\nFor Excel Spreadsheet: ECCS Simplified Method')
fprintf('\nThe ECCS characteristic buckling stress for meridional loading:
%.2f (N/mm^2)\n',N_xRkeccs)
% Excel
filename1='output1.xlsx';
outA=[A1, A2, A3, A_r, A_s, C11, C12, C14, C22, C25, C33, C44, C45, C55, C66,
C_phi, C_phitheta, C_theta, D_phi, D_phitheta, D_theta, E, G, I_rs, I_s,
I_tr, I_ts, P_nRcru, P_nRcrumin, d_r, d_s, e_r, e_s, j, ll, l_i, n, n_wav,
nu, omega, r, t];
% xlswrite(filename1,outA)

%fprintf('\nUnity Check 1: %.2f \n', UC1)
%fprintf('\nUnity Check: %s \n',UC1check)

```

Appendix D

Ansys Element Types

The following elements were used in the finite element analyses, the given information is taken from the Ansys Element Library (Ansys 13.0 Help System, SAS IP Inc., 2010), for further information readers are advised to consult this document.

BEAM188 Element Description

BEAM188 is suitable for analysing slender to moderately stubby/thick beam structures. The element is based on Timoshenko beam theory which includes shear-deformation effects. The element provides options for unrestrained warping and restrained warping of cross-sections. The element is a linear, quadratic, or cubic two-node beam element in 3-D. BEAM188 has six or seven degrees of freedom at each node. These include translations in the x, y, and z directions and rotations about the x, y, and z directions. A seventh degree of freedom (warping magnitude) is optional. This element is well-suited for linear, large rotation, and/or large strain nonlinear applications. The element includes stress stiffness terms, by default, in any analysis with large deflection. The provided stress-stiffness terms enable the elements to analyse flexural, lateral, and torsional stability problems (using eigenvalue buckling, or collapse studies with arc length methods or nonlinear stabilization). Elasticity, plasticity, creep and other nonlinear material models are supported. A cross-section associated with this element type can be a built-up section referencing more than one material.

SURF156 Element Description

SURF156 may be used for applying line pressure loads on structures. It may be overlaid onto the edge of any 3-D element. The element is applicable to 3-D structural analyses. Various loads and surface effects may exist simultaneously.

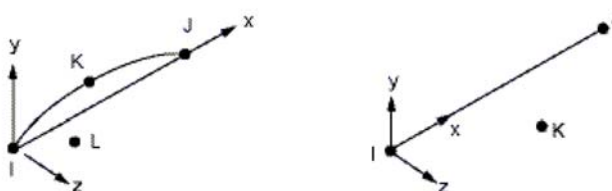


Figure 1: SURF156 Geometry

SHELL181 Element Description

SHELL181 is suitable for analysing thin to moderately-thick shell structures. It is a four-node element with six degrees of freedom at each node: translations in the x,y, and z directions, and rotations about the x, y, and z-axes. (If the membrane option is used, the element has translational degrees of freedom only). The degenerate triangular option should only be used as filler elements in mesh generation. SHELL181 is well-suited for linear, large rotation, and/or large strain nonlinear applications. Change in shell thickness is accounted for in nonlinear analyses. In the element domain, both full and reduced integration schemes are supported. SHELL181 accounts for follower (load stiffness) effects of distributed pressures. SHELL181 may be used for layered applications for modelling composite shells or sandwich construction. The accuracy in modelling composite shells is governed by the first-order shear-deformation theory (usually referred to as Mindlin-Reissner shell theory). The element formulation is based on logarithmic strain and true stress measures. The element kinematics allow for finite membrane strains (stretching). However, the curvature changes within a time increment are assumed to be small.

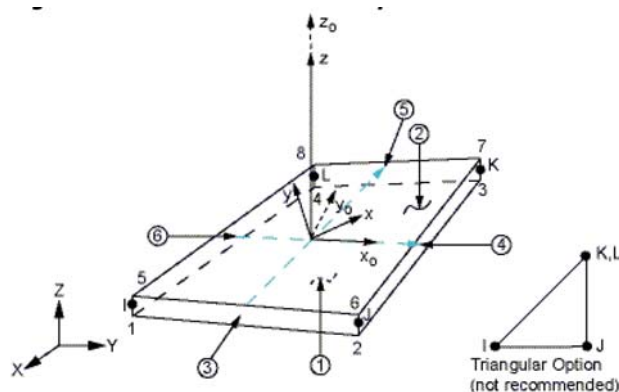


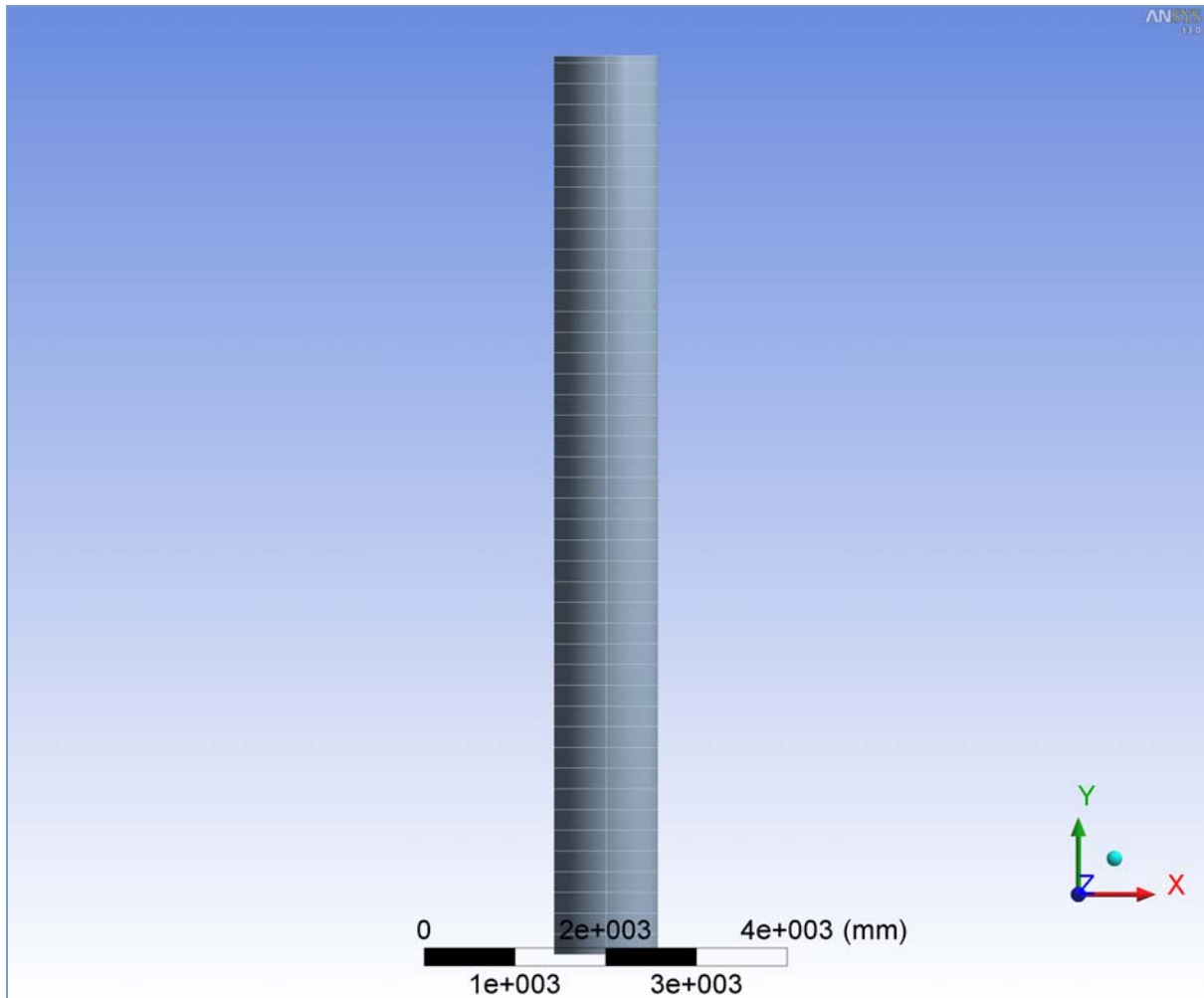
Figure 2: SHELL181 Geometry

Appendix E



Project

First Saved	Wednesday, December 12, 2012
Last Saved	Thursday, January 17, 2013
Product Version	13.0 Release



Contents

- [Units](#)
- [Model \(E4\)](#)
 - [Geometry](#)
 - [Surface Body](#)
 - [Coordinate Systems](#)
 - [Connections](#)
 - [Contacts](#)
 - [Mesh](#)
 - [Static Structural \(E5\)](#)
 - [Analysis Settings](#)
 - [Loads](#)
 - [Solution \(E6\)](#)
 - [Solution Information](#)
 - [Newton-Raphson Residual Force](#)
 - [Results](#)
 - [Force Reaction](#)
- [Material Data](#)
 - [Structural Steel](#)

Report Not Finalized

Not all objects described below are in a finalized state. As a result, data may be incomplete, obsolete or in error. [View first state problem](#). To finalize this report, edit objects as needed and solve the analyses.

Units

TABLE 1

Unit System	Metric (mm, kg, N, s, mV, mA) Degrees rad/s Celsius
Angle	Degrees
Rotational Velocity	rad/s
Temperature	Celsius

Model (E4)

Geometry

TABLE 2
Model (E4) > Geometry

Object Name	<i>Geometry</i>
State	Fully Defined
Definition	
Source	C:\Masters\Thesis\Matlab\Verification of Code\2-1C\Non-Linear\Non-Linear (Perfect)_files\dp0\SYS-2\DM\SYS-2.agdb
Type	DesignModeler
Length Unit	Millimeters
Element Control	Program Controlled
Display Style	Part Color
Bounding Box	
Length X	1142.8 mm

Length Y	9910. mm
Length Z	1142.8 mm
Properties	
Volume	6.9733e+007 mm ³
Mass	547.4 kg
Surface Area(approx.)	3.5578e+007 mm ²
Scale Factor Value	1.
Statistics	
Bodies	1
Active Bodies	1
Nodes	41760
Elements	41640
Mesh Metric	None
Preferences	
Parameter Processing	Yes
Personal Parameter Key	DS
CAD Attribute Transfer	Yes
CAD Attribute Prefixes	SDFEA;DDM
Named Selection Processing	No
Material Properties Transfer	No
CAD Associativity	Yes
Import Coordinate Systems	No
Reader Save Part File	No
Import Using Instances	Yes
Do Smart Update	Yes
Attach File Via Temp File	Yes
Temporary Directory	C:\Users\Eoin\AppData\Local\Temp
Analysis Type	3-D
Enclosure and Symmetry Processing	Yes

TABLE 3
Model (E4) > Geometry > Parts

Object Name	<i>Surface Body</i>
State	Meshed
Graphics Properties	
Visible	Yes
Glow	0
Shininess	1
Transparency	1
Specularity	1
Definition	
Suppressed	No
Stiffness Behavior	Flexible
Coordinate System	Default Coordinate System
Reference Temperature	By Environment
Thickness	1.96 mm
Thickness Mode	Refresh on Update
Offset Type	Middle(Membrane)
Material	
Assignment	Structural Steel
Nonlinear Effects	Yes
Thermal Strain Effects	Yes
Bounding Box	

Length X	1142.8 mm
Length Y	9910. mm
Length Z	1142.8 mm
Properties	
Volume	6.9733e+007 mm ³
Mass	547.4 kg
Centroid X	-3.908e-004 mm
Centroid Y	4955. mm
Centroid Z	1.1803e-002 mm
Moment of Inertia Ip1	4.5639e+009 kg·mm ²
Moment of Inertia Ip2	1.7774e+008 kg·mm ²
Moment of Inertia Ip3	4.5639e+009 kg·mm ²
Surface Area(approx.)	3.5578e+007 mm ²
Statistics	
Nodes	41760
Elements	41640
Mesh Metric	None

Coordinate Systems

TABLE 4
Model (E4) > Coordinate Systems > Coordinate System

Object Name	<i>Global Coordinate System</i>
State	Fully Defined
Definition	
Type	Cartesian
Coordinate System ID	0.
Origin	
Origin X	0. mm
Origin Y	0. mm
Origin Z	0. mm
Directional Vectors	
X Axis Data	[1. 0. 0.]
Y Axis Data	[0. 1. 0.]
Z Axis Data	[0. 0. 1.]

Connections

TABLE 5
Model (E4) > Connections

Object Name	<i>Connections</i>
State	Fully Defined
Auto Detection	
Generate Automatic Connection On Refresh	Yes
Transparency	
Enabled	Yes

TABLE 6
Model (E4) > Connections > Contacts

Object Name	<i>Contacts</i>
State	Fully Defined
Definition	
Connection Type	Contact
Scope	
Scoping Method	Geometry Selection
Geometry	All Bodies

Auto Detection	
Tolerance Type	Slider
Tolerance Slider	0.
Tolerance Value	25.102 mm
Face/Face	Yes
Face/Edge	Yes
Edge/Edge	Yes
Priority	Include All
Group By	Bodies
Search Across	Bodies

Mesh

TABLE 7
Model (E4) > Mesh

Object Name	<i>Mesh</i>
State	Solved
Defaults	
Physics Preference	Mechanical
Relevance	0
Sizing	
Use Advanced Size Function	On: Curvature
Relevance Center	Coarse
Initial Size Seed	Active Assembly
Smoothing	Medium
Span Angle Center	Coarse
Curvature Normal Angle	Default (30.0 °)
Min Size	10.0 mm
Max Face Size	30.0 mm
Growth Rate	Default
Minimum Edge Length	80.170 mm
Inflation	
Use Automatic Inflation	None
Inflation Option	Smooth Transition
Transition Ratio	0.272
Maximum Layers	2
Growth Rate	1.2
Inflation Algorithm	Pre
View Advanced Options	No
Advanced	
Shape Checking	Standard Mechanical
Element Midside Nodes	Program Controlled
Number of Retries	Default (4)
Extra Retries For Assembly	Yes
Rigid Body Behavior	Dimensionally Reduced
Mesh Morphing	Disabled
Defeaturing	
Use Sheet Thickness for Pinch	No
Pinch Tolerance	Default (9.0 mm)
Generate Pinch on Refresh	No
Sheet Loop Removal	No
Automatic Mesh Based Defeaturing	On
Defeaturing Tolerance	Default (7.50 mm)
Statistics	
Nodes	41760
Elements	41640

Mesh Metric	None
-------------	------

Static Structural (E5)

TABLE 8
Model (E4) > Analysis

Object Name	<i>Static Structural (E5)</i>
State	Not Solved
Definition	
Physics Type	Structural
Analysis Type	Static Structural
Solver Target	Mechanical APDL
Options	
Environment Temperature	22. °C
Generate Input Only	No

TABLE 9
Model (E4) > Static Structural (E5) > Analysis Settings

Object Name	<i>Analysis Settings</i>
State	Fully Defined
Restart Analysis	
Restart Type	Program Controlled
Load Step	1
Substep	38
Time	0.76 s
Step Controls	
Number Of Steps	1.
Current Step Number	1.
Step End Time	1. s
Auto Time Stepping	On
Define By	Substeps
Initial Substeps	50.
Minimum Substeps	50.
Maximum Substeps	50.
Solver Controls	
Solver Type	Program Controlled
Weak Springs	Program Controlled
Large Deflection	On
Inertia Relief	Off
Restart Controls	
Generate Restart Points	Program Controlled
Retain Files After Full Solve	No
Nonlinear Controls	
Force Convergence	Program Controlled
Moment Convergence	Program Controlled
Displacement Convergence	Program Controlled
Rotation Convergence	Program Controlled
Line Search	Program Controlled
Stabilization	Off
Output Controls	
Calculate Stress	Yes
Calculate Strain	Yes
Calculate Contact	No
Calculate Results At	All Time Points

Cache Results in Memory (Beta)	Never
Analysis Data Management	
Solver Files Directory	C:\Masters\Thesis\Matlab\Verification of Code\2-1C\Non-Linear\Non-Linear (Perfect)_files\dp0\SYS-2\MECH\
Future Analysis	None
Scratch Solver Files Directory	
Save MAPDL db	No
Delete Unneeded Files	Yes
Nonlinear Solution	Yes
Solver Units	Active System
Solver Unit System	nmm

TABLE 10
Model (E4) > Static Structural (E5) > Loads

Object Name	<i>Displacement</i>	<i>Simply Supported</i>	<i>Displacement 2</i>
State	Fully Defined		
Scope			
Scoping Method	Geometry Selection		
Geometry	1 Edge		
Definition			
ID (Beta)	646	648	650
Type	Displacement	Simply Supported	Displacement
Define By	Components		Components
Coordinate System	Global Coordinate System		Global Coordinate System
X Component	0. mm (ramped)		Free
Y Component	Free		-15. mm (ramped)
Z Component	0. mm (ramped)		Free
Suppressed	No		

FIGURE 1
Model (E4) > Static Structural (E5) > Displacement

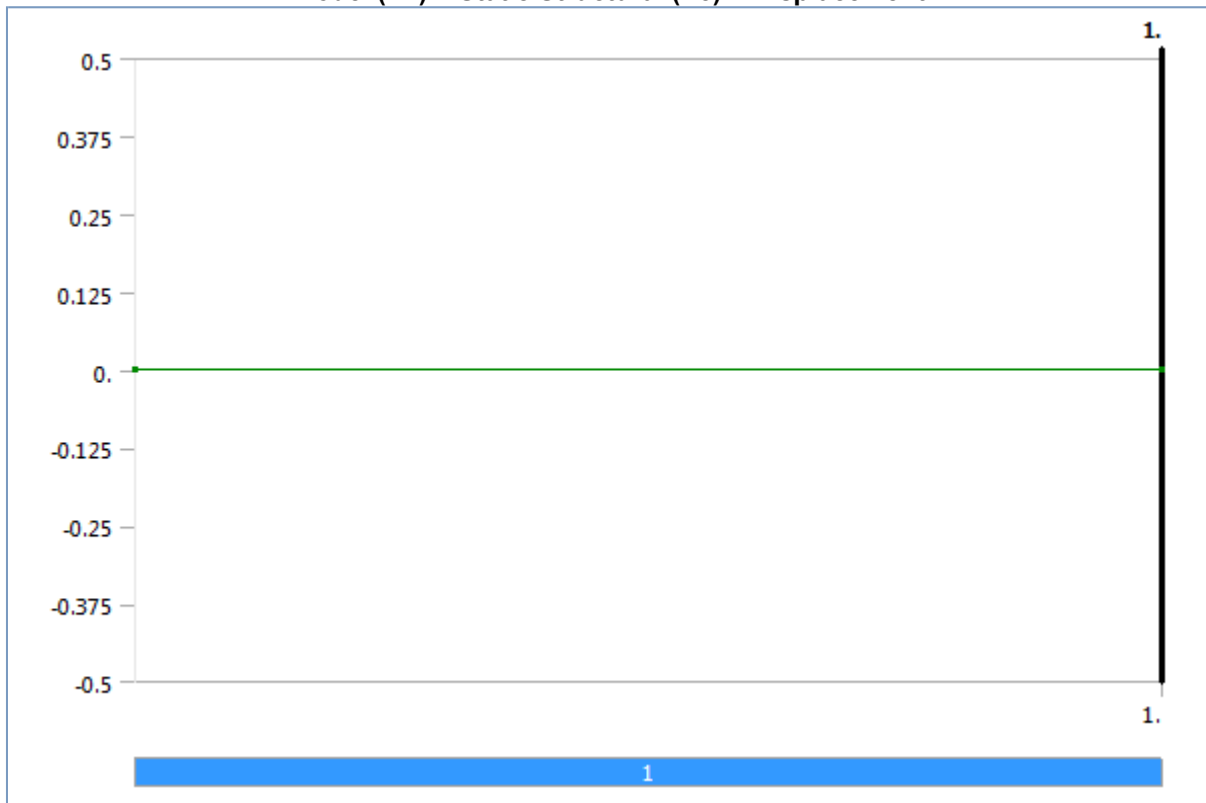


FIGURE 2
Model (E4) > Static Structural (E5) > Displacement 2

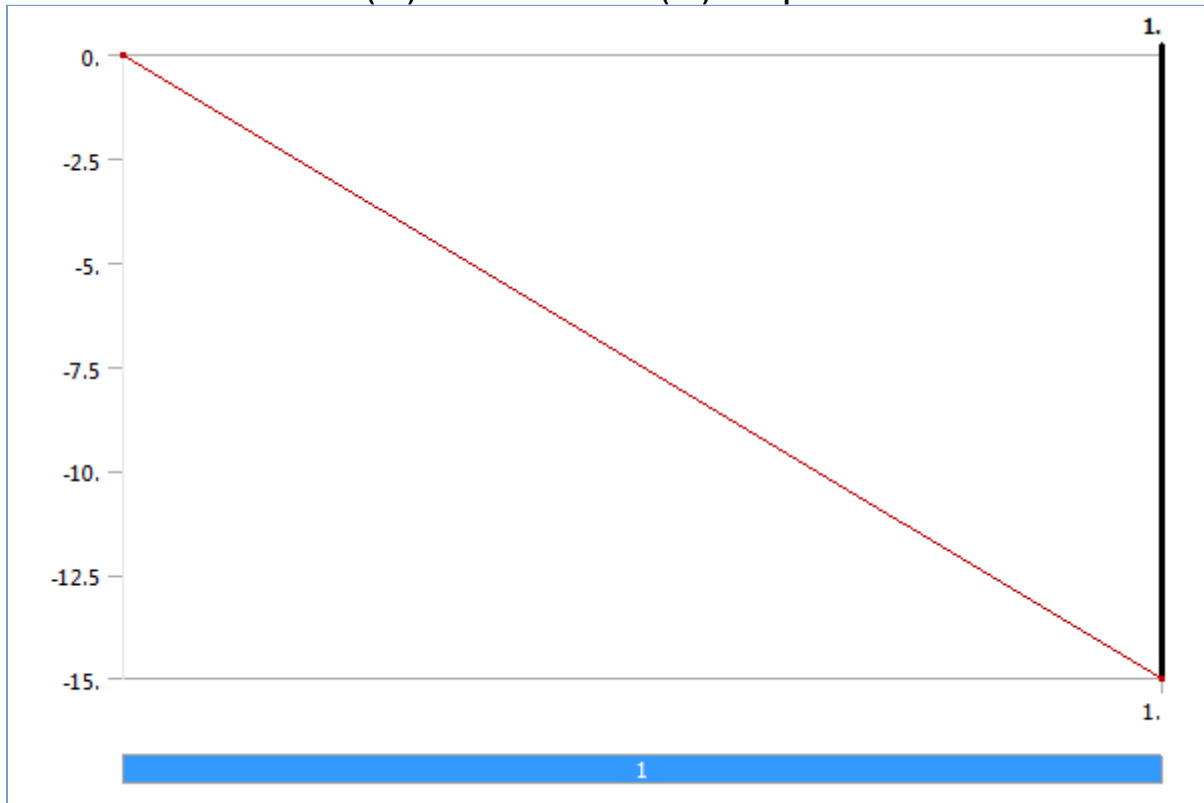


TABLE 11
Model (E4) > Static Structural (E5) > Command Snippet

Object Name	Commands (APDL)
State	Fully Defined
File	
File Name	
File Status	File not found
Definition	
Suppressed	No
Target	Mechanical APDL
Input Arguments	
ARG1	
ARG2	
ARG3	
ARG4	
ARG5	
ARG6	
ARG7	
ARG8	
ARG9	

Model (E4) > Static Structural (E5) > Commands (APDL)

```

NSEL,S,LOC,Y,-7.5,7.5
D,ALL,,0,,,,UX,UY,UZ,,,
CPINTF,UY,50

NSEL,S,LOC,Y,221.1,236.1
D,ALL,,0,,,,UX,UZ,,,,
CPINTF,UY,50

NSEL,S,LOC,Y,449.7,464.7

```

D,ALL,,0,,,,UX,UZ,,,,
CPINTE,UY,50

NSEL,S,LOC,Y,678.3,693.3
D,ALL,,0,,,,UX,UZ,,,,
CPINTE,UY,50

NSEL,S,LOC,Y,906.9,921.9
D,ALL,,0,,,,UX,UZ,,,,
CPINTE,UY,50

NSEL,S,LOC,Y,1135.5,1150.5
D,ALL,,0,,,,UX,UZ,,,,
CPINTE,UY,50

NSEL,S,LOC,Y,1364.1,1379.1
D,ALL,,0,,,,UX,UZ,,,,
CPINTE,UY,50

NSEL,S,LOC,Y,1592.7,1607.7
D,ALL,,0,,,,UX,UZ,,,,
CPINTE,UY,50

NSEL,S,LOC,Y,1821.3,1836.3
D,ALL,,0,,,,UX,UZ,,,,
CPINTE,UY,50

NSEL,S,LOC,Y,2049.9,2064.9
D,ALL,,0,,,,UX,UZ,,,,
CPINTE,UY,50

NSEL,S,LOC,Y,2278.5,2293.5
D,ALL,,0,,,,UX,UZ,,,,
CPINTE,UY,50

NSEL,S,LOC,Y,2507.1,2522.1
D,ALL,,0,,,,UX,UZ,,,,
CPINTE,UY,50

NSEL,S,LOC,Y,2735.7,2750.7
D,ALL,,0,,,,UX,UZ,,,,
CPINTE,UY,50

NSEL,S,LOC,Y,2964.3,2979.3
D,ALL,,0,,,,UX,UZ,,,,
CPINTE,UY,50

NSEL,S,LOC,Y,3192.9,3207.9
D,ALL,,0,,,,UX,UZ,,,,
CPINTE,UY,50

NSEL,S,LOC,Y,3421.5,3436.5
D,ALL,,0,,,,UX,UZ,,,,
CPINTE,UY,50

NSEL,S,LOC,Y,3650.1,3665.1
D,ALL,,0,,,,UX,UZ,,,,
CPINTE,UY,50

NSEL,S,LOC,Y,3878.7,3893.7
D,ALL,,0,,,,UX,UZ,,,,
CPINTE,UY,50

NSEL,S,LOC,Y,4107.3,4122.3
D,ALL,,0,,,,UX,UZ,,,,
CPINTE,UY,50

NSEL,S,LOC,Y,4335.9,4350.9
D,ALL,,0,,,,UX,UZ,,,,
CPINTE,UY,50

NSEL,S,LOC,Y,4564.5,4579.5
D,ALL,,0,,,,UX,UZ,,,,
CPINTE,UY,50

NSEL,S,LOC,Y,4793.1,4808.1
D,ALL,,0,,,,UX,UZ,,,,
CPINTE,UY,1

NSEL,S,LOC,Y,5021.7,5036.7

```
D,ALL,,0,,,,UX,UZ,,,,
CPINTF,UY,1

NSEL,S,LOC,Y,5250.3,5265.3
D,ALL,,0,,,,UX,UZ,,,,
CPINTF,UY,1

NSEL,S,LOC,Y,5478.9,5493.9
D,ALL,,0,,,,UX,UZ,,,,
CPINTF,UY,50
NSEL,S,LOC,Y,5707.5,5722.5
D,ALL,,0,,,,UX,UZ,,,,
CPINTF,UY,50
NSEL,S,LOC,Y,5936.1,5951.1
D,ALL,,0,,,,UX,UZ,,,,
CPINTF,UY,50
NSEL,S,LOC,Y,6164.7,6179.7
D,ALL,,0,,,,UX,UZ,,,,
CPINTF,UY,50
NSEL,S,LOC,Y,6393.3,6408.3
D,ALL,,0,,,,UX,UZ,,,,
CPINTF,UY,50
NSEL,S,LOC,Y,6621.9,6636.9
D,ALL,,0,,,,UX,UZ,,,,
CPINTF,UY,50
NSEL,S,LOC,Y,6850.5,6865.5
D,ALL,,0,,,,UX,UZ,,,,
CPINTF,UY,50
NSEL,S,LOC,Y,7079.1,7094.1
D,ALL,,0,,,,UX,UZ,,,,
CPINTF,UY,50
NSEL,S,LOC,Y,7307.7,7322.7
D,ALL,,0,,,,UX,UZ,,,,
CPINTF,UY,50
NSEL,S,LOC,Y,7536.3,7551.3
D,ALL,,0,,,,UX,UZ,,,,
CPINTF,UY,50
NSEL,S,LOC,Y,7764.900000000001,7779.900000000001
D,ALL,,0,,,,UX,UZ,,,,
CPINTF,UY,50
NSEL,S,LOC,Y,7993.500000000001,8008.500000000001
D,ALL,,0,,,,UX,UZ,,,,
CPINTF,UY,50
NSEL,S,LOC,Y,8222.100000000001,8237.100000000001
D,ALL,,0,,,,UX,UZ,,,,
CPINTF,UY,50
NSEL,S,LOC,Y,8450.700000000001,8465.700000000001
D,ALL,,0,,,,UX,UZ,,,,
CPINTF,UY,50
NSEL,S,LOC,Y,8679.300000000001,8694.300000000001
D,ALL,,0,,,,UX,UZ,,,,
CPINTF,UY,50
NSEL,S,LOC,Y,8907.900000000001,8922.900000000001
D,ALL,,0,,,,UX,UZ,,,,
CPINTF,UY,50
NSEL,S,LOC,Y,9136.500000000001,9151.500000000001
D,ALL,,0,,,,UX,UZ,,,,
CPINTF,UY,50
NSEL,S,LOC,Y,9365.100000000001,9380.100000000001
D,ALL,,0,,,,UX,UZ,,,,
CPINTF,UY,50
NSEL,S,LOC,Y,9593.700000000001,9608.700000000001
D,ALL,,0,,,,UX,UZ,,,,
CPINTF,UY,50
```

```

NSEL,S,LOC,Y,9822.30000000001,9837.30000000001
D,ALL,,0,,,,UX,UZ,,,,
CPINTF,UY,10
NSEL,S,LOC,Y,9902.50000000001,9917.50000000001
D,ALL,,0,,,,UX,UZ,,,,
CPINTF,UY,10
NSEL,ALL

```

Solution (E6)

TABLE 12
Model (E4) > Static Structural (E5) > Solution

Object Name	<i>Solution (E6)</i>
State	Solve Failed
Adaptive Mesh Refinement	
Max Refinement Loops	1.
Refinement Depth	2.
Information	
Status	Solve Required, Restart Available

TABLE 13
Model (E4) > Static Structural (E5) > Solution (E6) > Solution Information

Object Name	<i>Solution Information</i>
State	Solve Failed
Solution Information	
Solution Output	Force Convergence
Newton-Raphson Residuals	1
Update Interval	2.5 s
Display Points	All

FIGURE 3
Model (E4) > Static Structural (E5) > Solution (E6) > Solution Information



FIGURE 4

Model (E4) > Static Structural (E5) > Solution (E6) > Solution Information

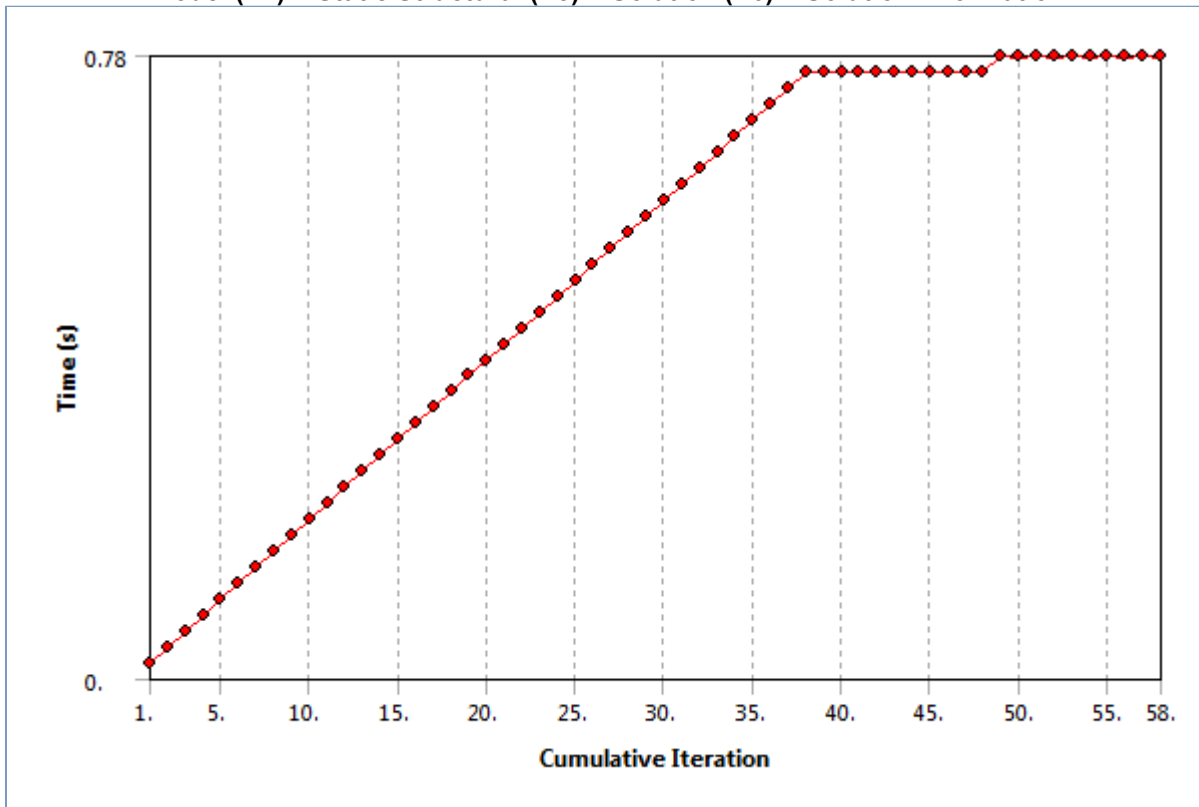


TABLE 14

Model (E4) > Static Structural (E5) > Solution (E6) > Solution Information > Results

Object Name	<i>Newton-Raphson Residual Force</i>
State	Solved
Definition	
Type	Newton-Raphson Residual Force
Results	
Minimum	1.1156e-030 N
Maximum	33338 N
Convergence	
Criterion	1920. N
Value	4.036e+005 N
Information	
Time	0.78 s
Load Step	1
Substep	39
Iteration Number	10

TABLE 15

Model (E4) > Static Structural (E5) > Solution (E6) > Results

Object Name	<i>Total Deformation</i>	<i>Directional Deformation</i>
State	Solved	
Scope		
Scoping Method	Geometry Selection	
Geometry	All Bodies	
Definition		
Type	Total Deformation	Directional Deformation
By	Time	
Display Time	0.76 s	
Calculate Time History	Yes	
Identifier		

Orientation		X Axis
Coordinate System		Global Coordinate System
Results		
Minimum	0. mm	-0.40042 mm
Maximum	11.4 mm	0.40062 mm
Minimum Value Over Time		
Minimum	0. mm	-211.71 mm
Maximum	0. mm	-5.904e-003 mm
Maximum Value Over Time		
Minimum	0.3 mm	5.9053e-003 mm
Maximum	446.43 mm	291.71 mm
Information		
Time	0.76 s	
Load Step	1	
Substep	38	
Iteration Number	48	

FIGURE 5
Model (E4) > Static Structural (E5) > Solution (E6) > Total Deformation

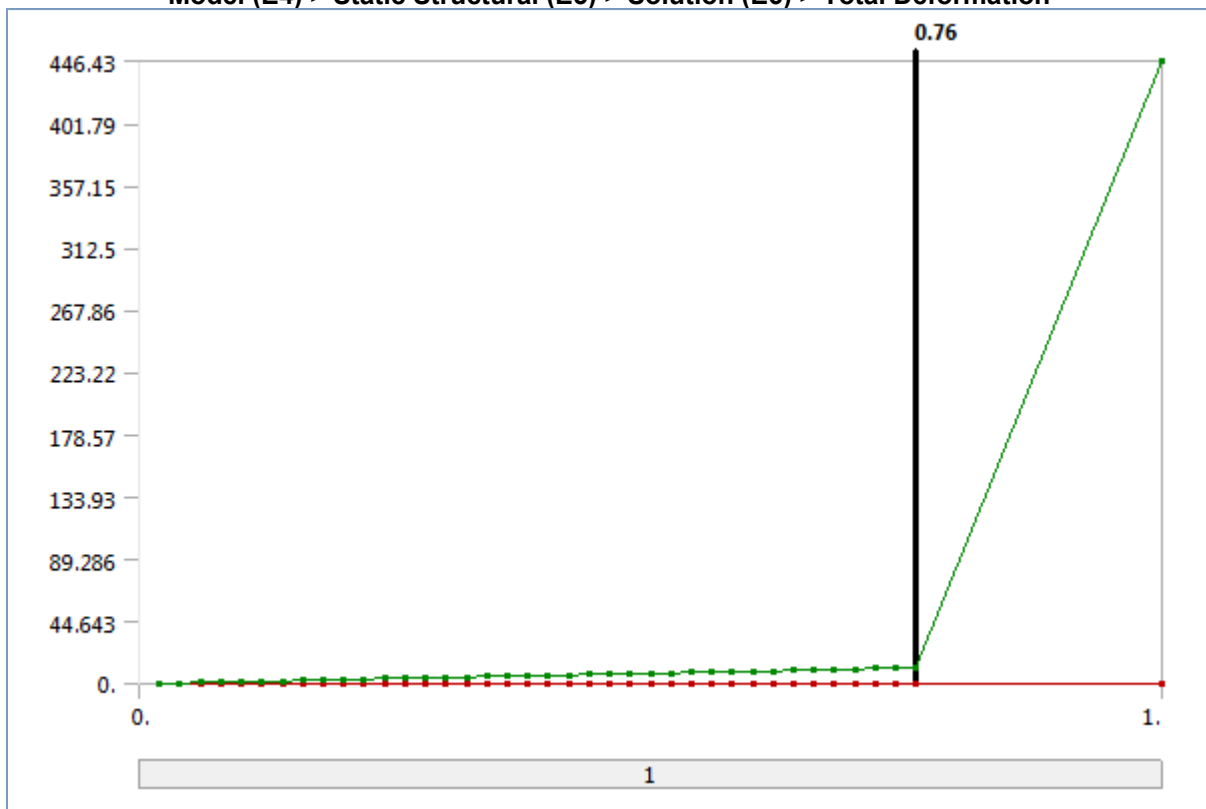


TABLE 16
Model (E4) > Static Structural (E5) > Solution (E6) > Total Deformation

Time [s]	Minimum [mm]	Maximum [mm]
2.e-002		0.3
4.e-002		0.6
6.e-002		0.9
8.e-002		1.2
0.1		1.5
0.12		1.8
0.14		2.1
0.16		2.4
0.18		2.7
0.2		3.

0.22		3.3
0.24		3.6
0.26		3.9
0.28		4.2
0.3		4.5
0.32		4.8
0.34		5.1
0.36		5.4
0.38		5.7
0.4		6.
0.42		6.3
0.44		6.6
0.46		6.9
0.48		7.2
0.5	0.	7.5
0.52		7.8
0.54		8.1
0.56		8.4
0.58		8.7
0.6		9.
0.62		9.3
0.64		9.6
0.66		9.9
0.68		10.2
0.7		10.5
0.72		10.8
0.74		11.1
0.76		11.4
1.		446.43

FIGURE 6
Model (E4) > Static Structural (E5) > Solution (E6) > Directional Deformation



TABLE 17
Model (E4) > Static Structural (E5) > Solution (E6) > Directional Deformation

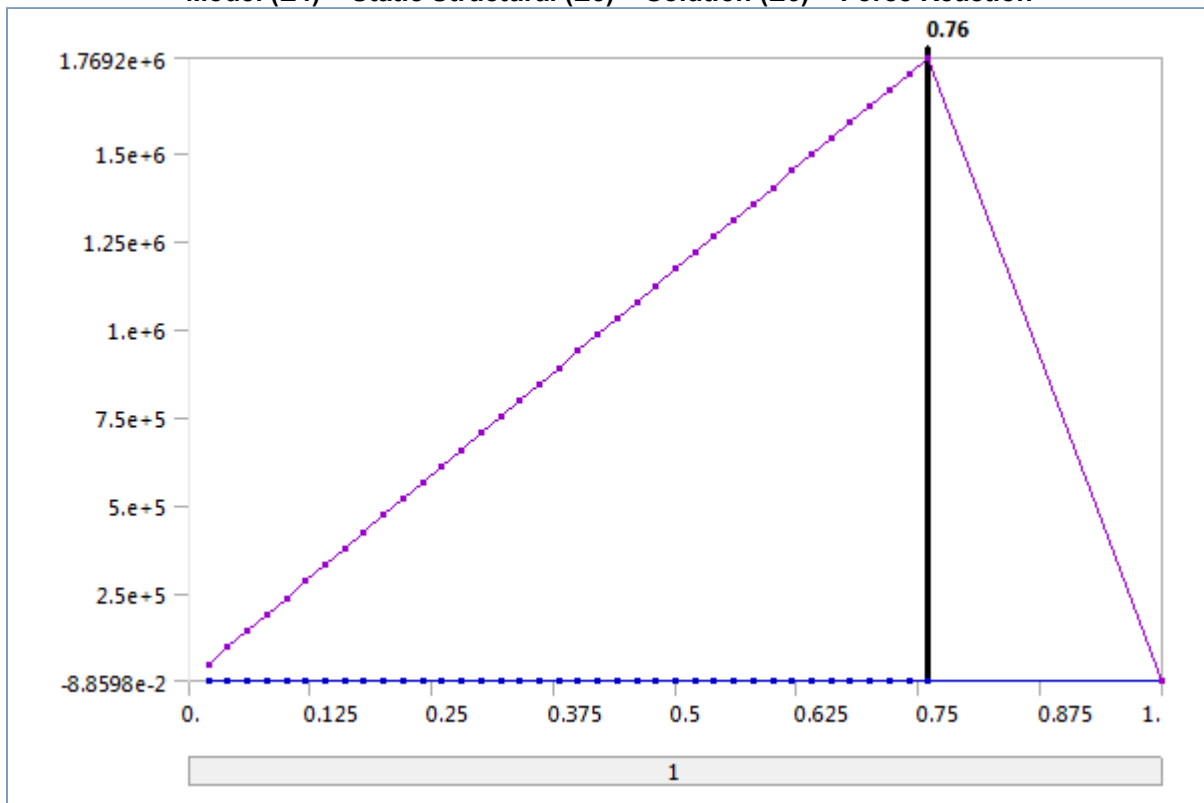
Time [s]	Minimum [mm]	Maximum [mm]
2.e-002	-5.904e-003	5.9053e-003
4.e-002	-1.1881e-002	1.1883e-002
6.e-002	-1.7883e-002	1.7887e-002
8.e-002	-2.3928e-002	2.3933e-002
0.1	-3.0016e-002	3.0022e-002
0.12	-3.6148e-002	3.6156e-002
0.14	-4.2326e-002	4.2336e-002
0.16	-4.8551e-002	4.8562e-002
0.18	-5.4823e-002	5.4836e-002
0.2	-6.1144e-002	6.1159e-002
0.22	-6.7516e-002	6.7532e-002
0.24	-7.3939e-002	7.3957e-002
0.26	-8.0416e-002	8.0435e-002
0.28	-8.6947e-002	8.6968e-002
0.3	-9.3534e-002	9.3557e-002
0.32	-0.10018	0.1002
0.34	-0.10688	0.10691
0.36	-0.11365	0.11368
0.38	-0.12048	0.12051
0.4	-0.12737	0.12741
0.42	-0.13434	0.13437
0.44	-0.14137	0.14141
0.46	-0.14847	0.14852
0.48	-0.15565	0.1557
0.5	-0.16291	0.16296
0.52	-0.17025	0.1703
0.54	-0.17768	0.17773
0.56	-0.18519	0.18524
0.58	-0.19279	0.19285
0.6	-0.20049	0.20055
0.62	-0.20829	0.20835
0.64	-0.21619	0.21626
0.66	-0.2242	0.22427
0.68	-0.23232	0.2324
0.7	-0.24056	0.24064
0.72	-0.24888	0.24897
0.74	-0.27482	0.27483
0.76	-0.40042	0.40062
1.	-211.71	291.71

TABLE 18
Model (E4) > Static Structural (E5) > Solution (E6) > Probes

Object Name	<i>Force Reaction</i>
State	Solved
Definition	
Type	Force Reaction
Location Method	Boundary Condition
Boundary Condition	Simply Supported
Orientation	Global Coordinate System
Options	
Result Selection	All
Display Time	0.76 s
Results	
X Axis	0.23244 N

Y Axis	1.7692e+006 N
Z Axis	11.413 N
Total	1.7692e+006 N
Maximum Value Over Time	
X Axis	0.23244 N
Y Axis	1.7692e+006 N
Z Axis	11.413 N
Total	1.7692e+006 N
Minimum Value Over Time	
X Axis	-5.1868e-002 N
Y Axis	0. N
Z Axis	-8.8598e-002 N
Total	0. N
Information	
Time	0.76 s
Load Step	1
Substep	38
Iteration Number	48

FIGURE 7
Model (E4) > Static Structural (E5) > Solution (E6) > Force Reaction



Material Data

Structural Steel

TABLE 19
Structural Steel > Constants

Density	7.85e-006 kg mm ⁻³
Coefficient of Thermal Expansion	1.2e-005 C ⁻¹
Specific Heat	4.34e+005 mJ kg ⁻¹ C ⁻¹
Thermal Conductivity	6.05e-002 W mm ⁻¹ C ⁻¹

Resistivity	1.7e-004 ohm mm
-------------	-----------------

TABLE 20
Structural Steel > Compressive Ultimate Strength

Compressive Ultimate Strength MPa
0

TABLE 21
Structural Steel > Compressive Yield Strength

Compressive Yield Strength MPa
293.2

TABLE 22
Structural Steel > Tensile Yield Strength

Tensile Yield Strength MPa
293.2

TABLE 23
Structural Steel > Tensile Ultimate Strength

Tensile Ultimate Strength MPa
460

TABLE 24
Structural Steel > Isotropic Secant Coefficient of Thermal Expansion

Reference Temperature C
22

TABLE 25
Structural Steel > Alternating Stress Mean Stress

Alternating Stress MPa	Cycles	Mean Stress MPa
3999	10	0
2827	20	0
1896	50	0
1413	100	0
1069	200	0
441	2000	0
262	10000	0
214	20000	0
138	1.e+005	0
114	2.e+005	0
86.2	1.e+006	0

TABLE 26
Structural Steel > Strain-Life Parameters

Strength Coefficient MPa	Strength Exponent	Ductility Coefficient	Ductility Exponent	Cyclic Strength Coefficient MPa	Cyclic Strain Hardening Exponent
920	-0.106	0.213	-0.47	1000	0.2

TABLE 27
Structural Steel > Isotropic Elasticity

Temperature C	Young's Modulus MPa	Poisson's Ratio	Bulk Modulus MPa	Shear Modulus MPa
	2.16e+005	0.3	1.8e+005	83077

TABLE 28
Structural Steel > Isotropic Relative Permeability

Relative Permeability
10000

TABLE 29
Structural Steel > Bilinear Isotropic Hardening

Yield Strength MPa	Tangent Modulus MPa	Temperature C
293.2	145	